Title
Structural Evaluation of a Bamboo Arch

Author
SHRIVASTAVA, RAHIL

Publication Date
2015

Peer reviewed|Thesis/dissertation

UNIVERSITY OF CALIFORNIA,
IRVINE

Structural Evaluation of a Bamboo Arch

THESIS

submitted in partial satisfaction of the requirements
for the degree of

MASTER OF SCIENCE

in CIVIL ENGINEERING

by

RAHIL SHRIVASTAVA

Thesis Committee:
Dr. Ayman S. Mosallam, Chair
Dr. Farzin Zareian
Dr. Anne Lemnitzer

2015

DEDICATION

To

my parents (Dr. Pratibha Shrivastava and Mr. J.M. Shrivastava),

my brother Mr. Kovid Shrivastava

and

my grandmother (Mrs. Triveni Shrivastava)

in helping me achieve my dreams.

My friends

(Mr. Aman Gaur, Mr. Shashank Chourey, Mr. Abhimanyu Manglam,

Miss Mayushi Jain, Miss Rasika Adhikari, Miss Sana Suri and Miss Aastha Maniar)

For always supporting and motivating me.

"In long term, economic sustainability depends on ecological sustainability"

TABLE OF CONTENTS

TABLE OF CONTENTS

LIST OF FIGURES

LIST OF TABLES

ACKNOWLEDGMENTS

I would like to express the deepest appreciation to my committee chair, Professor Ayman S. Mosallam, who has the attitude and the substance of a genius: he continually and convincingly conveyed a spirit of adventure in regard to research and scholarship, and an excitement in regard to teaching. Without his guidance and persistent help this dissertation would not have been possible.

I would like to thank my committee members, Professor Farzin Zareian and Professor Anne Lemnitzer, whose work and concern guided me in the dissertation. Their work in this field has always transcend academia and provides a quest for our times. The idea of this research was inspired by the pioneering work of Professor Khosrow Ghavami of Pontifícia Universidade Católica do Rio de Janeiro, Brazil. The effort of Professor Luciano Feo of the University of Salerno, Italy, for reviewing the technical content of the thesis is acknowledged. The design and fabrication of the bamboo structures were performed by Mr. Lucas Alves Ripper of Pontifícia Universidade Católica do Rio de Janeiro under the supervision of Professor Khosrow Ghavami.

I would also like to thank my fellow graduate researchers, Mr. Jivan Pachpande and Miss Surbhi Dadlani, who steered me in performing the experimental work and whose enthusiasm for the work kept the spirit high. Also, I thank my fellow undergraduate researchers, Mr. Khalid Bafakih and Miss Lusine Mezhlumyan for testing multiple samples of Bamboo strips for verification of material properties as a part of my thesis/dissertation. Financial support was provided by the University of California, Irvine.

ABSTRACT OF THE THESIS

Structural Evaluation of a Bamboo Arch

By

Rahil Shrivastava

Master of Science in Civil Engineering

University of California, Irvine, 2015

Professor Ayman S. Mosallam, Chair

With millions of poor and homeless people in the world and the presence of extensive bamboo resources in many regions, a part of the affordable housing problem can be solved by providing structural design for bamboo houses. In this study, structural evaluation of a bamboo arch was performed. In addition, a numerical finite element model using ANSYS software was developed to simulate the behavior of the bamboo structure. The study included a literature review of relevant published technical papers, books and reports. Experimental tests were conducted on the full-scale bamboo structure to verify the scissor action of joints to transfer load and to study the short-term creep behavior for controlling the deflection limits to satisfy the building standards as per CBC 2013. The finite element model was used to understand the expected behavior of the bamboo arch structure under gravity loading. The finite element model results were used to determine the possible improvement to stiffen the structural joints by using steel cables. This study is just a step towards providing an alternative for feasible housing design using bamboo as a structural material.

CHAPTER 1

INTRODUCTION

1.1 GENERAL

Throughout the history of civilization, engineering structures have been constructed to serve specific purpose of the society. The pyramids in Egypt and the Taj Mahal in India are a representative of many monuments that remind us of the accomplishment of ancient designers. In more recent times, the art of construction has been supplemented by new scientific and sophisticated approach of designing to provide safe and eco-friendly structures. A striking example which embodies both technological breakthrough and aesthetic quality of structure design is 'Bamboo Arch' and is as shown in Figure (1.1).

The elements of the bamboo arch are joined using nylon rope to allow the load transfer by scissor action between the members. Also, the bamboo tubes are spaced in three dimensions, and the structure is analyzed by computer FEM modelling using ANSYS software. The main reason in selecting the bamboo as main structural unit is due to its abundant growth and naturally occurring composite structure.

A typical bamboo consists of a cellulose fibre embedded in a lignin matrix. Cellulose fibers are aligned along the length of the bamboo providing maximum tensile strength, flexural strength and rigidity in direction parallel to that of the bamboo fibres, making it best to take axial force [2]. Every year many people struggle to build a shelter to live comfortably. But, sometimes due to lack of financial support or because of climate rudeness, they are unable

to construct a house. The main purpose of designing bamboo arch was to build temporary housing or emergency shelters.

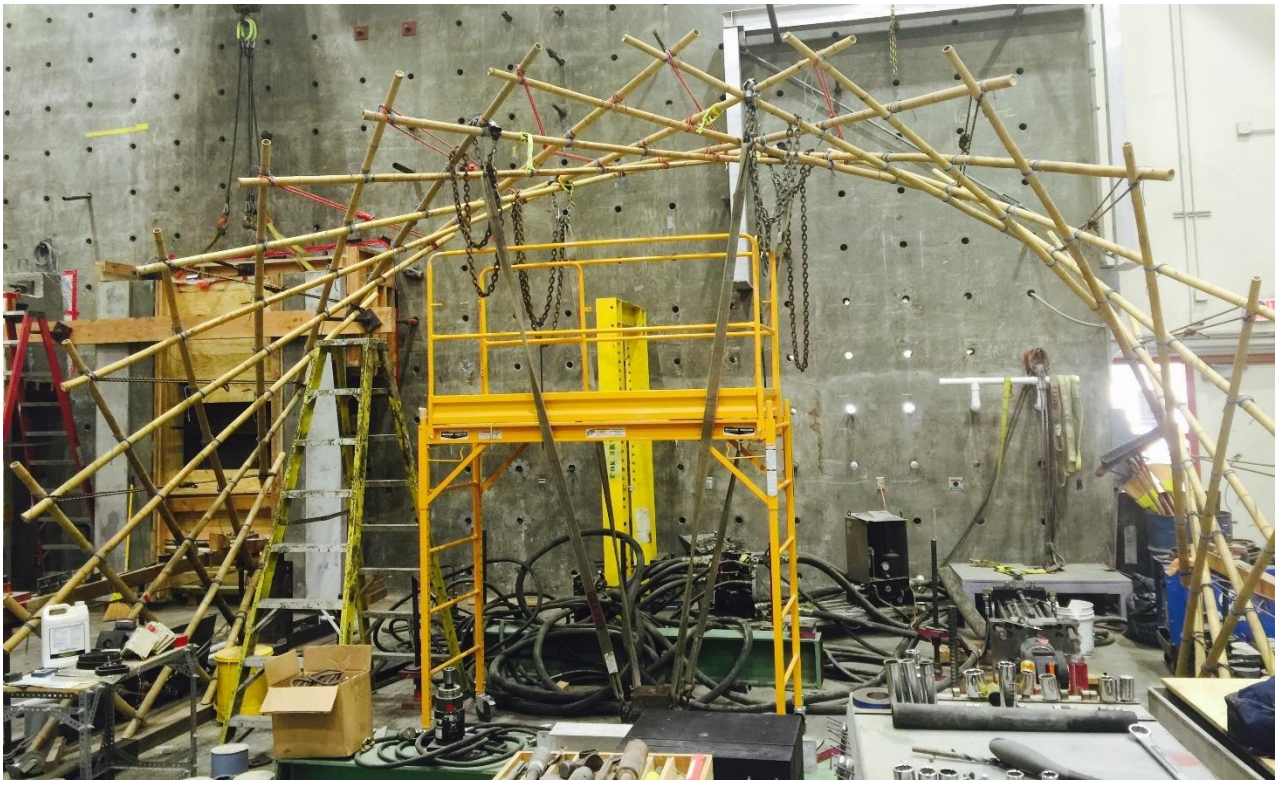

Figure (1.1): The Bamboo Arch

1.2 Benefits of Building with Bamboo: Bamboo houses can have the look of complete tranquility but it's not just aesthetics that has made bamboo so popular. It provides many benefits to the environment:

1. Bamboo is actually a grass and the fastest growing renewable resource Bamboo produces greater biomass and 30% more oxygen than a hardwood forest of the same area.

2. Bamboo absorbs 2/3 more carbon dioxide (CO_2) from the atmosphere than any other plants and in turn releases 2/3 more oxygen, producing super-oxygenated, pure air. Bamboo is flexible and evergreen. It bends but does not break, and
3. Bamboo can replenish itself very quickly and its growth and harvest have virtually no negative effects on the environment. The harvest time takes only 3-5 years versus 10-50 years for wood.

In this study, the structure geometry of a bamboo arch was analyzed experimentally and numerically using ANSYS software. To understand the load path, deformation and stability under constant loading was studied which provides strong foundation to understand the structural behavior. This study helps in improving the design to satisfy the International Building Standards for load and deflection limits. The details of the experiments involved performing, computer modelling, and analysis are explained in further chapters.

CHAPTER 2

LITERATURE REVIEW

2.1GENERAL

This chapter presents a literature review and background on technical information related to this research study. The literature review comprises of two parts: 1) review of bamboo material and 2) finite element analysis techniques review.

2.2 Bamboo as a construction material

Bamboo is one of the oldest building material used for construction purposes [5]. Over 1200 bamboo species have been identified globally [6]. It has been widely used for household products and extended to industrial applications by advancement in technology which has increases the market demand. In Asian countries, bamboo has been used for household utilities such as fishing poles, cricket boxes, handicrafts, chairs, etc. It has been widely used in building applications such as flooring, ceiling, walls, windows, doors, fences, housing roofs, trusses, rafters, purlins and also used in construction as structural materials for bridges, water-transportation facilities and skyscraper scaffoldings.

Bamboo is a hollow tube with thin walls. It is more difficult to join bamboo than pieces of wood. It has no ray or knot and hence stress is evenly distributed throughout the length of bamboo. Bamboo material do not contain chemical extractives unlike wood, and therefore,

can be glued very well [7]. These properties clearly show that bamboo is different from the conventional wood. Also the composite behavior of bamboo makes it much more easy to use for construction purpose [8].

The specific gravity of bamboo varies between 0.40 and 0.80 depending mainly on the anatomical structure. The moisture content of bamboo varies vertically from the bottom to the top portions and horizontally from the outer layer to the inner layers. Bamboo possesses very high moisture content. Green bamboo may have 100 percent moisture (oven-dry weight basis) and can be as high as 155 percent for the innermost layers to 70 percent for the peripheral layers. The vertical variation from the top (82%) to the bottom (110%) is comparatively less. The fiber saturation point of bamboo is around 20-22 percent [9].

Unlike wood, bamboo has no secondary growth and reaches its full height by addition of materials to its cells after the first year. Aging of a bamboo culm influences its physical, chemical, and mechanical properties [10]. In general, the properties of bamboo drop from the top portion to the bottom. The increase in weight is cumulative and directly related with age. Strength properties are reported to decrease in older culms [11]. There is also variation in strength properties along the culm height. Compressive strength tends to increase with height [12, 13, and 14]. The strength increases from the central to the outer part. There is more than 100 percent variation in strength from the inner to the outer layers [15]. In the United States, interest in bamboo has increased since several studies have been done to utilize its potential as an alternative to wood resource [16].

2.3 Dimensions of Elements of Bamboo Samples

Table (2.1): Variation of dimensions in Bamboo Samples used in Constructing the Bamboo Arch Structure

Samples	Outside diameter (D)		Average diameter (d_o)	Inside diameter (d)		Average diameter (d_i)	Thickness (t_o)
	side1	side2		side1	side2		
	inches (meter)						
1	1.5 (0.46)	1.5 (0.46)	1.5 (0.46)	1.2 (0.37)	1.1 (0.34)	1.2 (0.37)	0.3 (0.09)
2	1.6 (0.49)	1.6 (0.49)	1.6 (0.49)	1.2 (0.37)	1.2 (0.37)	1.2 (0.37)	0.4 (0.09)
3	1.5 (0.46)	1.6 (0.49)	1.5 (0.46)	1.2 (0.37)	1.2 (0.37)	1.2 (0.37)	0.3 (0.09)
4	1.4 (0.43)	1.3 (0.40)	1.4 (0.43)	1.1 (0.34)	1.1 (0.34)	1.1 (0.34)	0.3 (0.09)
5	1.4 (0.43)	1.4 (0.43)	1.4 (0.43)	1.1 (0.34)	1.1 (0.34)	1.1 (0.34)	0.3 (0.09)
	Average, D		1.5 (0.46)	Average, d		1.2 (0.37)	

The dimensions of long Bamboo stick (see Figure (2.2)) were recorded using Vernier Caliper and tabulated in Table (2.1) to get the generalized dimension of bamboo which was later used in numerical modeling. Further the properties of bamboo as orthotropic material were taken from past research work of Dr. A.N. Rao, Dr. Jules J. A. Janssen, and used in structural arch analysis.

Figure (2.1): A Foot Long Bamboo Samples

2.4 Properties of Nylon Rope (Joining Elements)

Nylon is a synthetic fiber, also known as polyamide. It is durable and strong with excellent abrasion resistance [19]. The fibers have good resistance towards oil, organic solvent, formaldehyde, alcohols and biological decompositions such as rot [19]. There are many different types of nylon ropes available in the market. The one which is used to tie the bamboo stick together were tested under axial loading to find out the stiffness of the rope. The nylon rope was attached to the ceiling and uniformly loaded by adding 4 lbs (17.8 N) of metal plates in the bucket attached to the rope (see Figure (2.2)).

Figure (2.2): Nylon Rope Axial Test Setup

The initial length of the rope was 37.5" (0.95 m) measured from celling to the connection at the bucket. It's then uniformly loaded and increase in length was recorded which was later used to calculate stiffness of the rope (see Figure (2.3)).

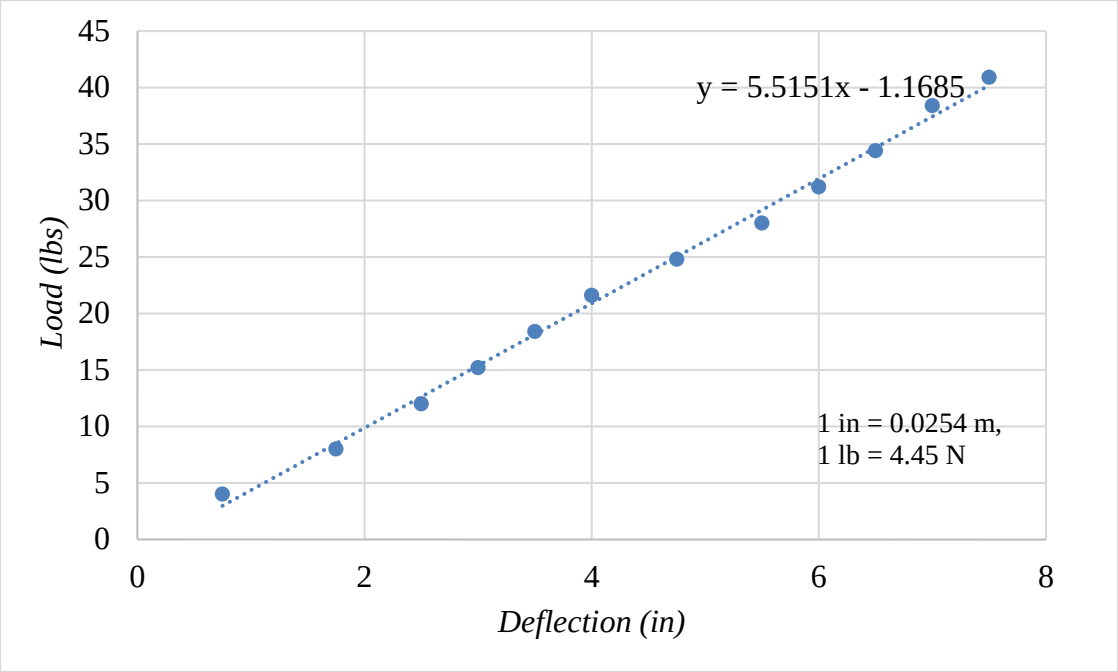

Figure (2.3): Load-Deflection Curve of Nylon rope

The slope of the load deflection curve is called stiffness ('K') of the nylon rope which is 5.5 lb/in (965.84 N/m). Therefore, modulus of elasticity using equation (2) is 1872.55 psi (12.9 MPa),

$$K = \frac{EA}{L} \tag{2.1}$$

where:

K: Axial Stiffness,

E: Modulus of Elasticity,

L: Original Length of Member.

This stiffness plays an important role when nylon ropes are connected transversely (see Figure (3.4)). It limits the deflection of the structure by acting as a spring (see Figure (2.4)) (discussed in following chapters).

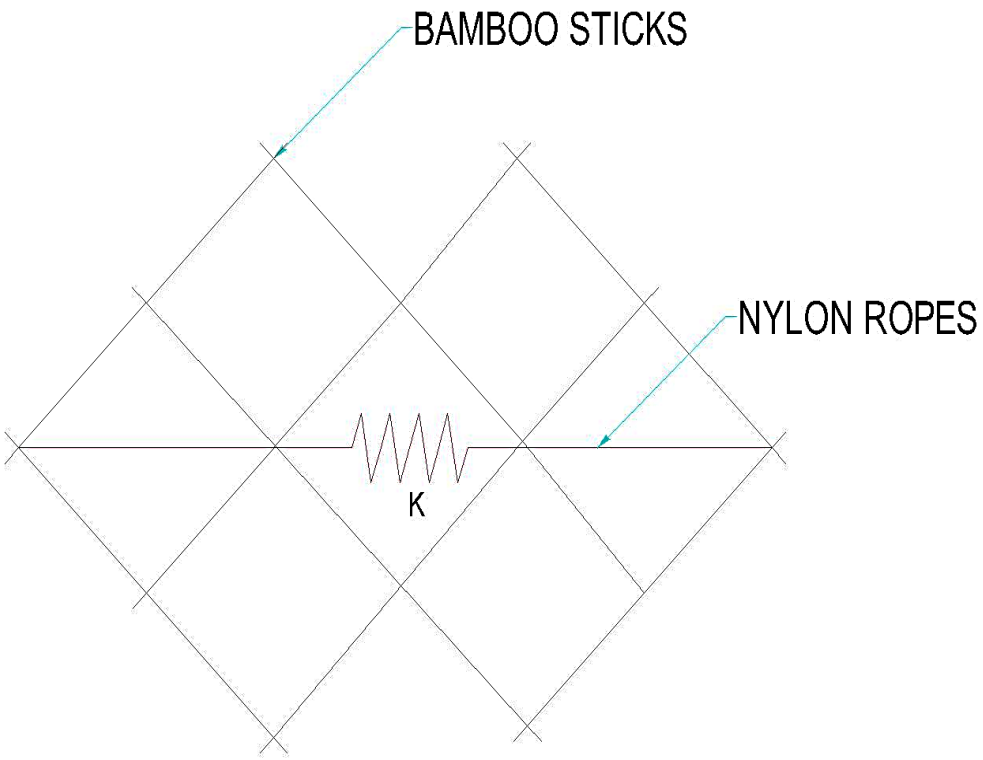

Figure (2.4): Spring Action of Nylon Rope Connection

2.5 FINITE ELEMENT NUMERICAL TECHNIQUES

The finite element analytical techniques were first conducted at the University of California, Berkeley during the period 1957 to 1970. The initial approach was a direct extension of classical methods of structural analysis which was used for one-dimensional elements only. The majority of the research conducted was to fulfill the needs to solve practical problems in aerospace, mechanical and civil engineering [4].

In the finite element analysis, displacement compatibility between adjacent elements and force equilibrium on an integral basis at a finite number of node points within the structure

are satisfied. It is apparent that for any mesh, the fundamental equilibrium equations have to be satisfied to find exact elasticity solution. This discrete element idealization is a different approach to find solution for continuum mechanics problems; hence, Clough coined the terminology finite element method [4]. The basic approach of structural analysis includes the following steps:

1. Recognize the actual problem.
2. Formulate the idealized problem.
3. Solve the idealized problem, and.
4. Interpret the solution of the idealized problem and draw the conclusion of the problem.

The first and last steps depend on the problem statement and an effort is made regularly to emphasize the important factors involved. But, the basic considerations in the formulation of problem may be outlined as mentioned below:

1. Analyze the forces and load path.
2. Study the deformations and the requirements of geometrical compatibility.
3. Establish the force-deformation relations from the properties of materials.

These steps were followed to analyze structural geometry which was precisely completed by ANSYS Software. The basic principles of finite element method are simple. The first step is to divide the domain into elements, and this process is called discretization. The elements distribution is called a mesh. The elements are connected at points called nodes. After the region is discretized, the governing equations for each element must be established for the

required physics. Material properties such as modulus of elasticity, thermal conductivity should be available. The element equations are assembled to obtain the global equation for the mesh which describes the behavior of the body as a whole. Generally, the global equation has the following form [2]:

$$[K]\{A\} = \{F\} \qquad (2.2)$$

where:

[K]: stiffness matrix,

{A}: nodal degree of freedom representing displacements vector in x-, y- and z- direction respectively, and

{F}: nodal external force vector.

This was the basic principle used in ANSYS software to analyze any structure.

CHAPTER 3

STRUCTURAL GEOMETRY AND SUPPORT SYSTEM OF BAMBOO ARCH STRUCTURE

In this chapter, the structural geometry and support system are described. The bamboo arch was constructed by Mr. Lucas Ripper of the Pontifícia Universidade Católica do Rio de Janeiro, Brazil. In building the arch structure, the bamboo sticks were joined together using nylon ropes forming multiple 2' x 2' (609.6mm X 609.6mm) rhombuses as shown in Figure (3.1).

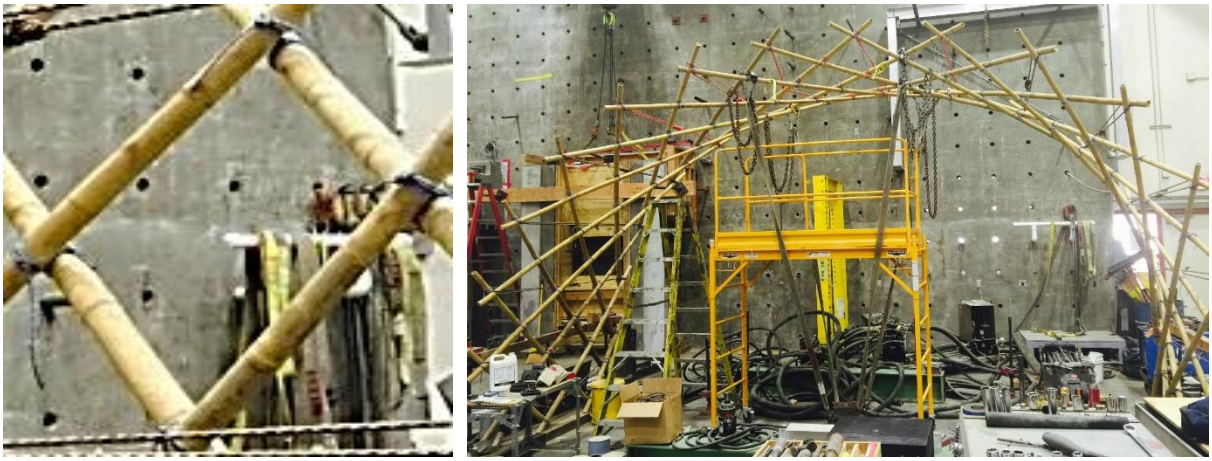

Figure (3.1): Rhombus formed by Joining Bamboo Sticks

The purpose of this prototype was to verify the scissor action behavior of the structural joints to transfer load and to find the possible improvement methods to create a safer design. The structure was purposefully constructed symmetrical for better understanding of the behavior and design criteria. Also, the numerical model in finite element codes was created

in ANSYS® software to test the deflections of structure in vertical direction and compared with allowable deflection as per CBC 2013 (see Table (6.1)).

The support was fixed at both ends (see Figure (3.2)) for the full scale bamboo arch. This type of fixity simulated the condition of temporary structures anchored in the ground.

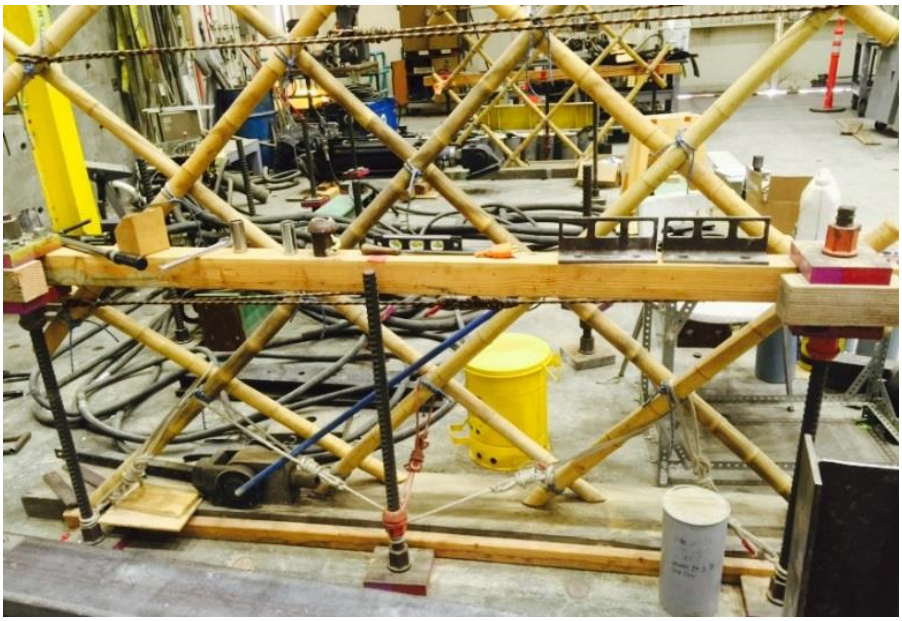

Figure (3.2): Support Condition for the Bamboo Structure

High-strength prestressing Dwydag® steel rods and nylon rope were used to fasten the base of the structure. The two bamboo sticks were connected together by clove hitch knot/general utility hitch (see Figure (3.3)). This simple joining method is easier to tie this type of knot around the bamboo sticks and also the joint formed by this arrangement is much stiffer to create the condition of moving together under loading especially for a structure subjected to very light loads. It can also be tightened by pulling one end and provides resilience and redundancy to the structure.

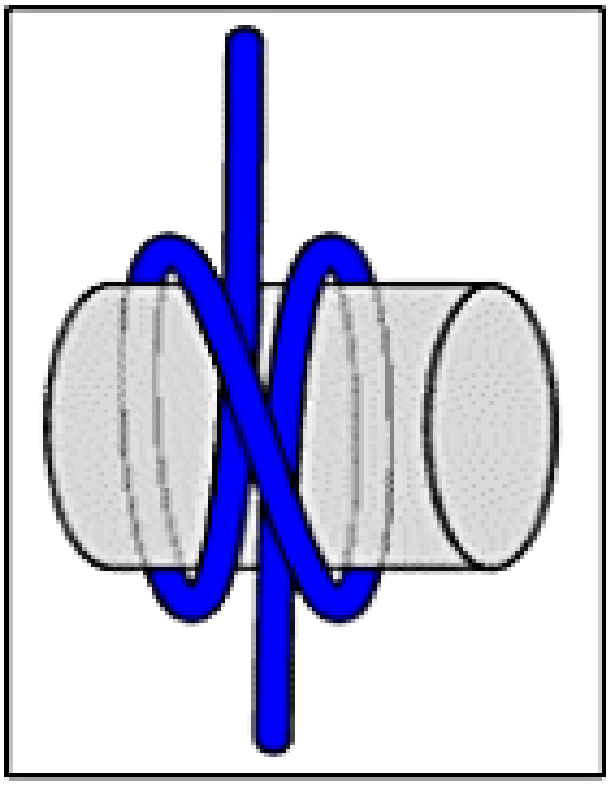

Figure (3.3): Clove Hitch Knot

The purpose of using clove knot is to create a joint which will allow rotation in all the directions and transfer loads in members but at the same time it should resist the relative movement of top and bottom bamboo sticks at a joint. In the numerical model, this type of joint was simulated with a nodes joint by nylon link which connects the bamboo sticks. Furthermore, in order to limit deflection of the structure in traverse direction (z-direction), the nylon ropes were attached to the extreme ends of three rhombuses in a row as shown in Figures (3.4) and (3.5). In Figure (3.4), the gray lines represent bamboo sticks which were joined together and joints are shown in green, blue and red colored circles. The transverse direction nylon ropes were represented in red color lines (see Figure (3.6)).

Nylon ropes in the transverse direction acts as a spring which resists z-deflection. To replicate this condition in finite element modeling the nylon ropes were modelled as link member and connected to the bamboo elements. The numerical model is shown in Figures (3.6) and (3.7).

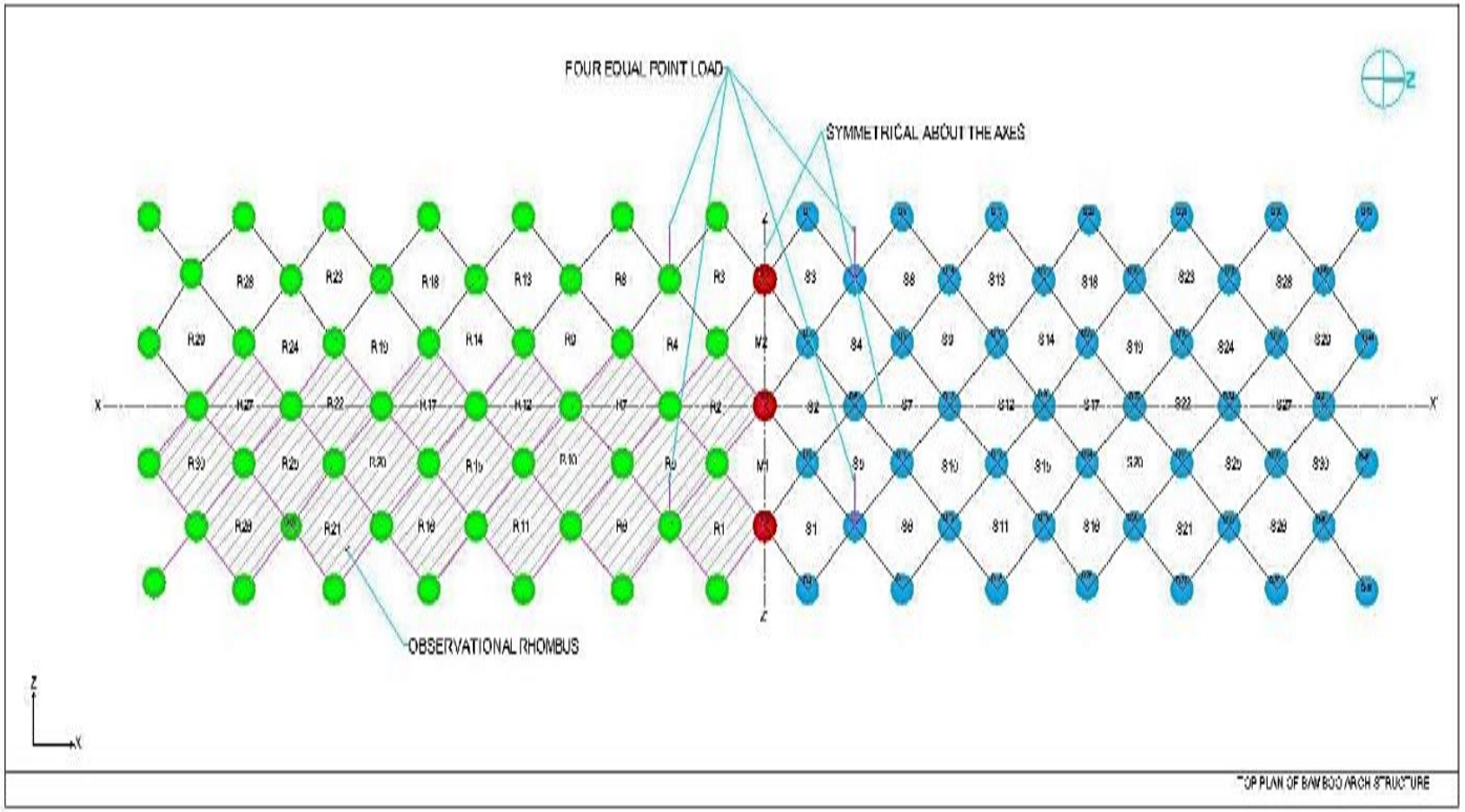

Figure (3.4): Top View CAD Sketch of the Structure

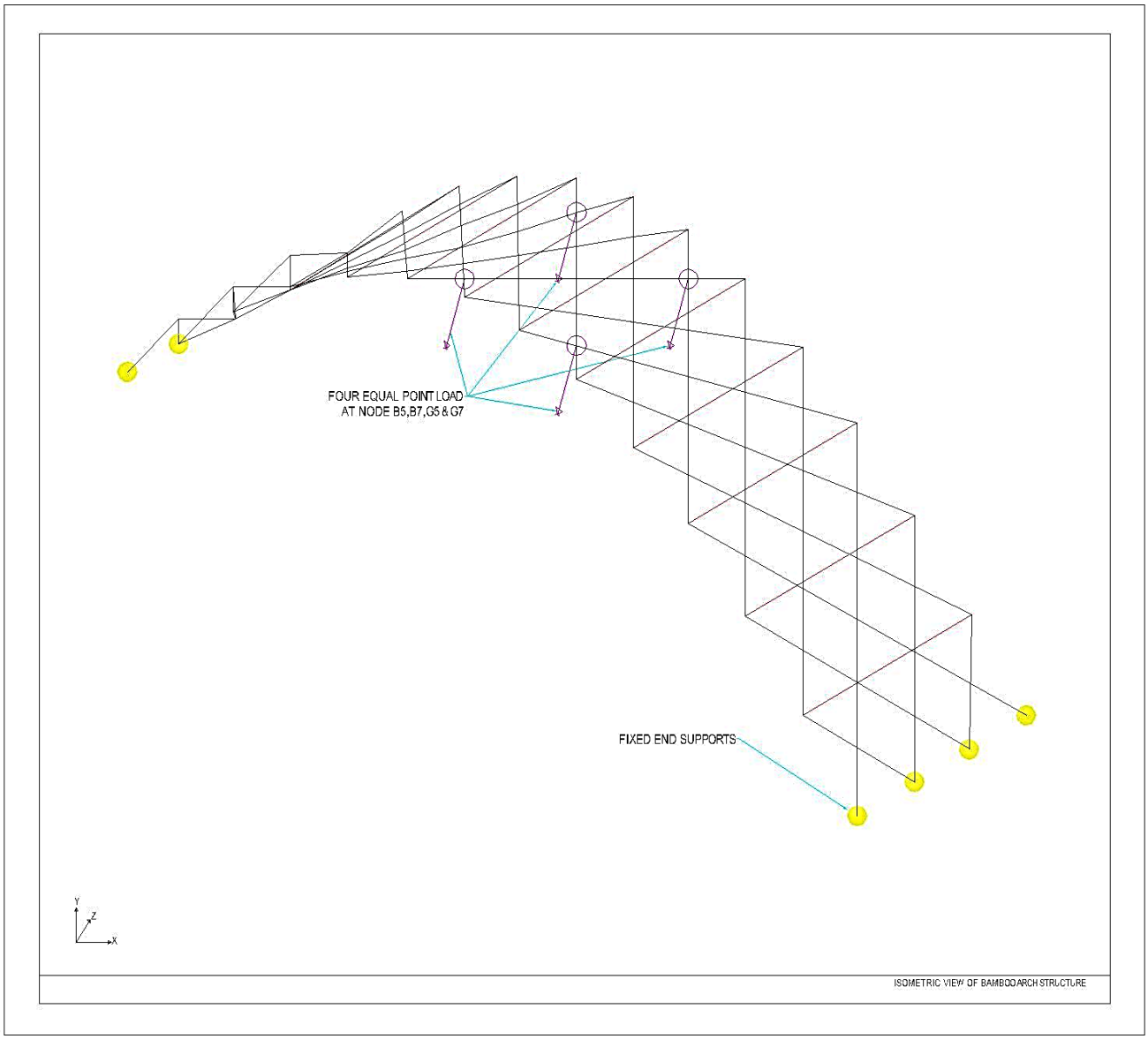

Figure (3.5): Isometric View of CAD Sketch of the Structure

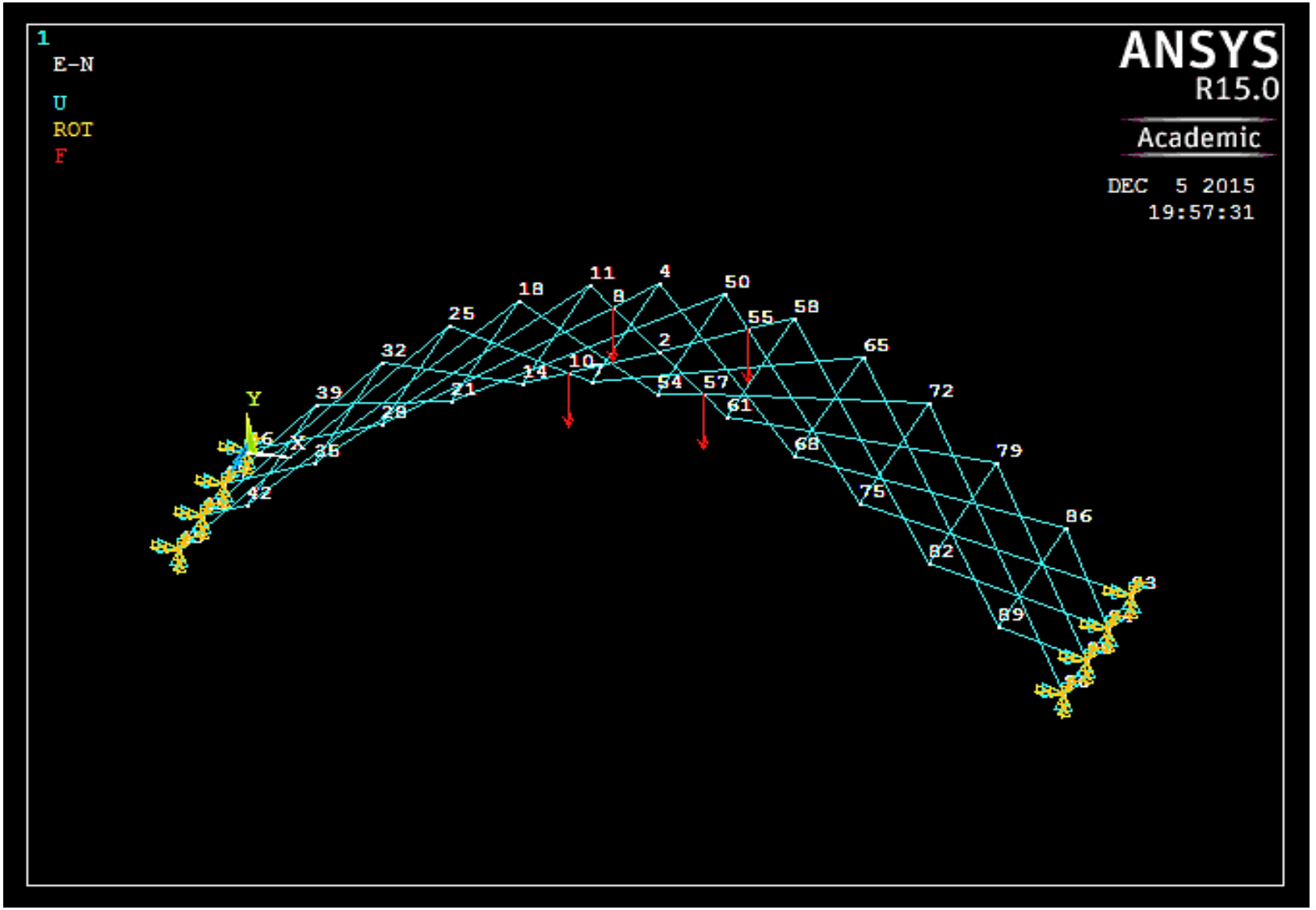

Figure (3.6): Finite element numerical model of the structure

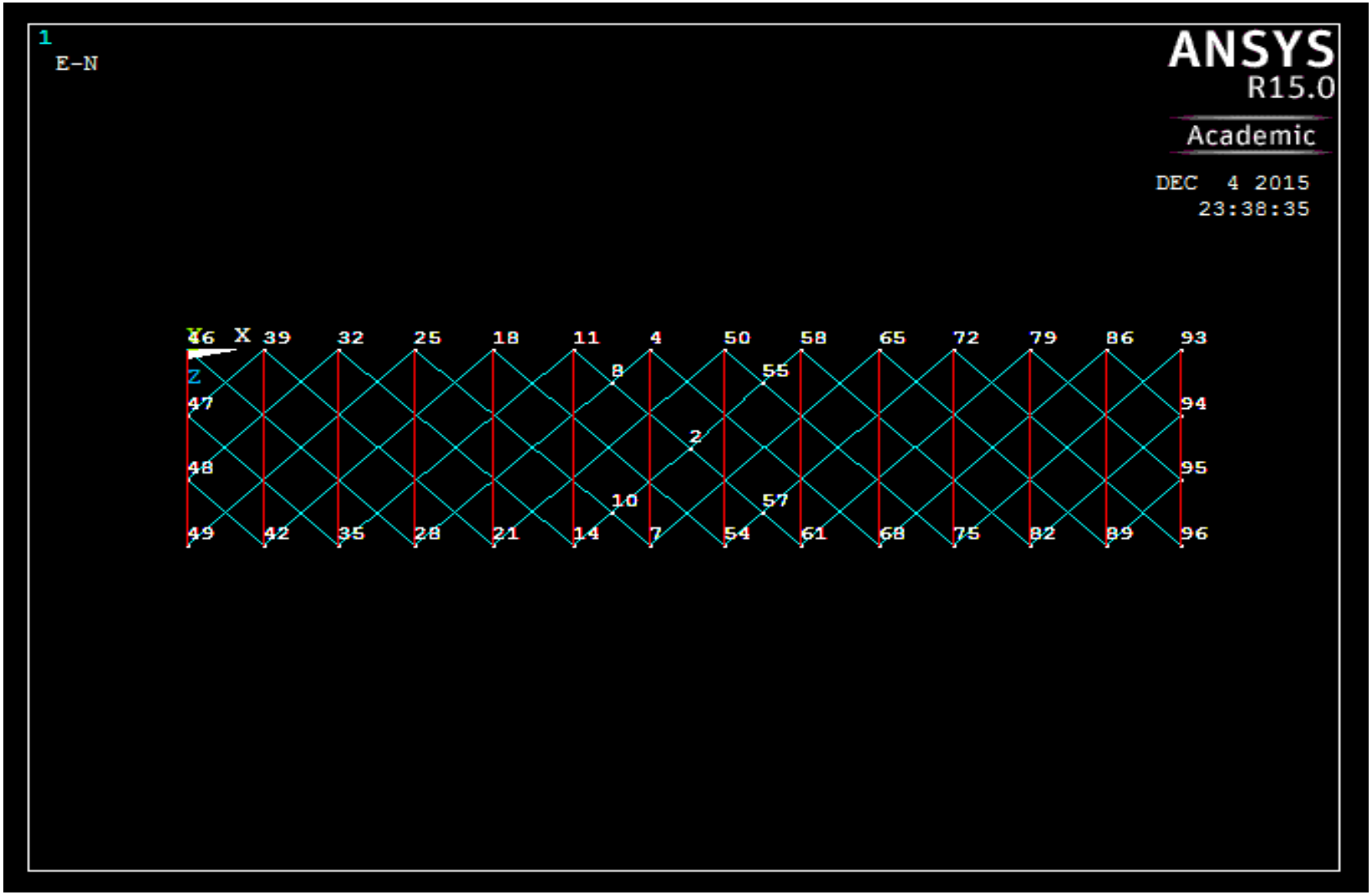

Figure (3.7): Finite element numerical model of the structure (Top View)

CHAPTER 4

EXPERIMENTAL EVALUATION OF BAMBOO ARCH STRUCTURE

4.1 GENERAL

This chapter describes the details and the results of non-destructive experimental tests that were performed on the bamboo arch.

4.2 EXPERIMENTAL EVALUATION OF BAMBOO ARCH

4.2.1 Loading Pattern and Joining Details of Bamboo Arch

The bamboo arch was subjected under four-point loads such that the resultant effect will be at the centroid of the structure as shown in Figure (4.1). In the CAD drawing (see Figure (4.1)) only the position of the applied loads are shown.

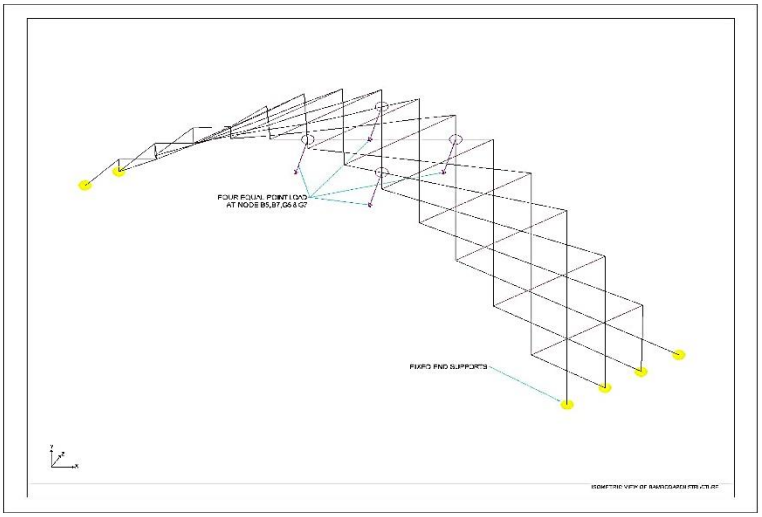

Figure (4.1): CAD Sketch of the Bamboo Arch Structure

The loads were applied progressively with a constant step of 10.0 lbs (44.80kN) up to maximum of 90.0 lbs (403.2kN). In order to avoid errors in collecting experimental measurements, each joint was assigned a distinct number and each rhombus was assigned a different designation number. After assigning each node identification number, the coordinates were recorded by assuming X-axis in longitudinal, Y-axis in elevation and Z-axis in transverse direction. The Table (4.1) presents the assigned numbers to the nodes and coordinates.

Table (4.1): Coordinates of Nodes of Bamboo

Nodes	X		Y		Z	
	U.S. Units	S.I. Units	U.S. Units	S.I. Units	U.S. Units	S.I. Units
	(foot)	(meter)	(foot)	(meter)	(foot)	(meter)
X1	14.3	4.4	9.0	2.7	3.1	0.9
X2	14.3	4.4	8.7	2.7	3.3	1.0
X3	14.3	4.4	9.0	2.7	3.4	1.0
1	13.2	4.0	9.2	2.8	2.0	0.6
2	13.2	4.0	8.7	2.7	2.2	0.7
3	13.2	4.0	8.7	2.7	2.3	0.7
4	13.2	4.0	9.2	2.8	2.5	0.8
5	12.1	3.7	8.7	2.7	1.1	0.3
6	12.1	3.7	8.4	2.6	1.3	0.4
7	12.1	3.7	8.7	2.7	1.4	0.4
8	11.0	3.4	8.7	2.7	0.0	0.0
9	11.0	3.4	8.1	2.5	0.2	0.1
10	11.0	3.4	8.1	2.5	0.3	0.1
11	11.0	3.4	8.7	2.7	0.5	0.2
12	9.8	3.0	7.8	2.4	9.1	2.8
13	9.8	3.0	7.5	2.3	9.3	2.8
14	9.8	3.0	7.8	2.4	9.4	2.9
15	8.7	2.7	7.6	2.3	8.0	2.4

16	8.7	2.7	7.1	2.2	8.2	2.5
17	8.7	2.7	7.1	2.2	8.3	2.5
18	8.7	2.7	7.6	2.3	8.5	2.6
19	7.6	2.3	6.7	2.0	7.1	2.2
20	7.6	2.3	6.3	1.9	7.3	2.2
21	7.6	2.3	6.7	2.0	7.4	2.3
22	6.5	2.0	6.2	1.9	6.0	1.8
23	6.5	2.0	5.7	1.7	6.2	1.9
24	6.5	2.0	5.7	1.7	6.3	1.9
25	6.5	2.0	6.2	1.9	6.5	2.0
26	5.4	1.6	5.0	1.5	5.1	1.6
27	5.4	1.6	4.8	1.5	5.3	1.6
28	5.4	1.6	5.0	1.5	5.4	1.6
29	4.3	1.3	4.3	1.3	4.0	1.2
30	4.3	1.3	3.9	1.2	4.2	1.3
31	4.3	1.3	3.9	1.2	4.3	1.3
32	4.3	1.3	4.3	1.3	4.5	1.4
33	3.3	1.0	3.0	0.9	3.1	0.9
34	3.3	1.0	2.9	0.9	3.3	1.0
35	3.3	1.0	3.0	0.9	3.4	1.0
36	2.2	0.7	2.2	0.7	2.0	0.6
37	2.2	0.7	1.9	0.6	2.2	0.7
38	2.2	0.7	1.9	0.6	2.3	0.7
39	2.2	0.7	2.2	0.7	2.5	0.8
40	1.1	0.3	1.9	0.6	1.1	0.3
41	1.1	0.3	1.9	0.6	1.3	0.4
42	1.1	0.3	1.9	0.6	1.4	0.4
43	0.0	0.0	0.0	0.0	0.0	0.0
44	2.2	0.7	0.0	0.0	2.2	0.7
45	4.3	1.3	0.0	0.0	4.3	1.3
46	6.5	2.0	0.0	0.0	6.5	2.0
1	15.3	4.7	9.2	2.8	4.0	1.2
2	15.3	4.7	8.7	2.7	4.2	1.3
3	15.3	4.7	8.7	2.7	4.3	1.3
4	15.3	4.7	9.2	2.8	4.5	1.4
5	16.4	5.0	8.7	2.7	5.1	1.6
6	16.4	5.0	8.4	2.6	5.3	1.6
7	16.4	5.0	8.7	2.7	5.4	1.6
8	17.5	5.3	8.7	2.7	6.0	1.8

9	17.5	5.3	8.1	2.5	6.2	1.9
10	17.5	5.3	8.1	2.5	6.3	1.9
11	17.5	5.3	8.7	2.7	6.5	2.0
12	18.6	5.7	7.8	2.4	7.1	2.2
13	18.6	5.7	7.5	2.3	7.3	2.2
14	18.6	5.7	7.8	2.4	7.4	2.3
15	19.7	6.0	7.6	2.3	8.0	2.4
16	19.7	6.0	7.1	2.2	8.2	2.5
17	19.7	6.0	7.1	2.2	8.3	2.5
18	19.7	6.0	7.6	2.3	8.5	2.6
19	20.8	6.3	6.7	2.0	9.1	2.8
20	20.8	6.3	6.3	1.9	9.3	2.8
21	20.8	6.3	6.7	2.0	9.4	2.9
22	21.8	6.6	6.2	1.9	10.0	3.0
23	21.8	6.6	5.7	1.7	10.2	3.1
24	21.8	6.6	5.7	1.7	10.3	3.1
25	21.8	6.6	6.2	1.9	10.5	3.2
26	22.9	7.0	5.0	1.5	11.1	3.4
27	22.9	7.0	4.8	1.5	11.3	3.4
28	22.9	7.0	5.0	1.5	11.4	3.5
29	24.0	7.3	4.3	1.3	0.0	0.0
30	24.0	7.3	3.9	1.2	0.2	0.1
31	24.0	7.3	3.9	1.2	0.3	0.1
32	24.0	7.3	4.3	1.3	0.5	0.2
33	25.1	7.7	3.0	0.9	1.1	0.3
34	25.1	7.7	2.9	0.9	1.3	0.4
35	25.1	7.7	3.0	0.9	1.4	0.4
36	26.2	8.0	2.2	0.7	2.0	0.6
37	26.2	8.0	1.9	0.6	2.2	0.7
38	26.2	8.0	1.9	0.6	2.3	0.7
39	26.2	8.0	2.2	0.7	2.5	0.8
40	27.3	8.3	1.9	0.6	3.1	0.9
41	27.3	8.3	1.9	0.6	3.3	1.0
42	27.3	8.3	1.9	0.6	3.4	1.0
43	28.3	8.6	0.0	0.0	4.0	1.2
44	28.3	8.6	0.0	0.0	2.2	0.7
45	28.3	8.6	0.0	0.0	4.3	1.3
46	28.3	8.6	0.0	0.0	6.5	2.0

The different colors in this table were adopted to represent the location of the nodes in the structure. For example, the brown color; represents the base of the structure on both sides, the red color represents the central nodes, while the blue and green colors represent the two symmetrical sides of the structure (refer to Figure (4.2)).

x-axis	**Coordinates of Bamboo Structure Nodes in x, y-axis**					**W**	**N**	**E**
							S	
	G43		G44		G45		G46	
	28-4,0		28-4,2-2		28-4,4-4		28-4,6-6	
		G40		G41		G42		
		27-3,1-1		27-3,3-3		27-3,5-5		
	G36		G37		G38		G39	
	26-2,0		26-2,2-2		26-2,4-4		26-2,6-6	
		G33		G34		G35		
		25-1,1-1		25-1,3-3		25-1,5-5		
	G29		G30		G31		G32	
	24,0		24,2-2		24,4-4		24,6-6	
		G26		G27		G28		
		22-11,1-1		22-11,3-3		22-11,5-5		
	G22		G23		G24		G25	
	21-10,0		21-10,2-2		21-10,4-4		21-10,6-6	
		G19		G20		G21		
		20-9,1-1		20-9,3-3		20-9,5-5		
	G15		G16		G17		G18	
	19-8,0		19-8,2-2		19-8,4-4		19-8,6-6	
		G12		G13		G14		
		18-7,1-1		18-7,3-3		18-7,5-5		
	G8		G9		G10		G11	
	17-6,0		17-6,2-2		17-6,4-4		17-6,6-6	
		G5		G6		G7		
		16-5,1-1		16-5,3-3		16-5,5-5		
	G1		G2		G3		G4	
	15-4,0		15-4,2-2		15-4,4-4		15-4,6-6	

	X1		X2		X3		
	14-3,1-1		14-3,3-3		14-3,5-5		
B1		B2		B3		B4	
13-2,0		13-2,2-2		13-2,4-4		13-2,6-6	
	B5		B6		B7		
	12-1,1-1		12-1,3-3		12-1,5-5		
B8		B9		B10		B11	
11,0		11,2-2		11,4-4		11,6-6	
	B12		B13		B14		
	9-9,1-1		9-9,3-3		9-9,5-5		
B15		B16		B17		B18	
8-8,0		8-8,2-2		8-8,4-4		8-8,6-6	
	B19		B20		B21		
	7-7,1-1		7-7,3-3		7-7,5-5		
B22		B23		B24		B25	
6-6,0		6-6,2-2		6-6,4-4		6-6,6-6	
	B26		B27		B28		
	5-5,1-1		5-5,3-3		5-5,5-5		
B29		B30		31		B32	
4-4,0		4-4,2-2		4-4,4-4		4-4,6-6	
	B33		B34		B35		
	3-3,1-1		3-3,3-3		3-3,5-5		
B36		B37		B38		B39	
2-2,0		2-2,2-2		2-2,4-4		2-2,6-6	
	B40		B41		B42		
	1-1,1-1		1-1,3-3		1-1,5-5		
B43		B44		B45		B46	
0,0		0,2-2		0,4-4		0,6-6	
y-axis							

Figure (4.2): X, Y Axis Coordinates of the Bamboo Arch Structure

For the experimental analysis, existence of symmetry was used and changes in only quarter part of the arch structure (see Figure (3.4)) were recorded. Further the loads were applied by steel plates connected by high strength strap and chains to transfer the loads perpendicular to the structure at the joints as shown in Figures (4.3) and (4.4).

Table (4.2): Identity Number of Rhombus of Structure

Rhombus ID	Rhombus	Symmetrical Rhombus About X1X2X3	
M1	X1B2X2G2		
M2	X2B3X3G3		
R1	X1G1G7G2	S1	X1B1B7B2
R2	X2G2G6G3	S2	X2B2B6B3
R3	X3G3G5G4	S3	X3B3B5B4
R4	G2G7G9G6	S4	B2B7B9B6
R5	G3G6G10G5	S5	B3B6B10B5
R6	G7G8G14G9	S6	B7B8B14B9
R7	G6G9G13G10	S7	B6B9B13B10
R8	G5G10G12G11	S8	B5B10B12B11
R9	G9G14G16G13	S9	B9B14B16B13
R10	G10G13G17G12	S10	B10B13B17B12
R11	G14G15G21G16	S11	B14B15B21B16
R12	G13G16G20G17	S12	B13B16B20B17
R13	G12G17G19G18	S13	B12B17B19B18
R14	G16G21G23G20	S14	B16B21B23B20
R15	G17G20G24G19	S15	B17B20B24B19
R16	G21G22G28G23	S16	B21B22B28B23
R17	G20G23G27G24	S17	B20B23B27B24
R18	G19G24G26G25	S18	B19B24B26B25
R19	G23G28G30G27	S19	B23B28B30B27
R20	G24G27G31G26	S20	B24B27B31B26
R21	G28G29G35G30	S21	B28B29B35B30
R22	G27G30G34G31	S22	B27B30B34B31
R23	G26G31G33G32	S23	B26B31B33B32
R24	G30G35G37G34	S24	B30B35B37B34
R25	G31G34G38G33	S25	B31B34B38B33
R26	G35G36G42G37	S26	B35B36B42B37
R27	G34G37G41G38	S27	B34B37B41B38
R28	G33G38G40G39	S28	B33B38B40B39
R29	G37G42G44G41	S29	B37B42B44B41
R30	G38G41G45G40	S30	B38B41B45B40

Figure (4.3): Plate Connection to the High Strength Strap

Figure (4.4): Nodes to Chain Connection

4.2.2 Bamboo Arch Test Description

As stated earlier, the bamboo arch was tested by progressive loading of 44.5 N (10.0lbs). The aim of the experiment was to find out the behavior of joints and load path in the structure. The apparatus used in experimental procedure was explained earlier.

The short-term creep tests were performed on the bamboo arch structure. Prior to conducting the test #2, simple loading tests were performed to improve the design of both the support system and the joining details in test #2. Test #2 was verified performing finite element modeling to confirm the proposed improvements to the final non-destructive tests. Table (4.3), is a list of the observational nodes and rhombus which were analyzed at the time of experiment.

Table (4.3): Observational Nodes and Rhombus in the Structure

Rhombus I.D.	Rhombus	Rhombus Nodes
1	R1	X1G1G7G2
2	R2	X2G2G6G3
3	R5	G2G7G9G6
4	R6	G7G8G14G10
5	R7	G6G9G13G10
6	R10	G9G14G16G13
7	R11	G14G15G21G16
8	R12	G13G16G27G17
9	R15	G16G21G23G27
10	R16	G21G22G28G23
11	R17	G27G23G27G24
12	R20	G23G28G30G27
13	R21	G28G29G35G30
14	R22	G27G30G34G31
15	R25	G30G35G37G34
16	R26	G35G36G42G37
17	R27	G34G37G41G38
18	R30	G37G42G44G41

Using measuring tapes, the change in distance and angles were recorded for the observational rhombuses. In a rhombus, 'α' and 'β' are the angles measurements parallel to z-, x- axes respectively (see Figure (4.5)). The change in both direction angles for each rhombus is graphically represented. Initially, the rhombus angles, 'α' and 'β' were 90° respectively.

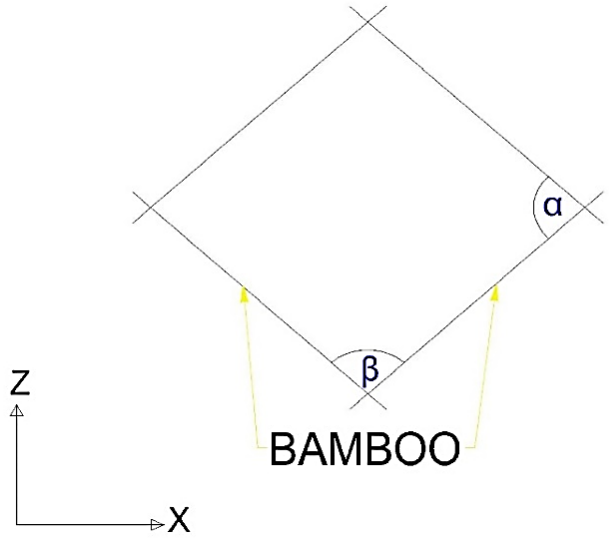

Figure (4.5): Angle Notation in a Rhombus

4.2.3 Test #1: Joints with Nylon Ropes Only

Case #1: Loading of Structure (Uniform Loading with Load Step of 4.5 kg (10.0lbs) to maximum load of 40.8 kg (90.0lbs)): The change in angles were recorded which shows that alternate expansion and contraction happens due to loads in the system. Increasing the value of 'α' and decreasing the value of 'β' verifies scissor action behavior of bamboo at that joint. The angle change of quarter side of bamboo structure verifies the scissor action at the

joints. Consider the observational rhombus R1, R2 and R5 which are shown in Figure (4.6), the change in angles were recorded and results are shown in Figures (4.7), (4.8) and (4.9).

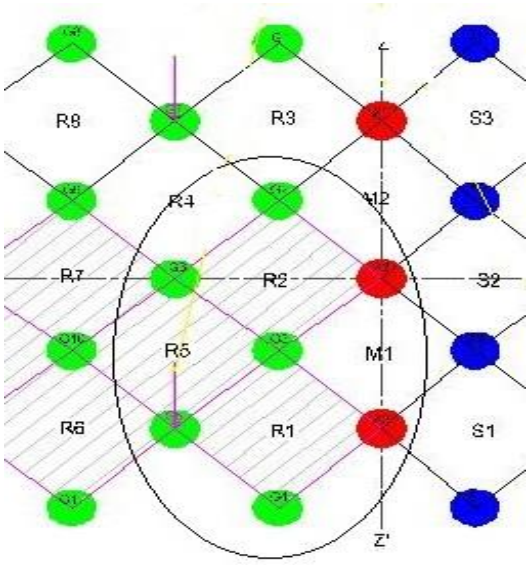

Figure (4.6): Observational Area in the Structure

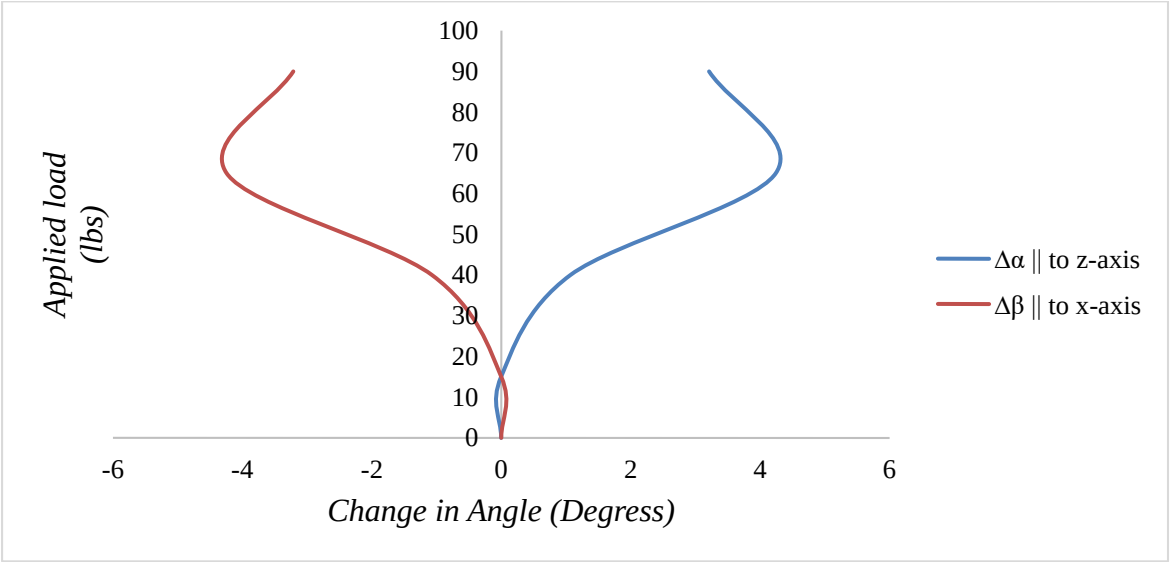

Figure (4.7): Records of Change in Angle in Rhombus 'R1' while Loading

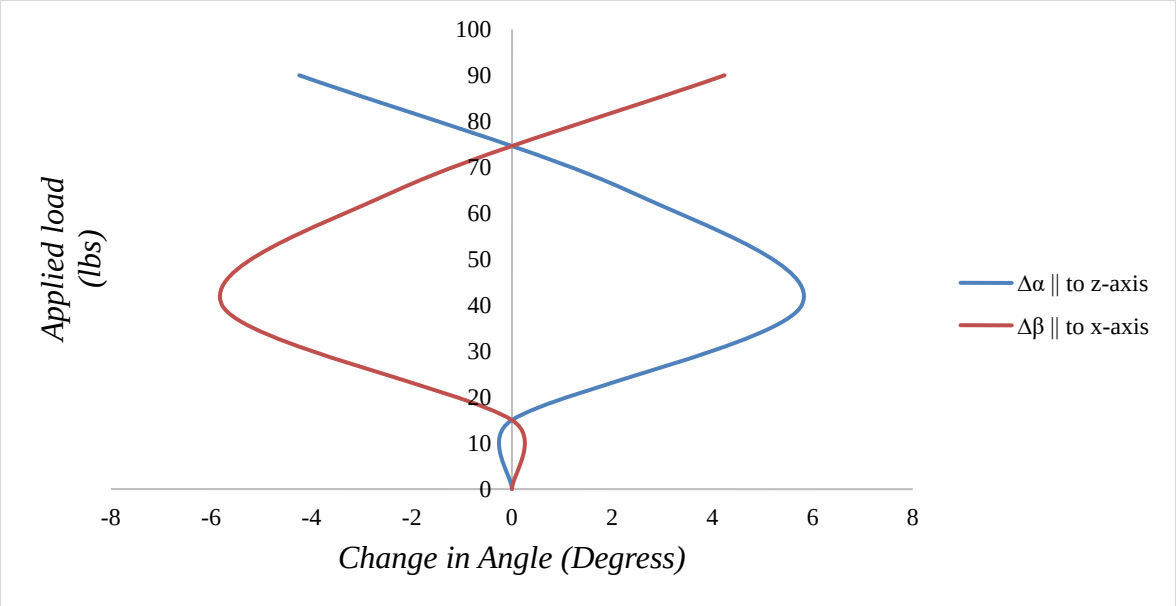

Figure (4.8): Records of Change in Angle in Rhombus 'R2' while Loading

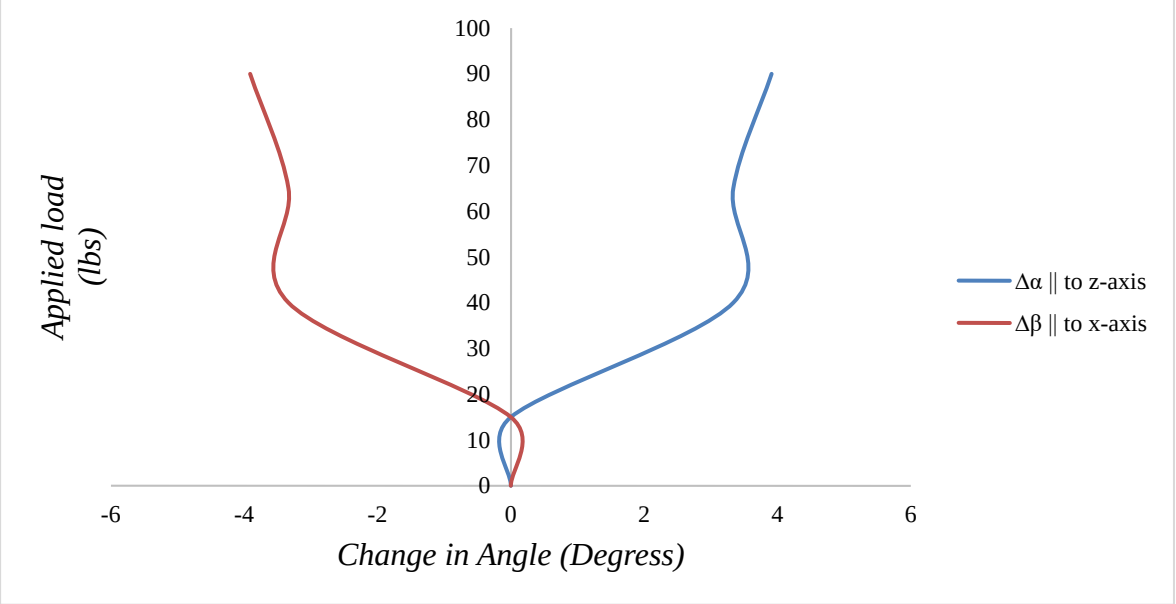

Figure (4.9): Records of Change in Angle in Rhombus 'R5' while Loading

The records of change in angle with the increase in loads (Figures (4.7) through (4.9)), indicate that rhombus R1, R2 expands in z direction while rhombus R5 closes in z direction.

It was also verified for all the observational rhombuses (see Figure (3.4)) by recording angular change which is described in Appendix A.

In order to understand the structural deflection pattern, vertical deflections at quarter, half and third-quarter of span were measured at each increment of load (refer to Figure (4.10)). As mentioned earlier, the tests performed in this study are non-destructive in nature and for this reason loads were applied in smaller range of magnitudes. The main purpose of these tests is to evaluate the structure stiffness and to bring the design under acceptable range of deflection as per CBC 2013 building codes. The measured central deflection at a load level of 40.8 N (90.0lbs) was 152.0 mm (6.0”).

Bamboo is considered a viscoelastic material, and hence it is sensitive to sustained loading. In order to evaluate the time-dependent behavior of such structures, creep and recovery tests are essential. In order to assess the bamboo arch creep behavior, a load of 66.72N (15.0lbs) was initially applied and was gradually increased to 400.34 N (90.0lbs) which were applied for a period of twelve hours. During the loading period, deflection was recorded at every 10.0 lbs (4.5 kg) increment of load. This time-dependent deflection is termed as short term creep as shown in Figure (4.11).

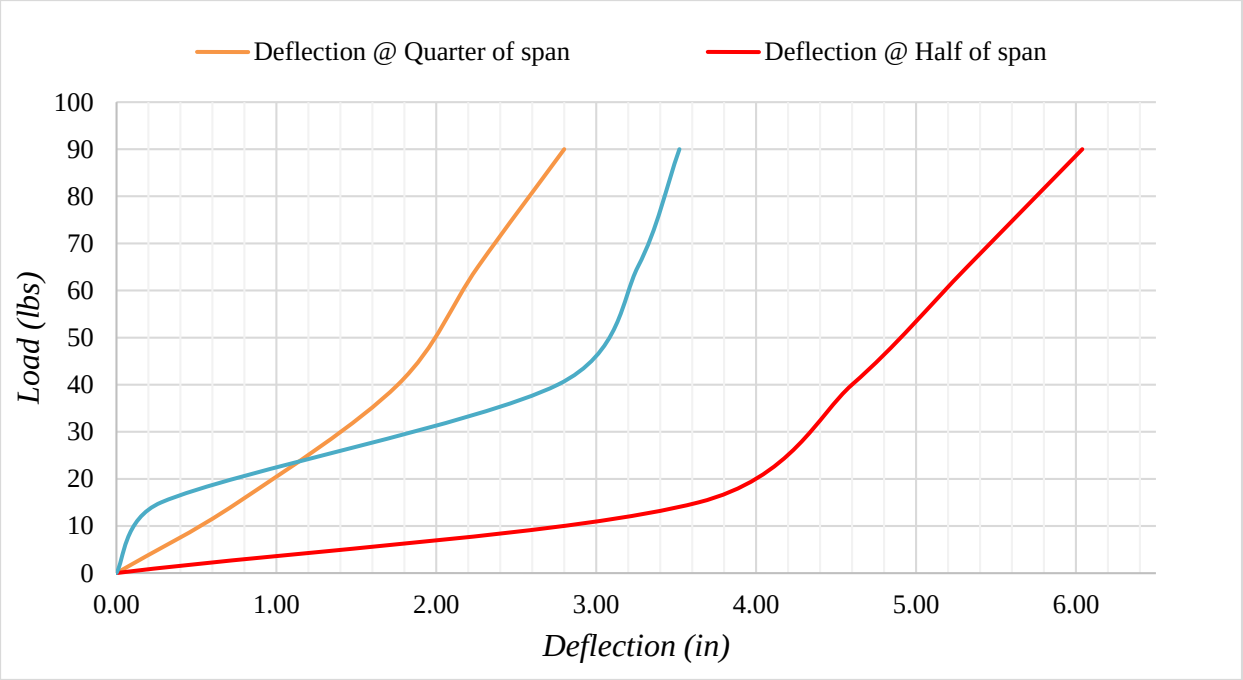

Figure (4.10): Vertical Deflection as per Load Application

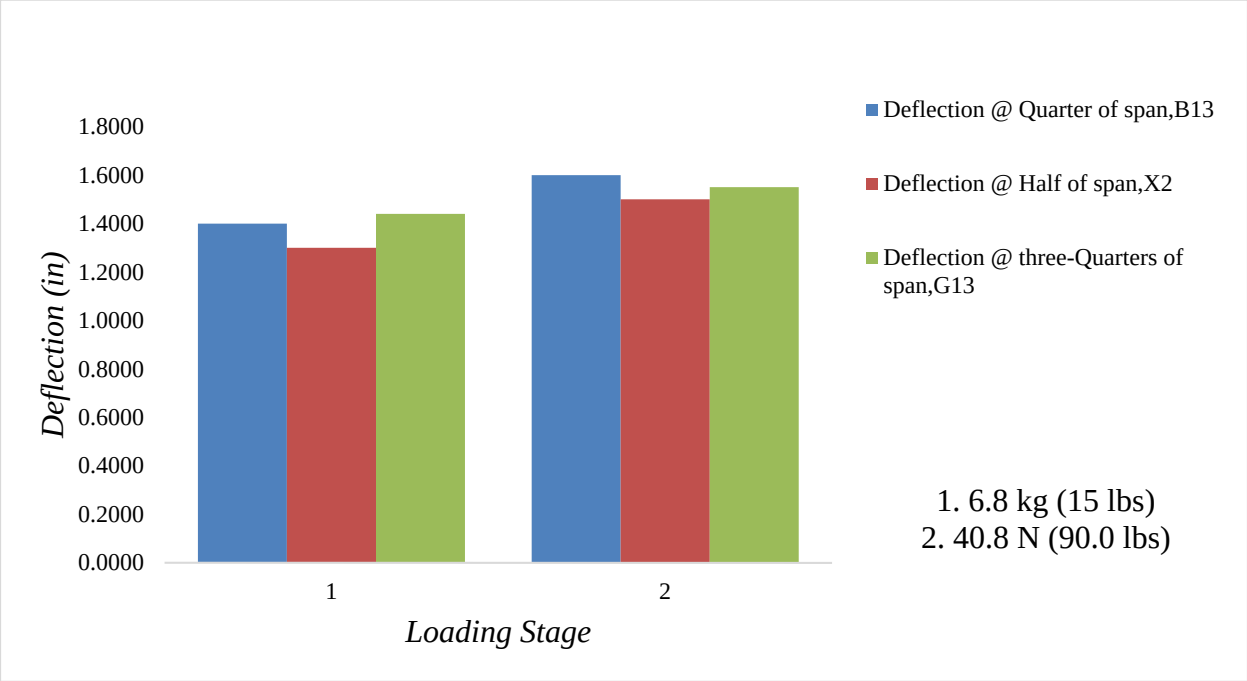

Figure (4.11): Short-Term Creep as per Load Application

Case #2: Uniform Unloading with Load Step of 4.5 kg (10.0lbs) to maximum load of 40.8kg (90.0lbs)): Unloading was performed by removing the loads at the unloading rate of 4.50 kg (10.0lbs) and angular change of each rhombus along with deflection was recorded. The time-dependent angular readings were shown in Figure (4.12), (4.13) and (4.14).

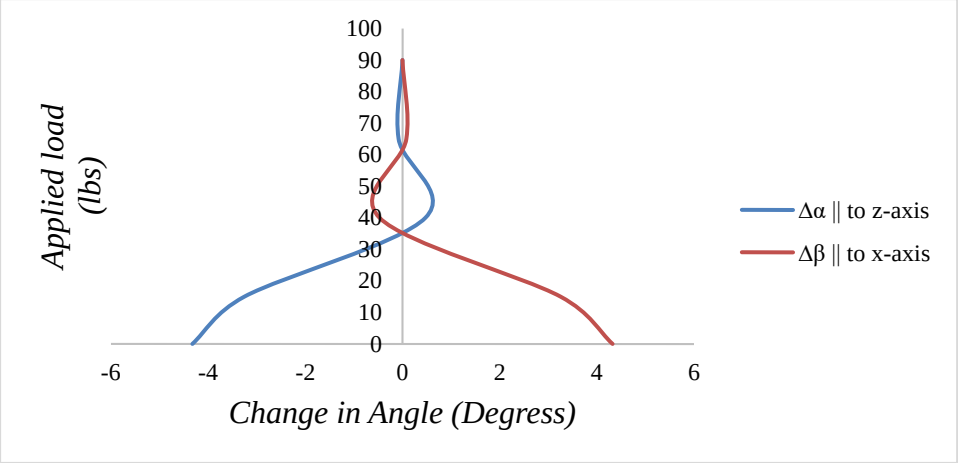

Figure (4.12): Records of Change in Angle in Rhombus 'R1' while Unloading

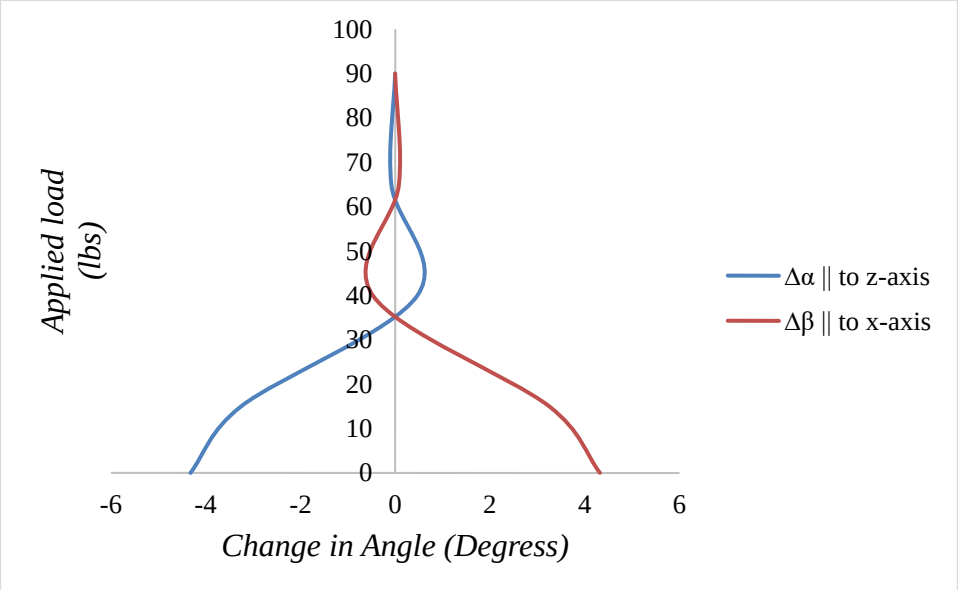

Figure (4.13): Records of Change in Angle in Rhombus 'R2' while Unloading

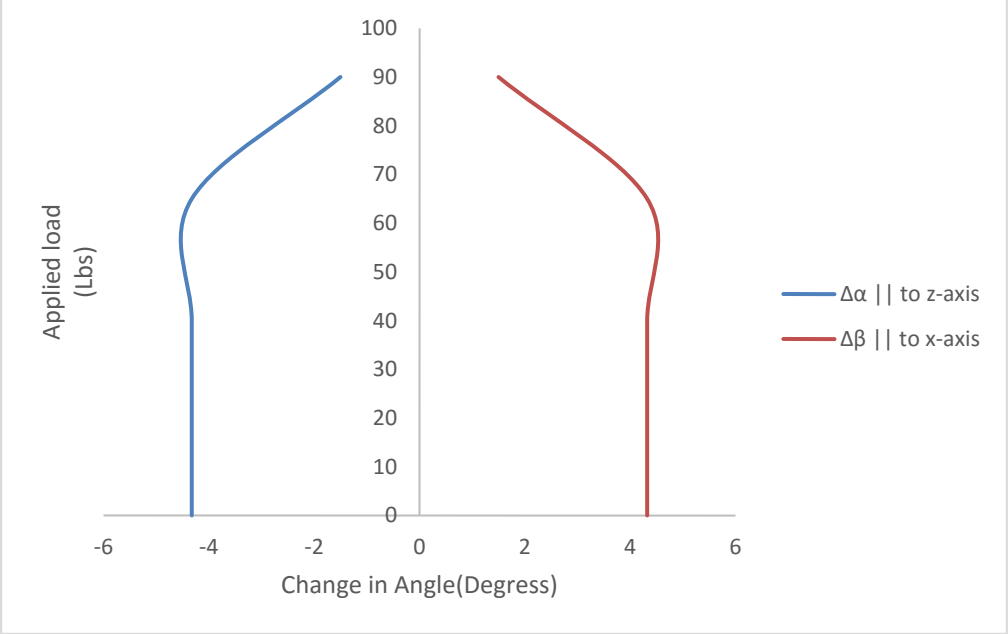

Figure (4.14): Records of Change in Angle in Rhombus 'R5' while Unloading

The scissor action of structural joints was shown in unloading also. The vertical deflections (see Figure (4.15)) were also recorded by following same procedure as in loading. The permanent settlement was found at the end of unloading of structure which is due to inelastic extension happened in nylon ropes attached at the joints. As it is shown in Figure (4.15), the unloading was also uniform with a rate of 4.5 kg/record (10.0lbs/record). On removal of complete 40.8 kg (90.0lbs) of loads, it was found that only 6.4 cm (2.5") of re-bounce to original position occurred. It was observed that creep deformation of 8.9 cm (3.5") occurred.

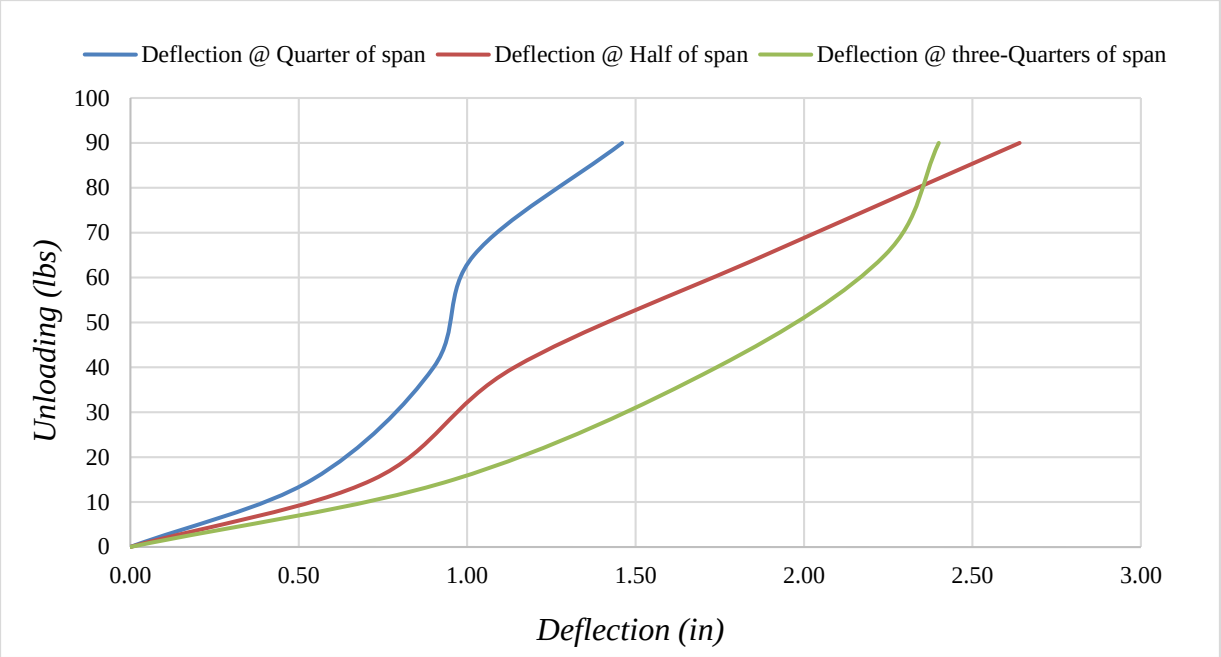

Figure (4.15): Vertical Re-bounce as per Release of Load Application

4.2.4 Test #2: When Joints Were Tied by Nylon Ropes and Cable Ties

Based on the experimental results, the structure was permanently settled at about 6.6 cm (2.6") which was caused due to nylon stretching. This problem can be solved by providing stiffness to the joints which makes them work together. Therefore, the stiffness was provided using 35.6 cm (14") commercial electric cable ties of loop tensile strength of 33.6 kg (74.0lbs). This cable ties were operational at temperature range of -25˚C to 85˚C (-13˚F to 185 ˚F). The cable ties were looped around the two crossing bamboo to form a stiff joint (see Figure (4.16) and (4.17)).

Figure (4.16): Cable Ties Looped Around the Joint

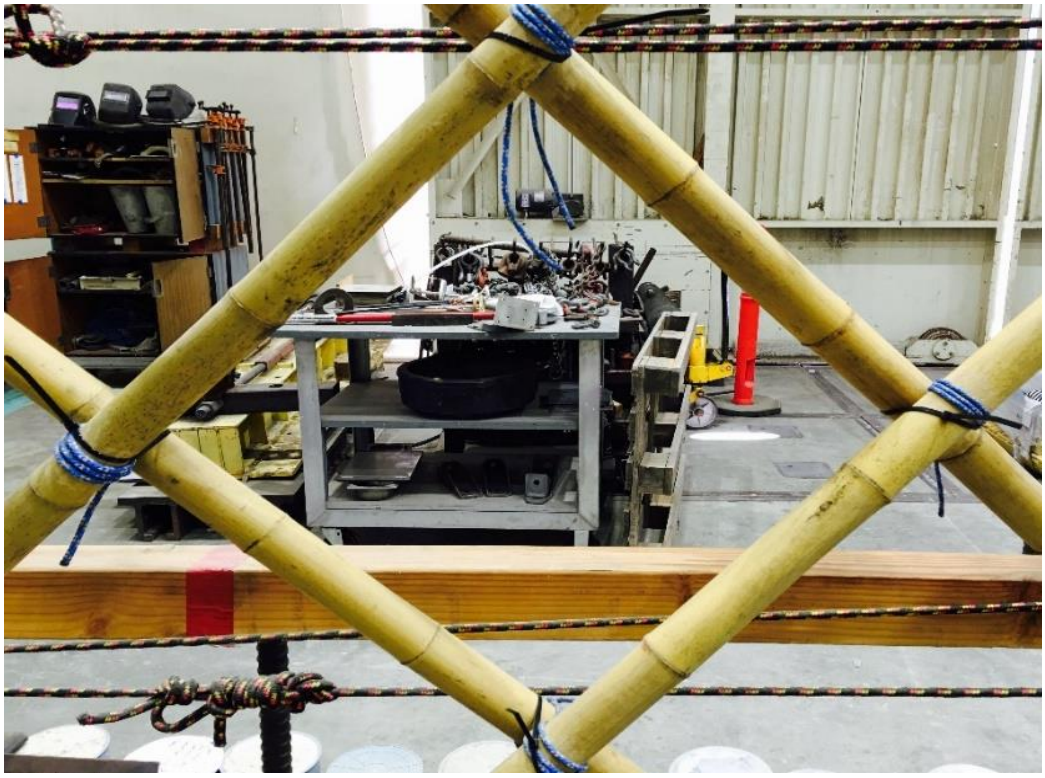

Figure (4.17): Bamboo Rhombus with Cable Ties Attached

Case #1: Loading of Structure (Uniform Loading with Load Step of 4.5 kg (10.0lbs) to maximum load of 40.8 kg (90.0lbs)): By following the same procedure of test #1, angular changes of observational rhombuses and vertical deflection of the structure at every

increment of load were recorded. For rhombuses R1, R2, R5 and other observational rhombuses, recorded data was presented in Figures (4.18), (4.19), (4.20) and Appendix B respectively. The records of test #2 verify that pair of three rhombuses and pair of two rhombuses in transverse direction (z-direction) of the structure have opened and closed respectively which verifies the scissor action of joints. In order to check the effect of cable ties, vertical deflection was recorded (see Figure (4.21)).

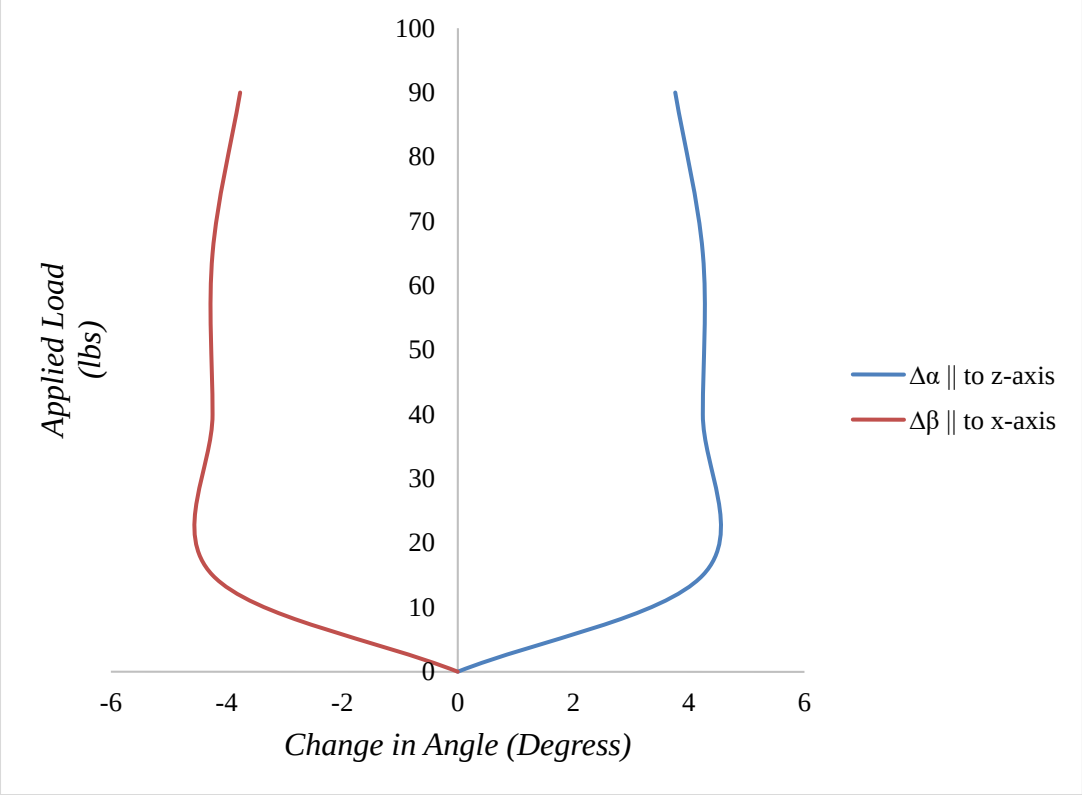

Figure (4.18): Records of Change in Angle in Rhombus 'R1' while Loading

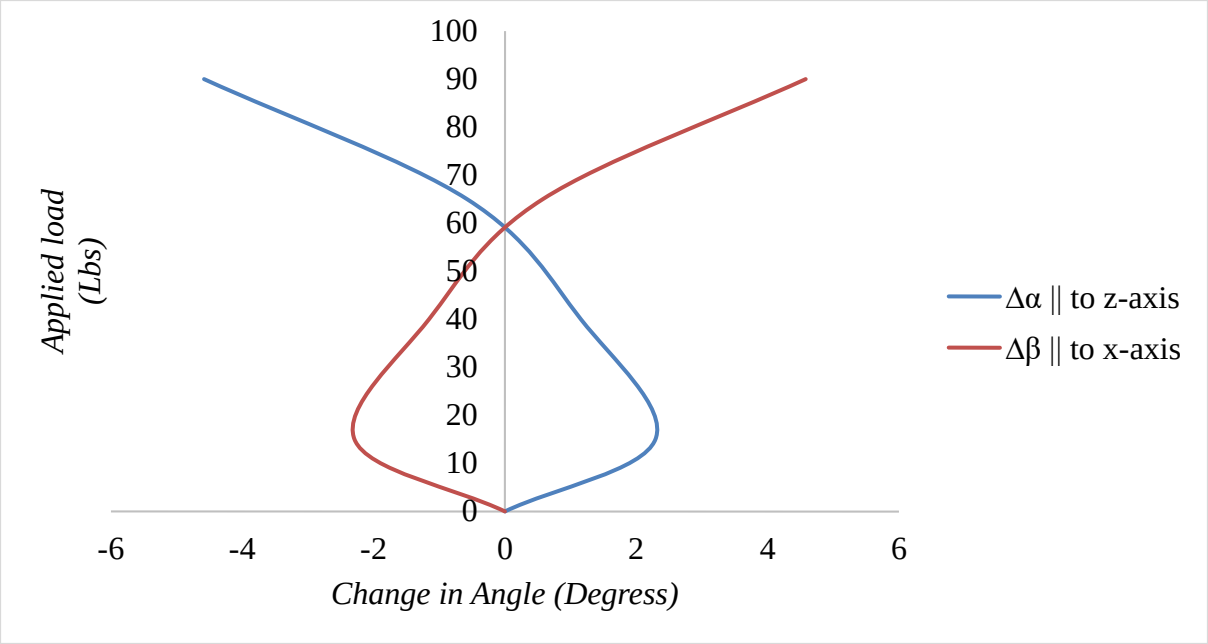

Figure (4.19): Records of Change in Angle in Rhombus 'R2' while Loading

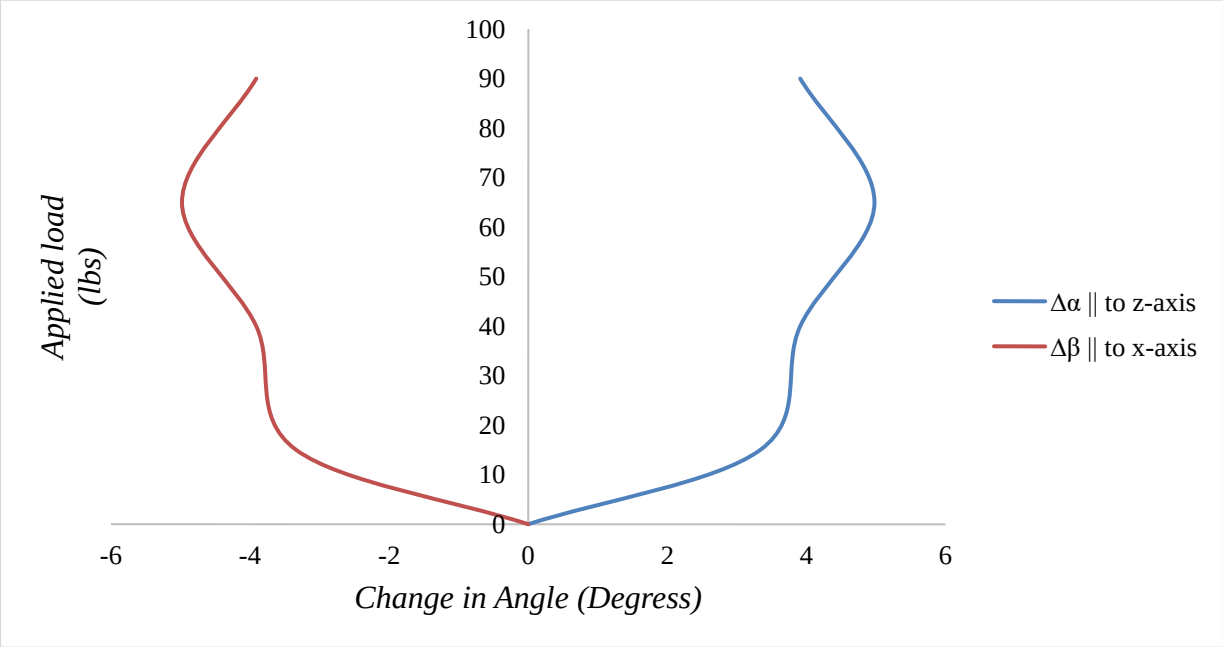

Figure (4.20): Records of Change in Angle in Rhombus 'R5' while Loading

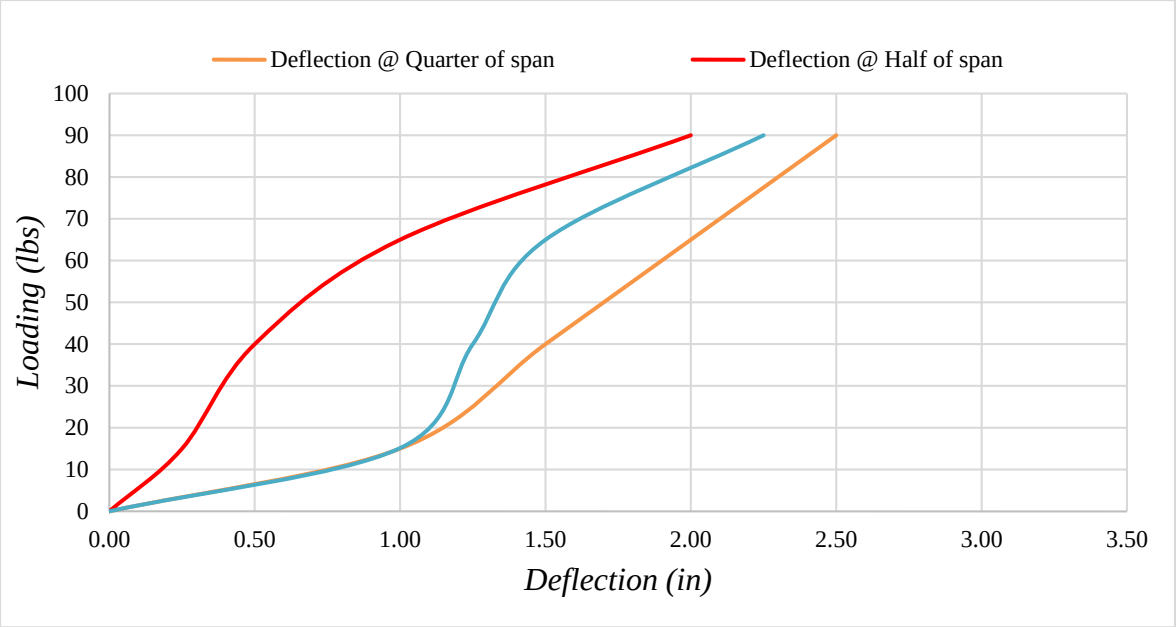

Figure (4.21): Vertical Deflection Records while Loading

Figure (4.21) shows that by adding cable ties, the stiffness of joints was increased and vertical deflection of central node got reduced from 15.2 cm (6") to 6.4 cm (2.5"). The same behavior of joints was observed for nodes at quarter and three-quarter of span. Also, the short- term creep was recorded (see Figure (4.22)).

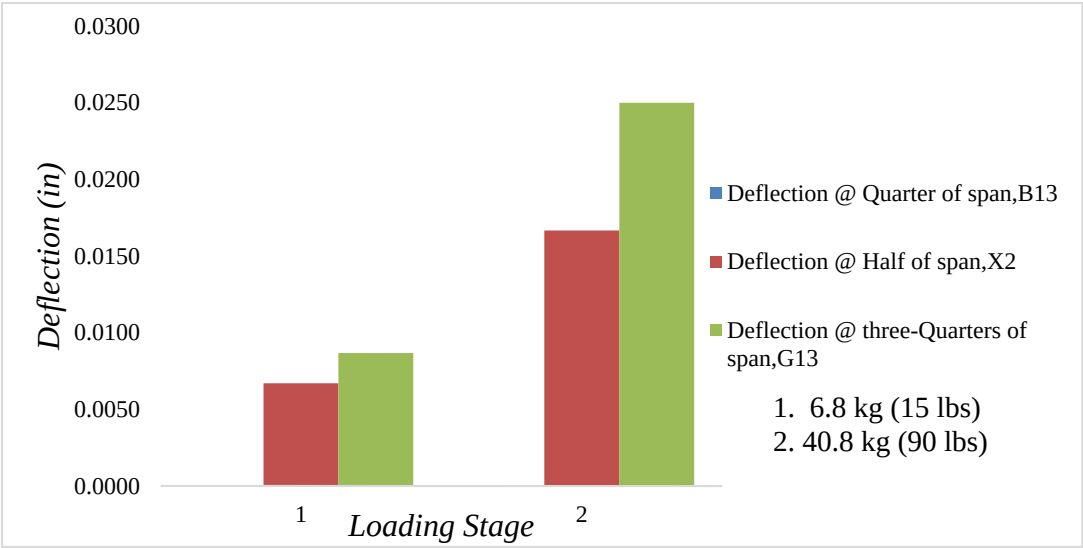

Figure (4.22): Short-Term Creep as per Load Application

With the increase in joint stiffness, the vertical deflection was decreased. it was observed that vertical central node deflection was decreased by almost 60% in test#2. To check any permanent settlement, the unloading was performed following the same procedure as test #1.

Case 2: Unloading of structure (Uniform Unloading Load Step of 4.5 kg (10.0lbs) to maximum load of 40.8 kg (90.0lbs)): Unloading was performed by following the same procedure as previously in test #1, angular changes and vertical restoring deflection was recorded. The results were shown in Figures (4.23), (4.24) and (4.25) for rhombuses R1, R2, R5 and other observational rhombuses recorded data is presented in Appendix C.

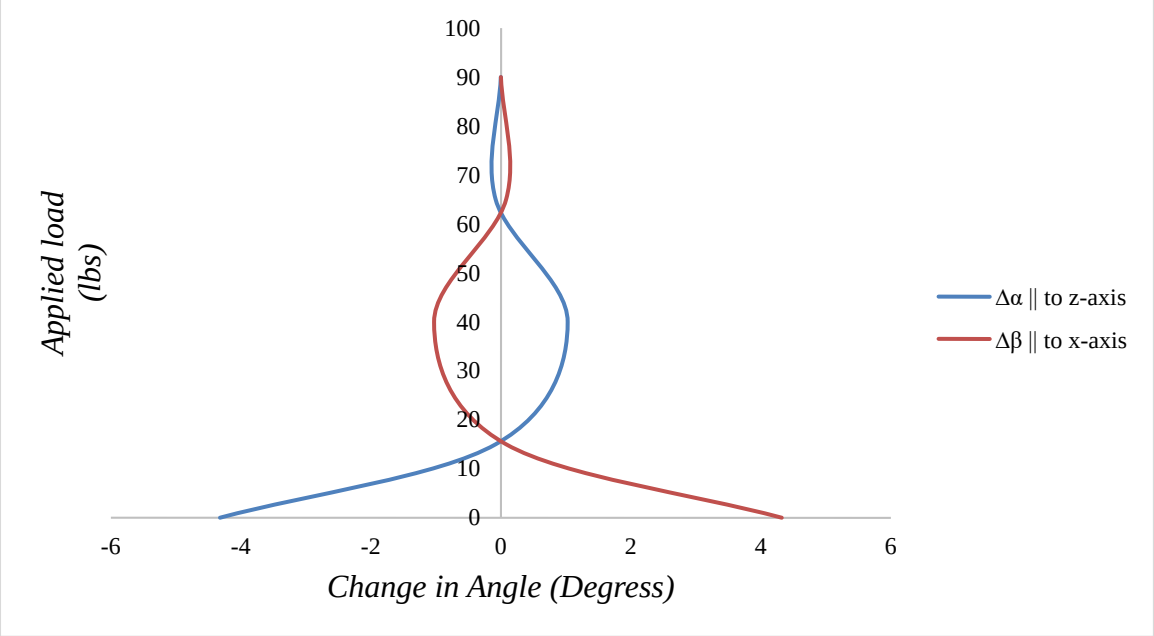

Figure (4.23): Records of Change in Angle in Rhombus 'R1' while Unloading

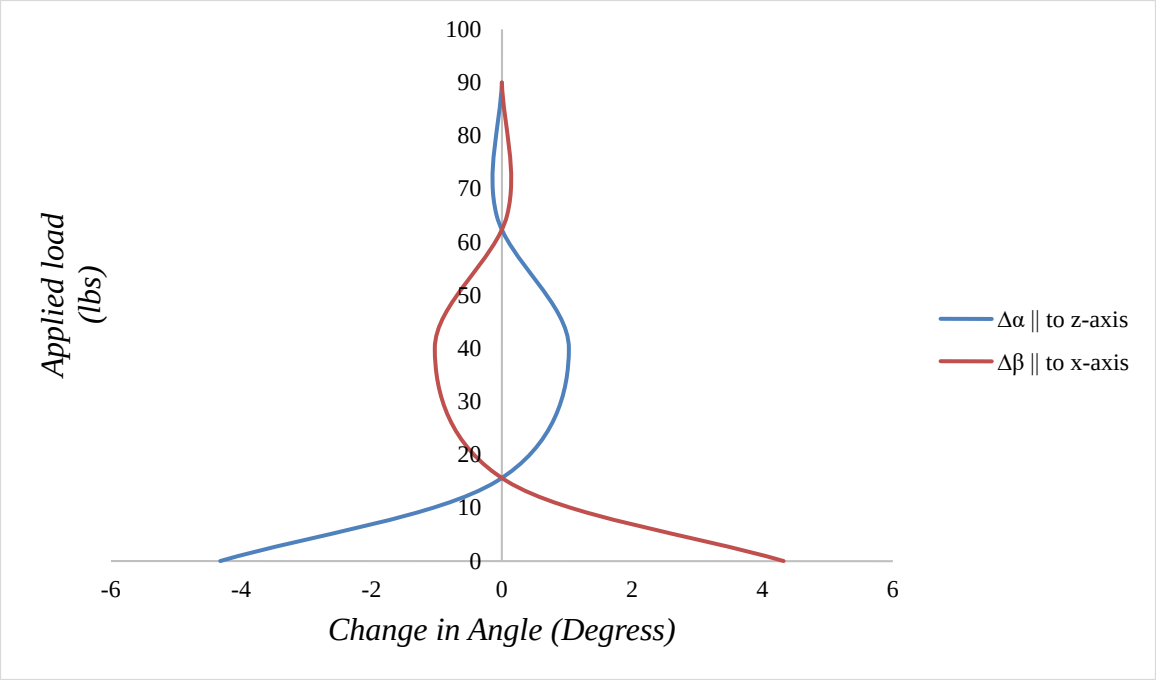

Figure (4.24): Records of Change in Angle in Rhombus 'R2' while Unloading

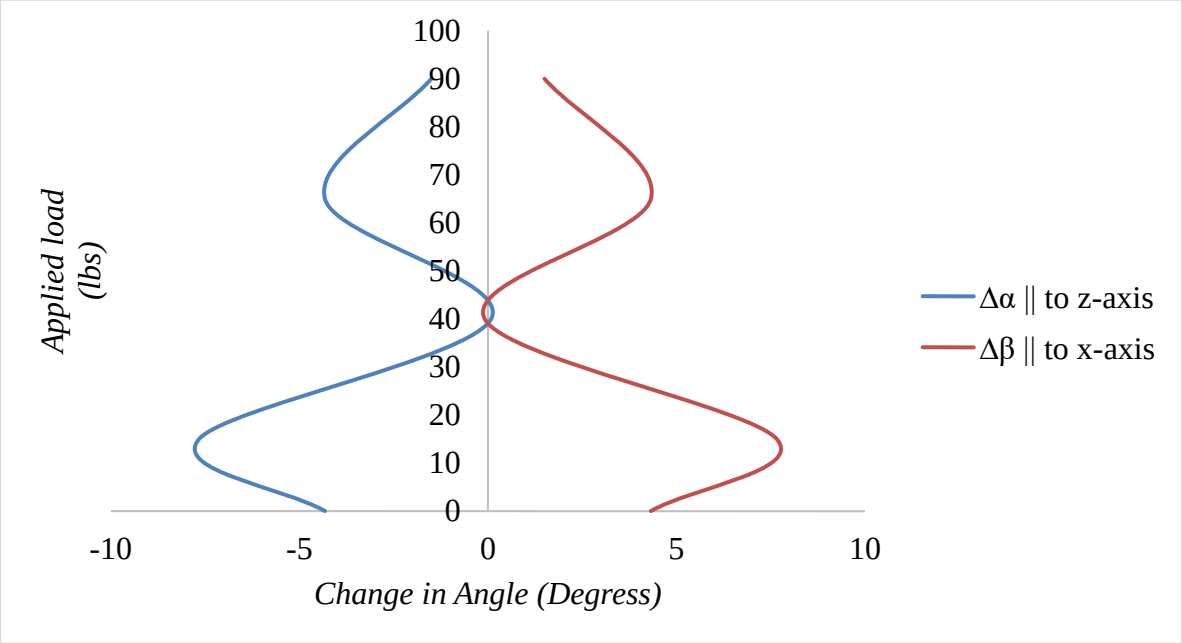

Figure (4.25): Records of Change in Angle in Rhombus 'R5' while Unloading

Vertical deflection of structure was recorded in Figure (4.26) and it shows that the structure came back to its original location completely.

Due to very less stretching of nylon ropes, the structure was coming back to its location as loads were released. It shows that by increasing stiffness of the joints of structure, the permanent settlement was decreased significantly. Furthermore, studies were performed by using finite element analysis in ANSYS software to get the optimum design.

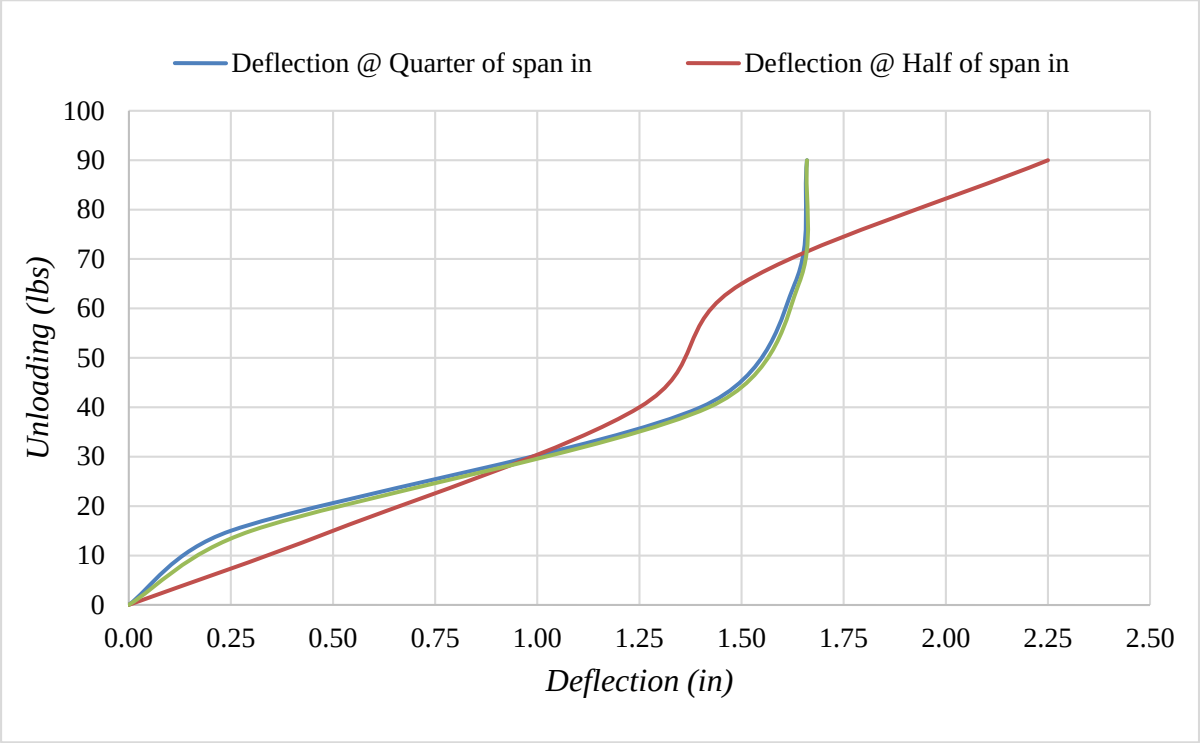

Figure (4.26): Vertical Re-bounce as per Release of Load Application

4.2.5 Short-term Creep Test: This test was performed to evaluate the viscoelastic behavior of the bamboo arch structure with the modifications described in test #2. Applying a sustained load, will generate time depended strain in bamboo sticks. The duration of this

short-term creep test was forty-eight hours (2,880 minutes) of loading. It is well known that both short- and long-term structural performance of bamboo relies heavily on moisture content and creep [21]. Although creep behavior of bamboo may be susceptible to loading parallel to the fibers, loads perpendicular to the fibers which induce longitudinal splitting behavior are commonly reported as the dominant mode of failure in bamboo members [22]. The strain of the central node was observed via two strain gauges that were bonded; one on the top of bamboo stick and another on the bottom. The 100.0lbs (448.0N) sustained point load was applied at the central node as shown in Figures (4.27) and (4.28) and strain changes with time were recorded. The plates (each weighing 25.0lbs/111.20N) were added to attach making the total sustained point load to be 100.0lbs (448.0N). Over the duration of test, both room temperature and relative humidity were recorded and results are presented in Table (4.4). The strain with respect to time was recorded and it was found that after initial loading the strain became constant throughout the time period (see Figures (4.28)). As shown in the figure, the primary (instantaneous) creep was large up to 0.0015 after which the rate of change was negligible. The large value of the primary creep is attributed to the creep component of the low level of the nylon materials. However, since the stiffness of the bamboo is much higher than for the nylon the contribution of the bamboo creep is very minimal due to the lower value of the imposed sustained load of 100lbs (448.0N). The negligible value of the transit (or secondary creep) is attributed to two factors including low strain level and the short duration of the test. In addition, since the strain gages were bonded to the top portion of the bamboo structure, as the load was applied, stretching of the nylon rope took place, allowing the top central bamboo members to come to a straight flat position (see Figure (4.29)) where the original arched strain was neutralized resulting in a minimal

amount of time dependent strain as observed in this test. In fact, the highest deformable portion is towards the support where the arched portion will become more strained as the load is applied and sustained over time.

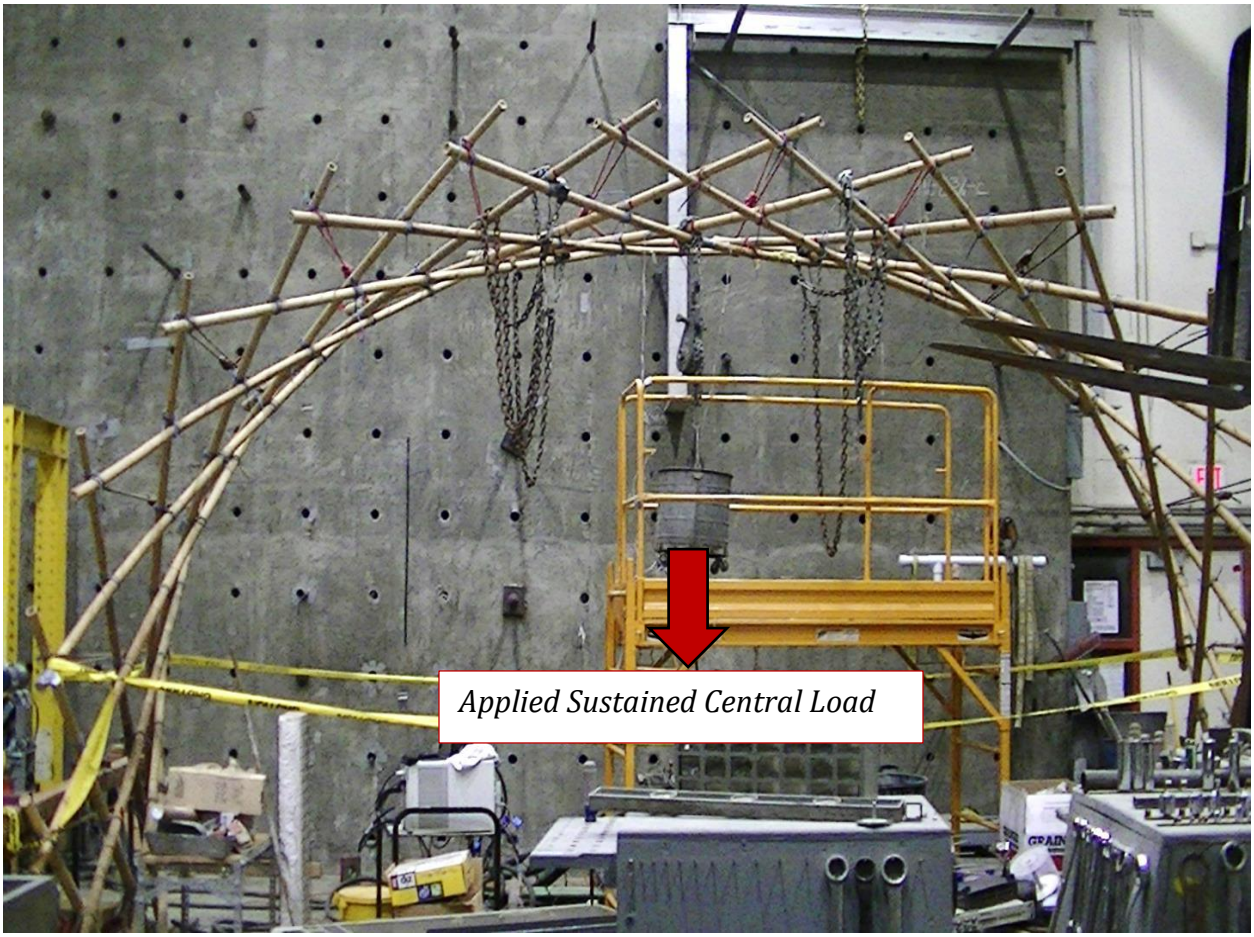

Figure (4.27): Loading at Central Node of Structure

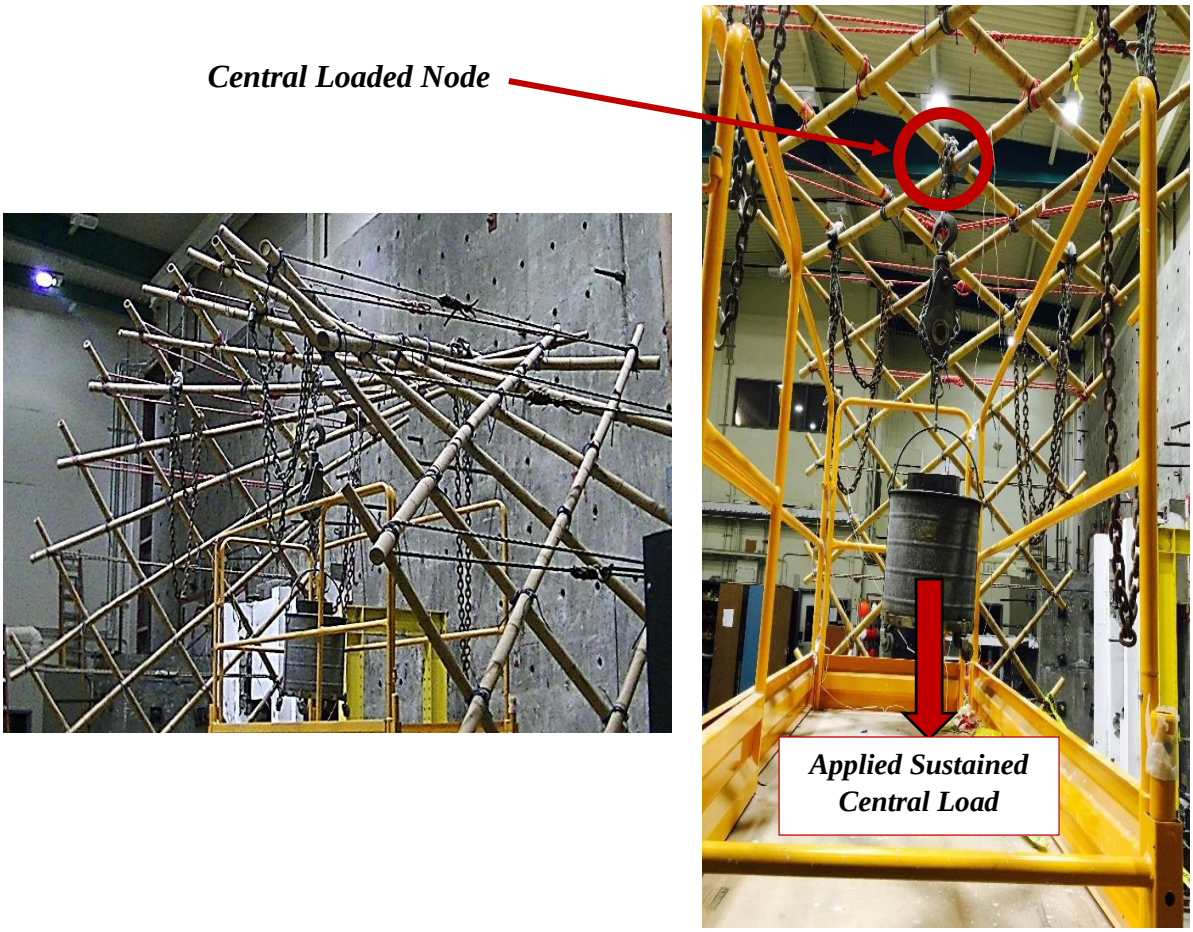

Figure (4.28): Details of Loading Regime of the Bamboo Arch Structure

Table (4.4): Temperature and Humidity Record

Date	Time	Temperature		Humidity
(mm/dd/yyyy)	(Hr:Min)	˚C	˚F	%
12/08/2015	3:00 PM	19	66	42
12/09/2015	3:00 AM	7	44	62
12/09/2015	3:00 PM	16	61	16
12/10/2015	3:00 AM	11	51	35
12/10/2015	3:00 PM	21	69	78

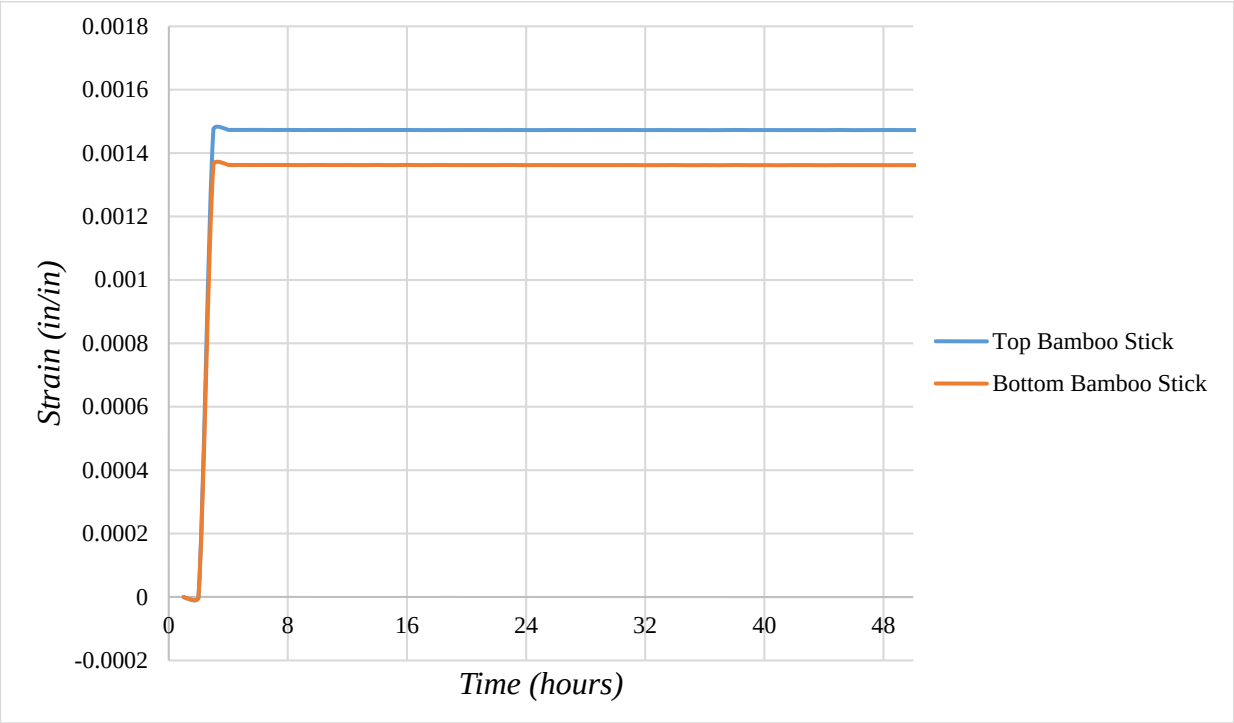

Figure (4.29): Strain Change Record for an Hour of Loading

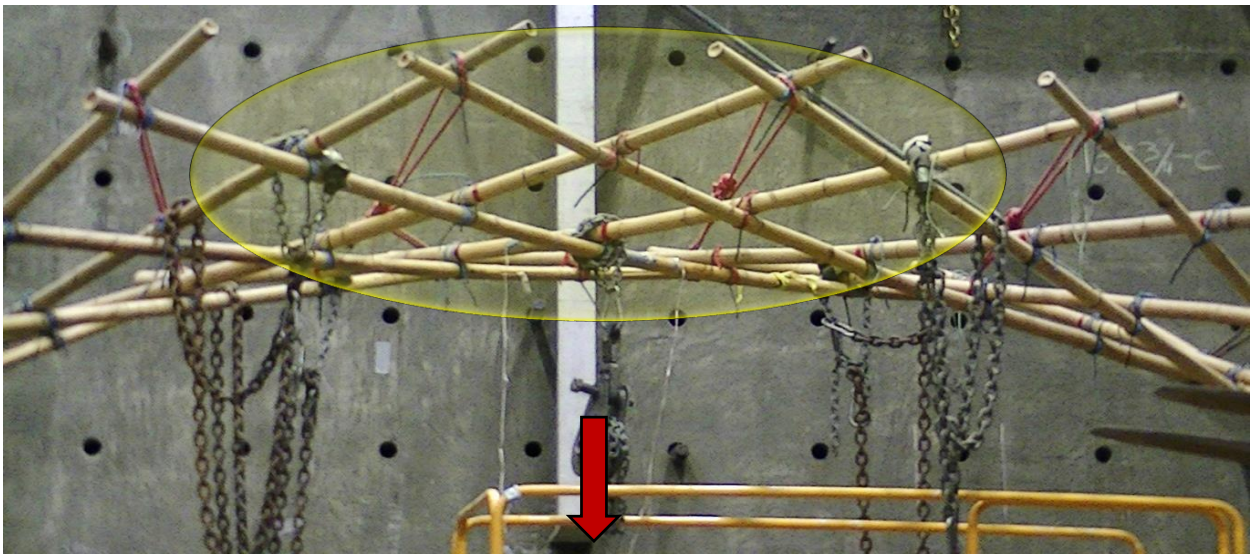

Figure (4.30): As the Load was Applied the Arch Central Portion of Bamboo Members Flattened

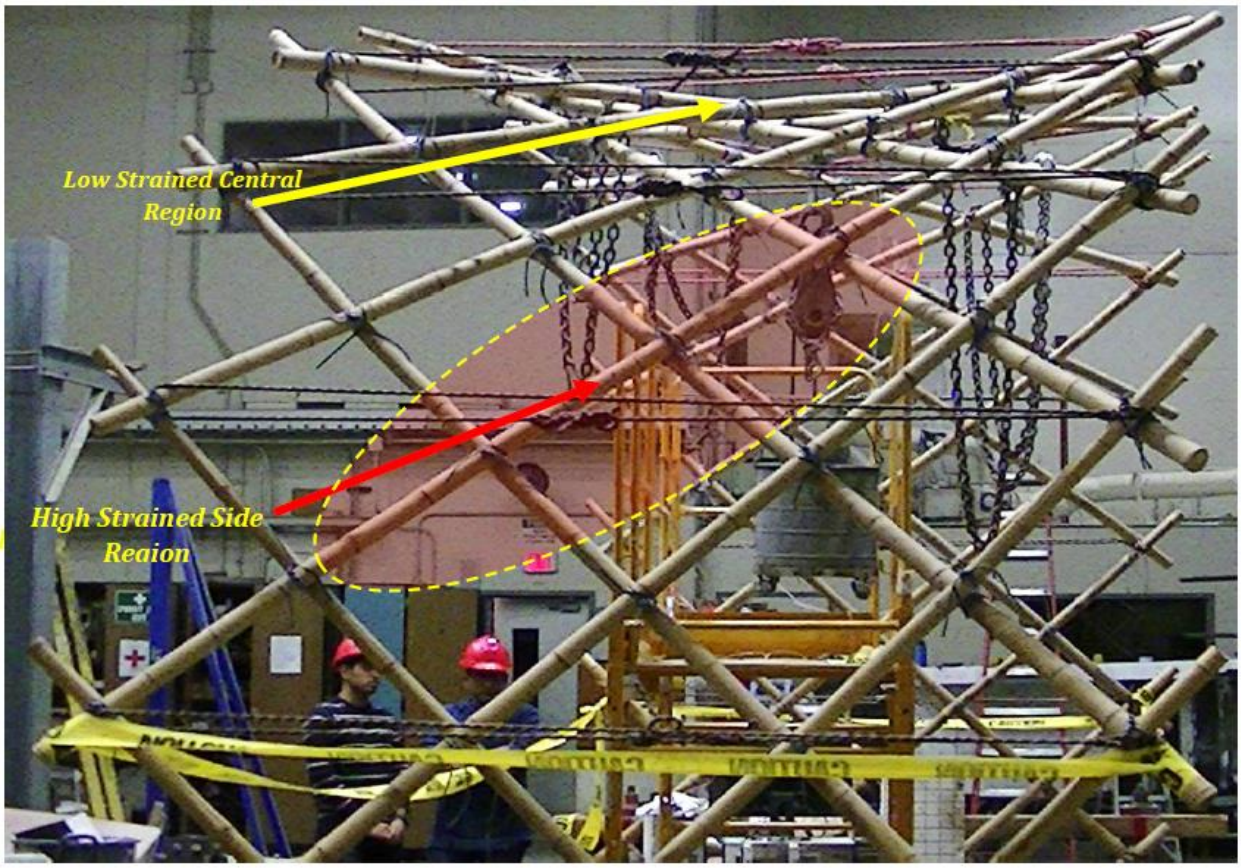

Figure (4.31): High and Low Strained Portion of Loaded Bamboo Arch

Chapter 5

NUMERICAL MODELING OF BAMBOO ARCH STRUCTURE

5.1 GENERAL

In this chapter, a finite element (FE) numerical model for the bamboo arch structure was developed. The numerical model was used initially to simulate the behavior of the arch structure under gravity loads and was used in designing the test setup and the supporting system. It was also used to improve the joining details of the arch structure. The numerical analysis was carried using the ANSYS® commercial FE code.

5.2 FINITE ELEMENT ANALYSIS (FEA)

The prototype was modelled in ANSYS and procedure is explained in Appendix F, to understand the numerical model simulation and the results were compared with experimental data. The 3D numerical model was created. A time increasing force was applied on the numerical model to match the test #1 loading conditions (see Figure (5.1)). The model was analyzed and displacements in all three directions were recorded.

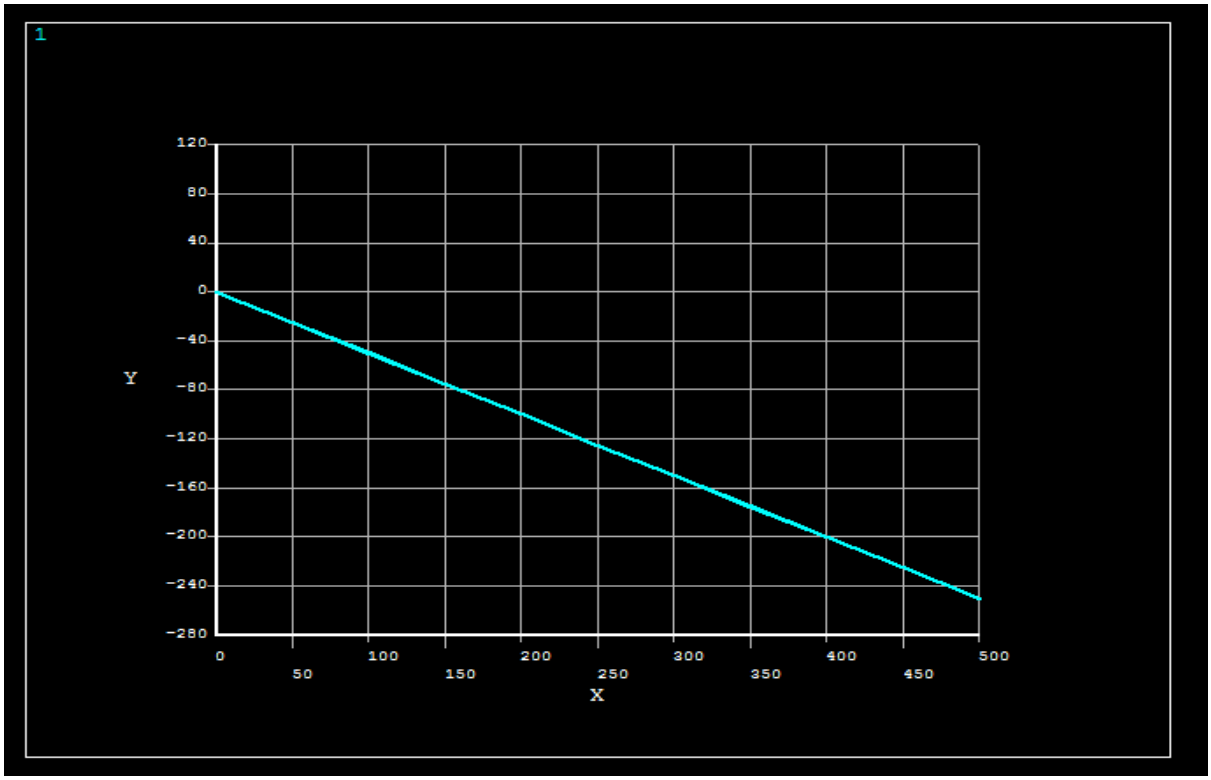

Figure (5.1): Force Function Applied at Four Nodes Respectively

Force function (Y) was linear time dependent function which was defined as $-0.5 * X$, where 'X' is time in seconds and negative sign indicates the downward direction of loading. The ANSYS finite element software meshed the bamboo element into 8 parts (see Figure (5.2)) and then analyzed for the structural characteristics.

5.2.1 Verification of ANSYS model with the Experimental Results

The model was first created to replicate the test #1 results, in order to check the accuracy of the numerical model and analysis result. The same linearly increasing force function was applied to reach a maximum load of 40.8 kg (90.0 lbs) . The deformed shape and central vertical deflection of both ANSYS finite element software model and test #1 basic model was

compared (see Figure (5.4)). The deformed shape of ANSYS finite element model is shown in Figure (5.3). In this blue and dashed gray lines were elements of structure after deformation and initially unloaded structure respectively. Now, to check this model the applied load vs vertical central node deflection was plotted (see Figure (5.4)) and compared.

The ANSYS finite element model was used for further analysis for design improvement. To overcome the structure design flaws, some alteration was performed in design and then analyzed.

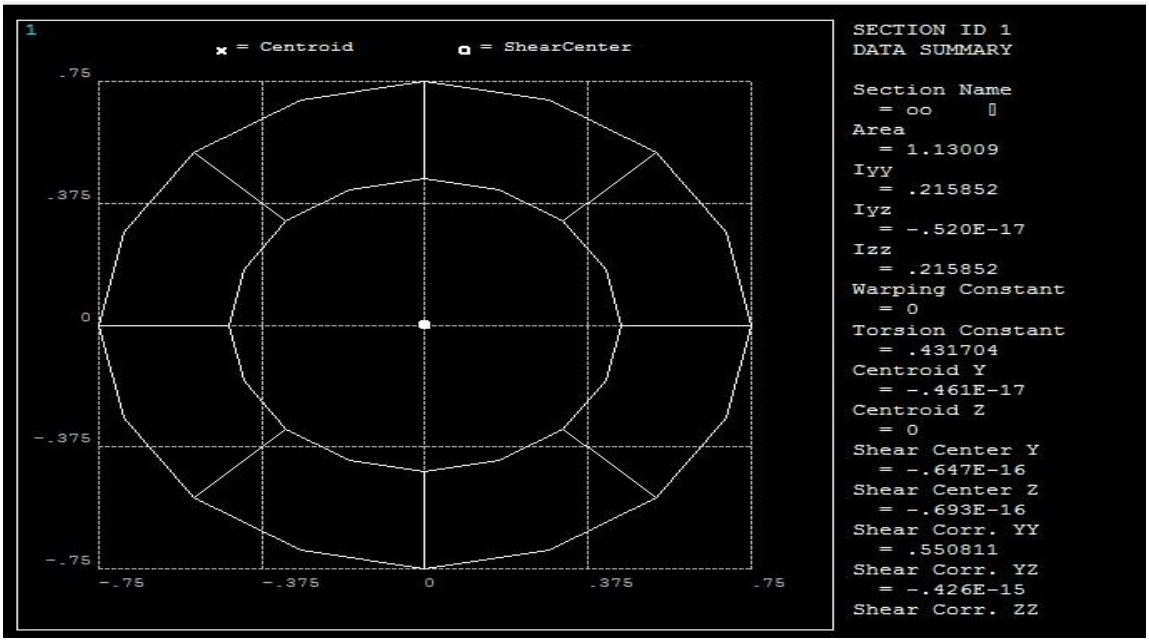

Figure (5.2): Bamboo Element Mesh and its Geometrical Properties

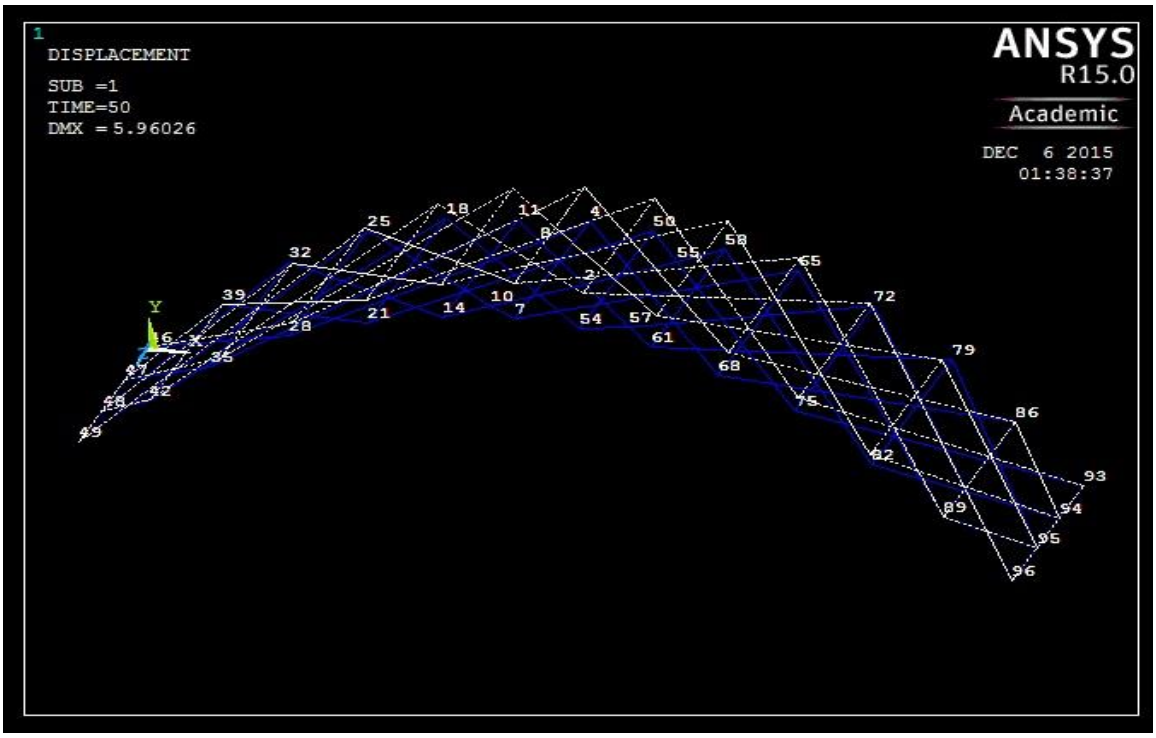

Figure (5.3): Deformed Shape under Loading

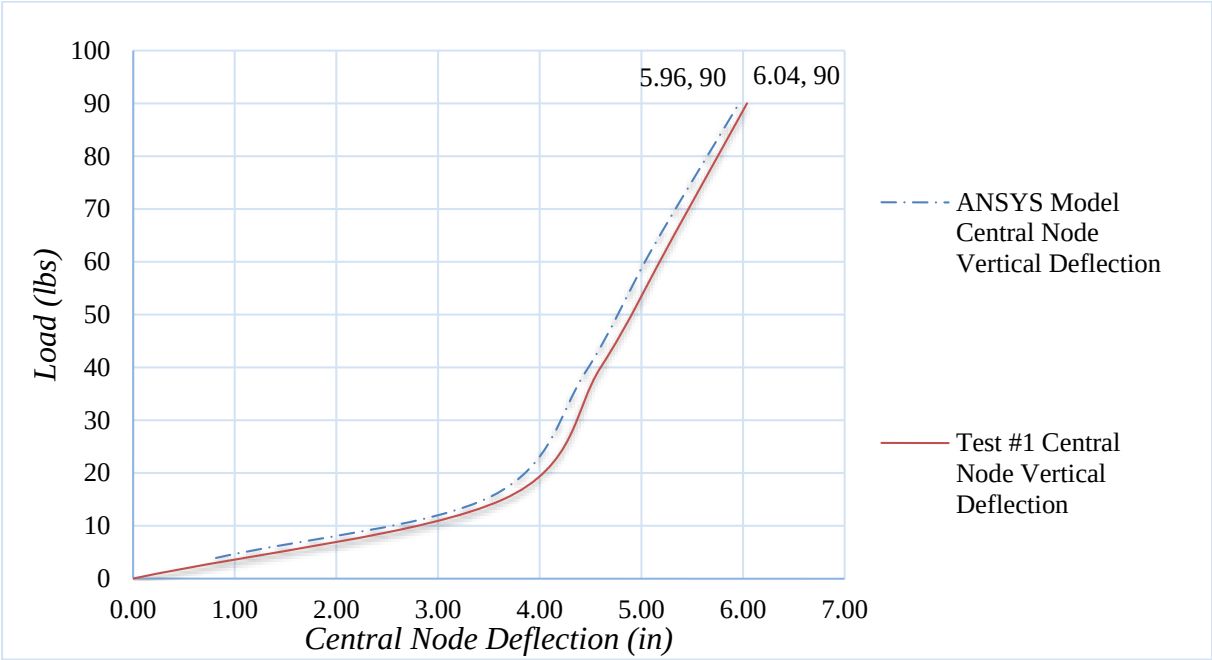

Figure (5.4): Comparison of Finite Element Model and Experimental Model (Test #1)

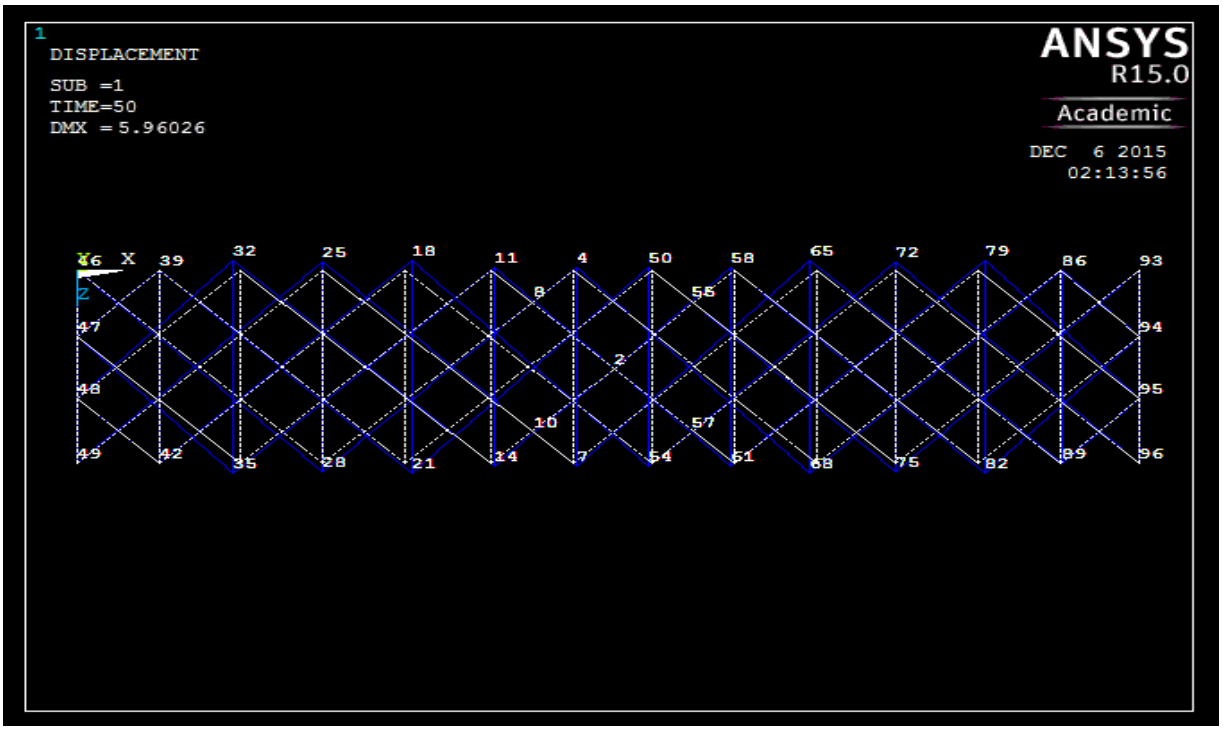

Figure (5.5): Top view of Deformed Shape under Loading

5.2.2 Design Improvement

"Bamboo Arch with Steel Cable Connecting Alternate End Joints Replacing Nylon Ropes"

The Nylon was modelled as a link member as shown in Figure (3.7) in red colored lines. In this design, the nylon ropes were replaced by steel cables in transverse direction (z-direction) in terms of its material properties and analyzed in ANSYS software (see Figures (3.7) and (5.6)). The 8 mm (0.31") steel cables with elastic modulus of 20.1 GPa (3 X10^6 psi) were used to replace nylon ropes.

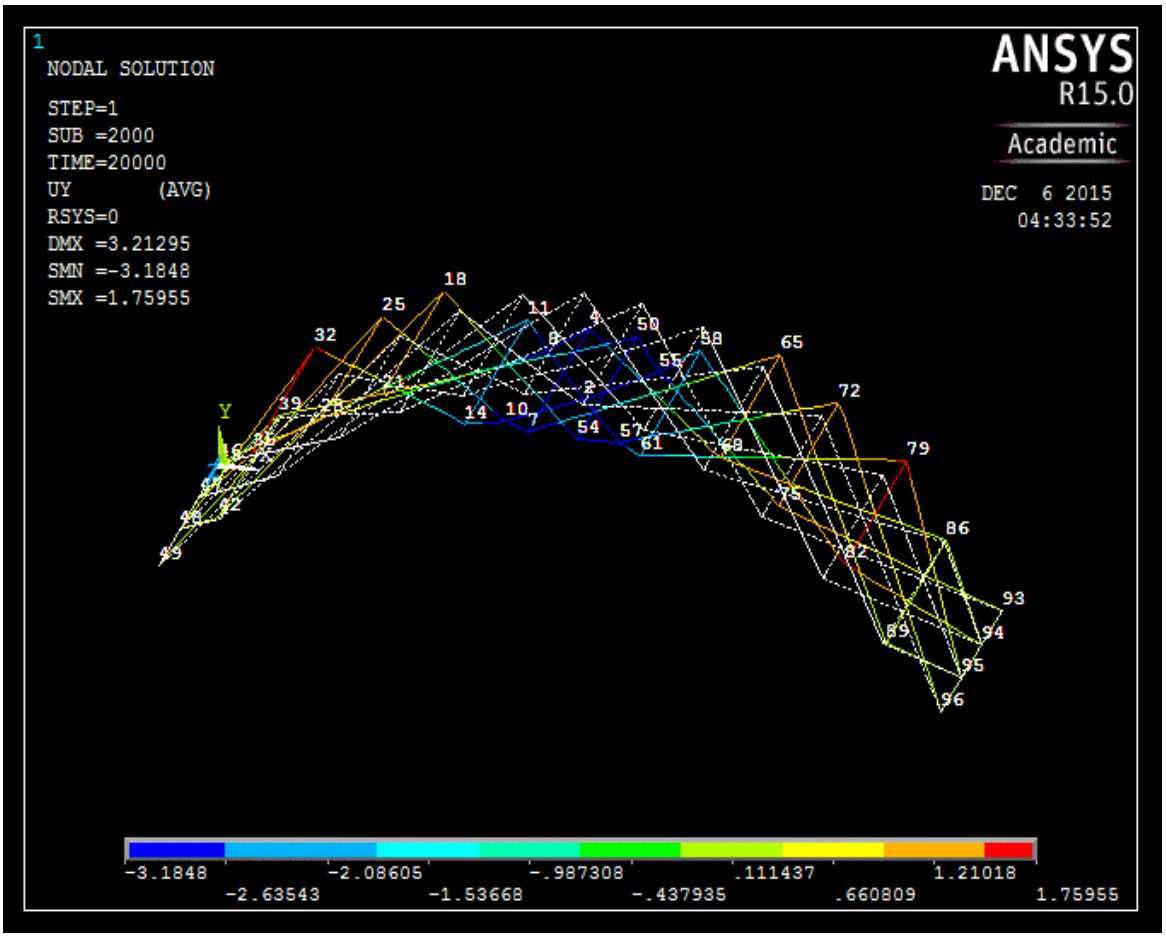

Figure (5.6): Un-deformed and Deformation Shape

In this design, the vertical deflection of structure was decreased (see Figure (5.6)) by providing steel cables in transverse direction (z-directions). The steel cables increase the stiffness of joints which helps in resisting displacement of nodes as shown in Figures (5.7) and (5.8). The z-direction deflection values were also less in case of using the steel cables. Also, by this design the structure has become much stiffer with rigid joints than the basic design in which nylon ropes were used. Improved design showed that the elastic behavior under uniform loading is due to the major difference in stiffness of steel cables and nylon ropes. The stiffness of steel cables are almost 15000 times higher than nylon ropes stiffness.

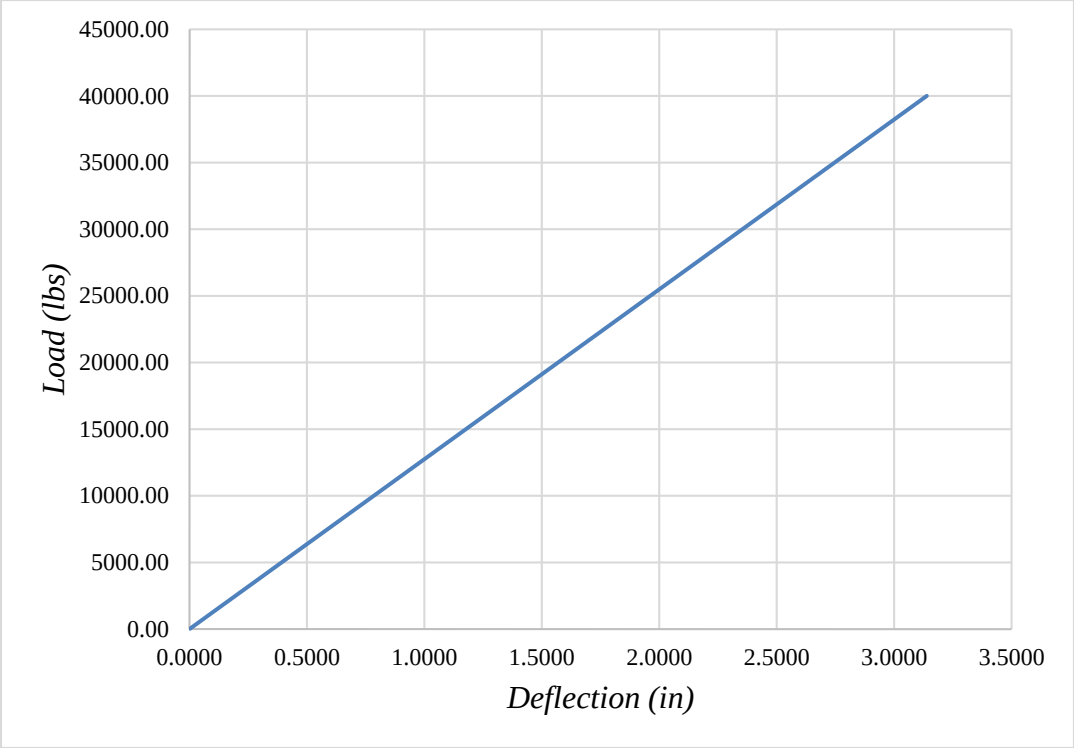

Figure (5.7): Central Node Vertical Deflection

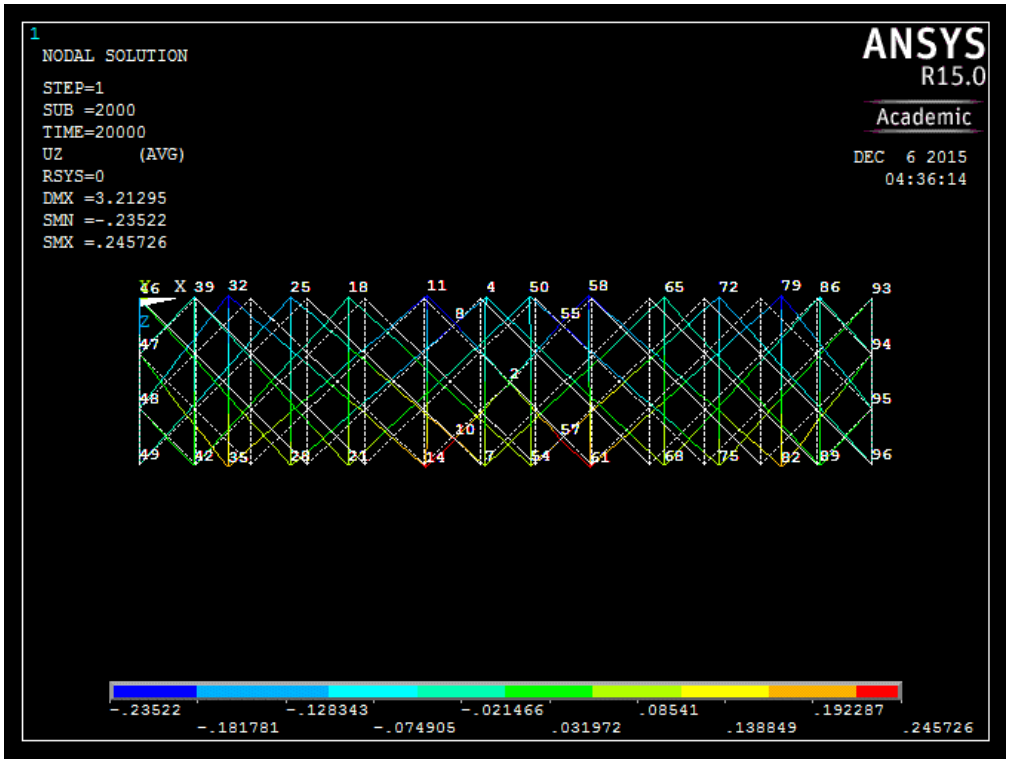

Figure (5.8): Z- Deflection Distribution

CHAPTER 6

CONCLUSIONS AND RECOMMENDATIONS FOR FUTURE RESEARCH

6.1 GENERAL

In this chapter, a summary of major observations, conclusions and recommendations for future research are presented.

6.2 CONCLUSIONS

In this study, the behavior of a bamboo arch structure was investigated. The study was divided in two parts: experimental and numerical. In the experimental phase, the bamboo arch structure was tested under point loading to examine both instantaneous as well as short-term creep behavior. ANSYS finite element code was used to simulate these behaviors (see Appendix F) and to optimize the joint details of the arch. The numerical results matched well with the experimental results confirming the validity of using such model in simulating the bamboo arch behavior. With the aid of the FE model, a stiffer nodal joining detail using steel cables was developed and implemented, that assisted in decreasing the deflection of the arch at the central region.

One of the major observations that was learned from this study is that the arch has higher stresses at the ends(support) when central load is applied (see Figures (4.30) and (4.31)). In the central region, bamboo members are pre-arched (pre-strained) and get flattened upon the load application at the central area (see Figure (4.30)). The pre-strained central portion

of the arch, flattened due to both member and rigid body rotation of the nodes, releases the strain from the pre-arched bamboo member.

Based on the lab test observation, in the portion of the bamboo arch close to the support, the pre-arched members were exposed to additional straining action that may lead to failure of the bamboo (see Figure (4.31)). However, this issue cannot be confirmed since all the tests performed in this study were non-destructive. This issue is very important when performing creep tests and identifies the proper locations where strain gages should be located in order to gather time-dependent strain values.

The serviceability of the arch structure subjected to a load of 400.34N (90.0lbs), that was implemented in the experimental program, was assessed by comparing the central vertical deflection with limiting values specified by California Building Code (CBC) 2013, Table 1604 A.3. This requires a deflection limit for the non-supporting ceiling roof members of L/180, where L is the total-span. Table (6.1) summarizes the findings for both original and new nodal joining details of the arch structure. It is clearly shown that replacing the flexible nylon ropes with steel cables makes a substantial improvement in the resulting central deflection of the bamboo arch structure.

Figure (6.1) show that the numerical model simulating stiff joints has higher capacity as compared to the nylon joint detail. It can be concluded that, in order to use this type of structure for different application, a stiffer joining details is essential.

Table (6.1): Structural Design Evaluation

Bamboo Structure Designs	**Structural Evaluation**	
(Two ANSYS models compared)	Deflection Comparison at 40.8 kg (90.0 lbs)	CBC 2013 requirement (Deflection L/180) *Allowable Deflection 4.8 cm (1.9")*
Bamboo arch constructed with nylon ropes	15.1 cm (5.96") (see Figure (5.26))	It passed the deflection limit at very small range of loading due to flexible nylon rope.
Bamboo arch model with steel cable	0.02 cm (0.0075") (see Figure (5.31))	It passes the deflection limit at 107.07 kN (24.20 kips) which is comparability capacity.

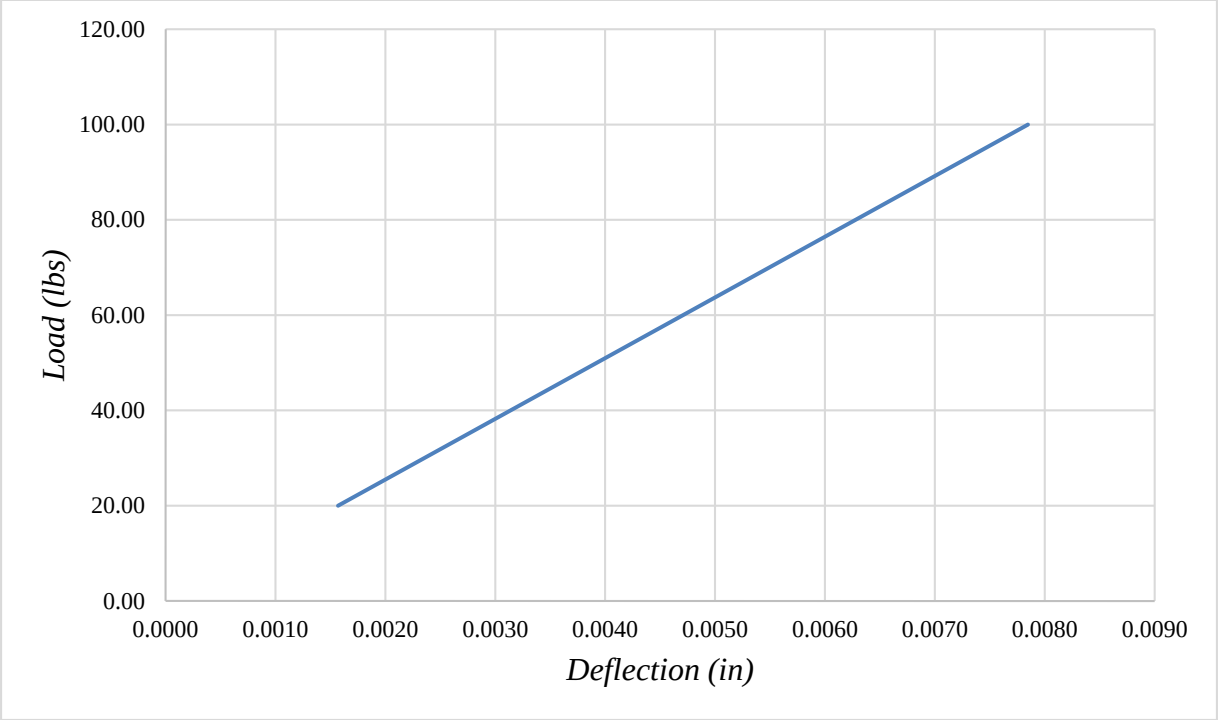

Figure (6.1): Central Node Vertical Deflection at a limit of 90.0 lbs (400.34N) Load

6.3 RECOMMENDATIONS FOR FUTURE RESEARCH

Based on the results of this study, the following areas for future research were identified:

1. The influence of different end support details will influence the overall behavior of the arch structure. For this reason, additional investigations are recommended to evaluate the issue.

2. As it was revealed and discussed from this study, nodal joining details play an essential role in defining the load-displacement characteristics of the structure. Therefore, more studies on improving the connectivity of such structures are needed.

3. This study focused on the behavior of the bamboo arch structure when exposed to gravity-simulated loading. Future study should investigate the behavior of such structure when exposed to lateral loads such as wind, impact and seismic ground forces.

4. This study included only non-destructive evaluation of the bamboo arch structure. It is important to perform tests to determine the ultimate capacity of such structures and identify the associated failure modes.

5. Short-term creep tests were performed in this study, however, more creep test with longer duration, up to a year or more, is also recommended in order to develop a mathematical model to describe the viscoelastic behavior of such structure.

6. The dynamic characterization and damping properties need to be identified through analytical as well as experimental studies.

7. Bamboo material are sensitive to moisture and temperature. For this reason, studies on the behavior of arch bamboo structure under such conditions are also recommended.

REFERENCE

[1] Tung AU and Paul Christiano, 1993; Fundamentals of Structural Analysis, Prentice Hall,: 16-50,

[2] Lakkad, S.C. and J.M. Patel. 1980; Mechanical properties of bamboo, a natural composite. Fiber Science Technology 14: pp. 319-322,

[3] M. Asghar Bhatti, 2005; Fundamental-Finite-Element-Analysis-and-Applications, Wiley: pp. 50-283,

[4] Ray W. dough & Edward L. Wilson, 1999. Early Finite Element Research at Berkeley, Present at the Fifth U.S. National Conference on Computational Mechanics, Aug. 4-6, 1999,

[5] Abd.Latif, M., W.A. W. Tarmeze, and A. Fauzidah. 1990. Anatomical features and mechanical properties of three Malaysian bamboos. J. Tropical Forest Sci. 2(3): pp. 227-234,

[6] Wang, D., and S.J. Shen. 1987. Bamboos of China. Timber Press, Portland, Oregon. pp. 428.

[7] Janssen, J.J.A. 1995. Building with bamboo (2nd ed.). Intermediate Technology Publication Limited, London. pp. 65,

[8] Amada, S., Y. Ichikawa, T. Munekata, Y. Nagase, and K. Shimizu. 1997. Fiber texture and mechanical graded structure of bamboo. Composite Part B. 28(B): 13-20,

[9] Kishen, J., D.P. Ghosh, and M.A. Rehman. 1956. Studies on moisture content, shrinkage, swelling and intersection point of mature (*Dendrocalamus strictus*) male bamboo. Indian For. Rec. 1: 1-30,

[10] Chauhan, L., S. Dhawan, and S. Gupta. 2000. Effect of age on anatomical and physicomechanical properties of three Indian bamboo species. J. of the T.D.A.. 46:11-17.

[11] Zhou, F.C.. 1981. Studies on physical and mechanical properties of bamboo woods. J.

of Nanjing Technology College of Forest Products. 2: 1-32,

[12] Espiloy, Z. 1987. Physico-mechanical properties and anatomical relationships of some Philippine bamboos, Proceedings of the International Bamboo Workshop, Hangzhou, China, 6-14 October 1985. Chinese Academy of forestry, Beijing, China; International Development Research Centre, Ottawa, Canada. pp. 257-264.

[13] Liese, W. and G. Weiner. 1996. Ageing of bamboo culms, a review. Wood Science Technology 30: pp. 77-89,

[14] Sattar, M.A., M.F. Kabir, and D.K. Battacharjee. 1994. Effect of age and height position. on muli (*Melocanna baccifera*) and borak (*Bambusa balcooa*) bamboos on their physical and mechanical properties,

[15] Narayanmurti, D. and B.S. Bist. 1947. Preliminary studies on building boards from bamboos. Indian Forestry Leaflet No.103,

[16] Lee, A.W.C, X.S. Bai, and P.N. Peralta. 1994. Selected physical and mechanical properties of giant timber bamboo grown in South Carolina. Forest Prod. J.. 44(9):40-46,

[17] American Society for Testing and Materials (ASTM). 1994. Standard methods of evaluating the properties of wood based fiber and particle panel materials. ASTM D 1037-94,

[18] A. N. Rao et al, 1998; Jules J. A. Janssen, 1981; M. Ahmad & F. A. Kamke, 2005; International Network for Bamboo.

[19] Changjun Zhua, Chonghui Zhanga, Yixin Zhang; Study on Raman spectra of aliphatic polyamide fibers.

[20] Han Yuan, Eric Courteille, Dominique Deblaise; Static and dynamic stiffness analyses of cable-driven parallel robots with non-negligible cable mass and elasticity.

[21] Xu Q, Harries KA, Li X, Lui Q, Gottron J; Mechanical properties of structural bamboo following immersion in water. Eng Struct; 2014.

[22] Jennifer Gottron , Kent A. Harries, Qingfeng Xu; Creep behavior of bamboo

[23] Jo Scheer, Jules J. A. Janssen; Bamboo Technologies, 1981: p153-226

APPENDIX (A)

RECORD OF TEST #1 UNDER LOADING

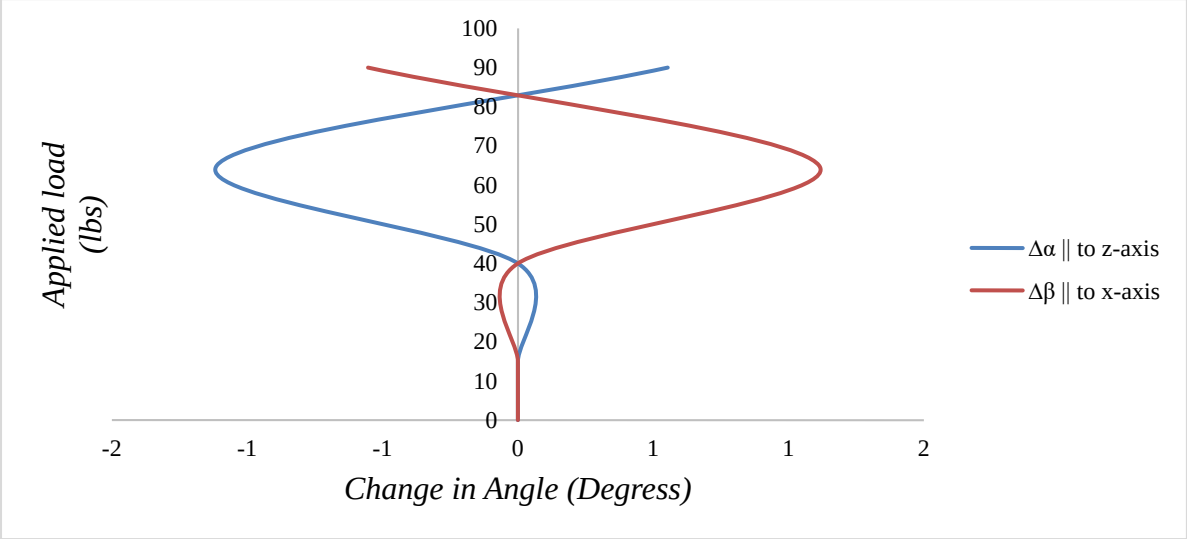

Figure (A.1): Records of Change in Angle in Rhombus 'R6' while Loading

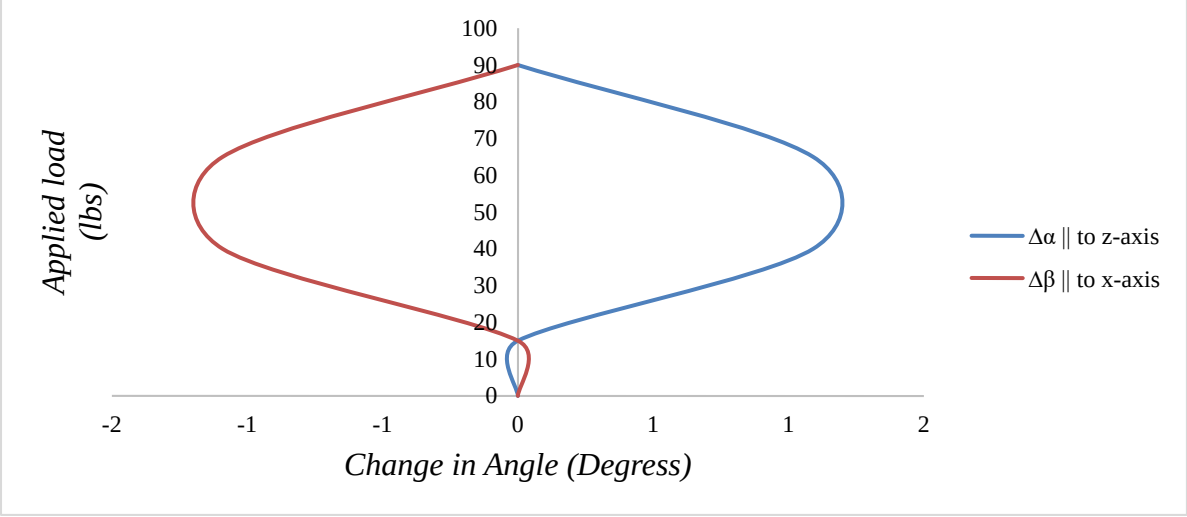

Figure (A.2): Records of Change in Angle in Rhombus 'R7' while Loading

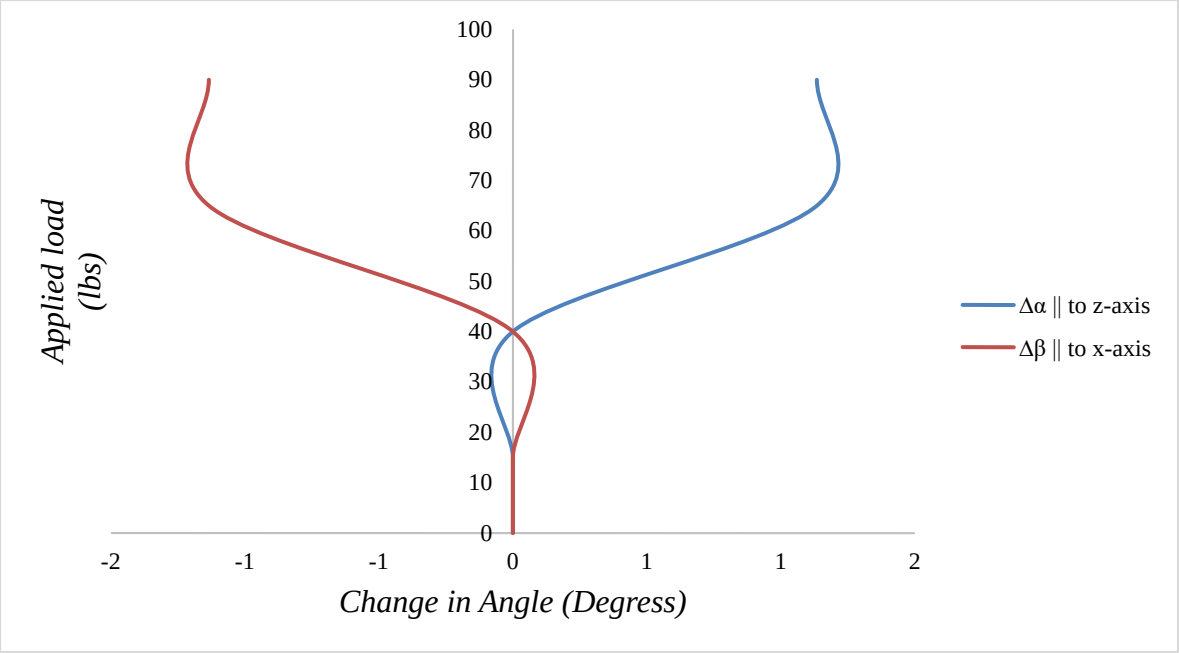

Figure (A.3): Records of Change in Angle in Rhombus 'R10' while Loading

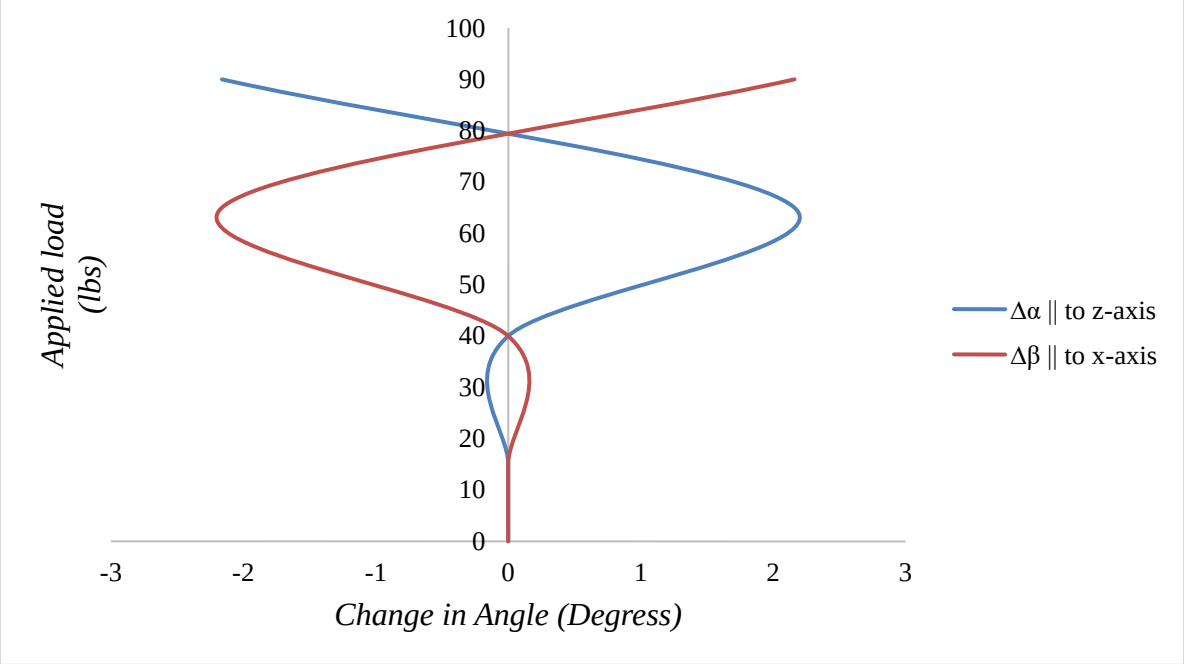

Figure (A.4): Records of Change in Angle in Rhombus 'R11' while Loading

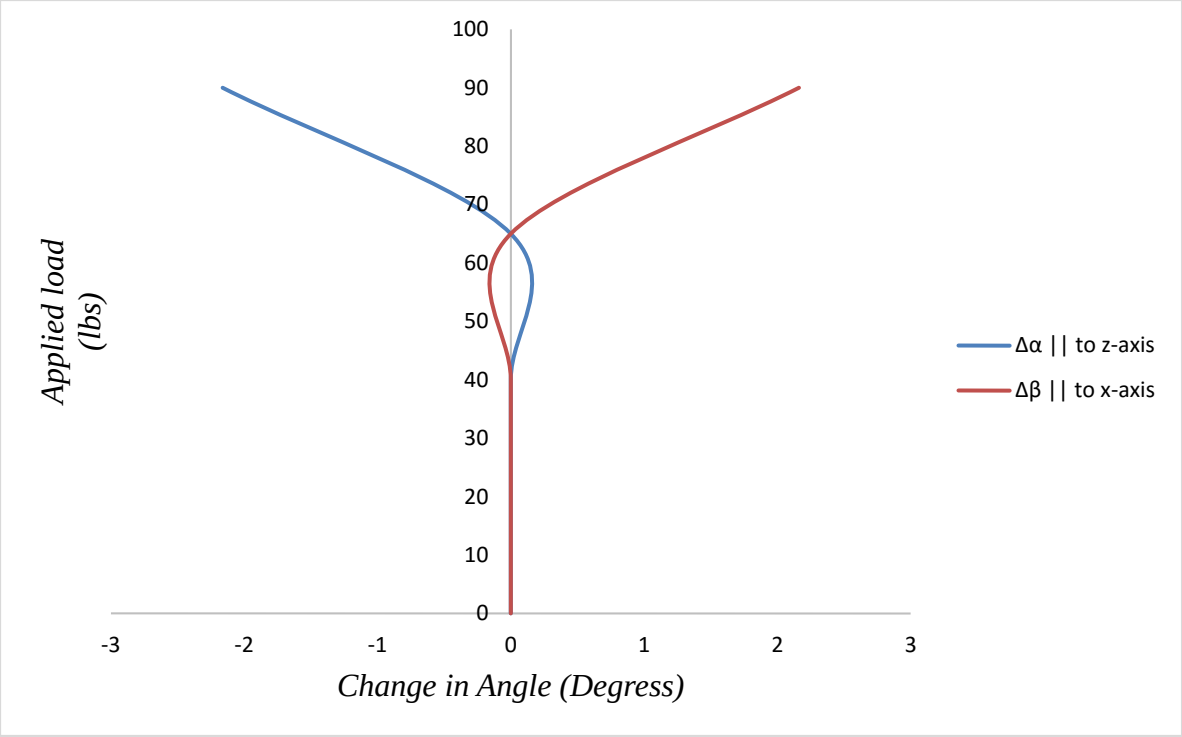

Figure (A.5): Records of Change in Angle in Rhombus 'R12' while Loading

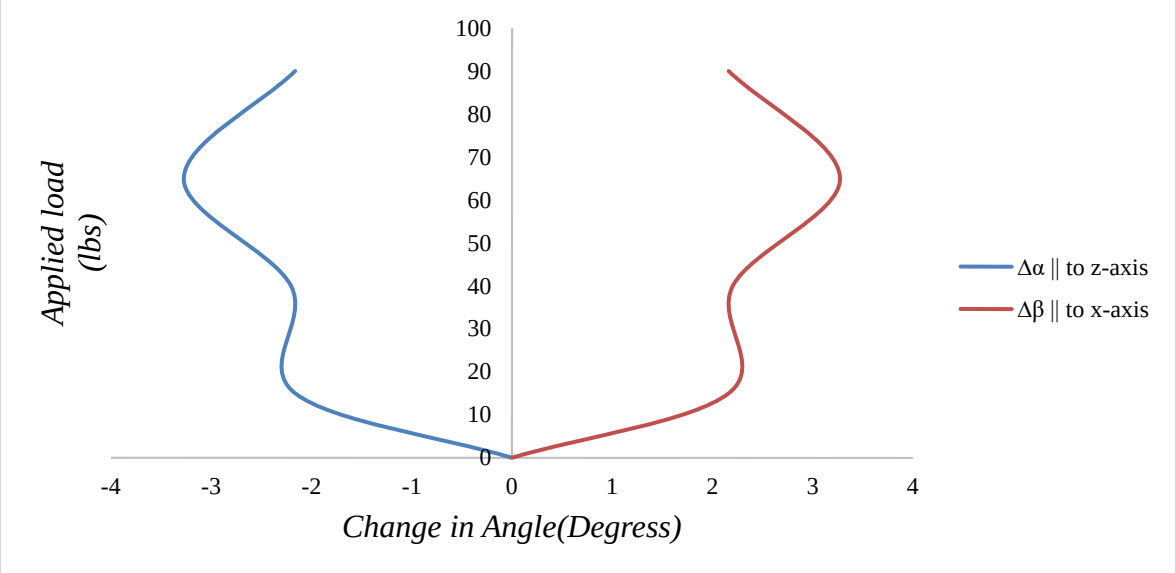

Figure (A.6): Records of Change in Angle in Rhombus 'R15' while Loading

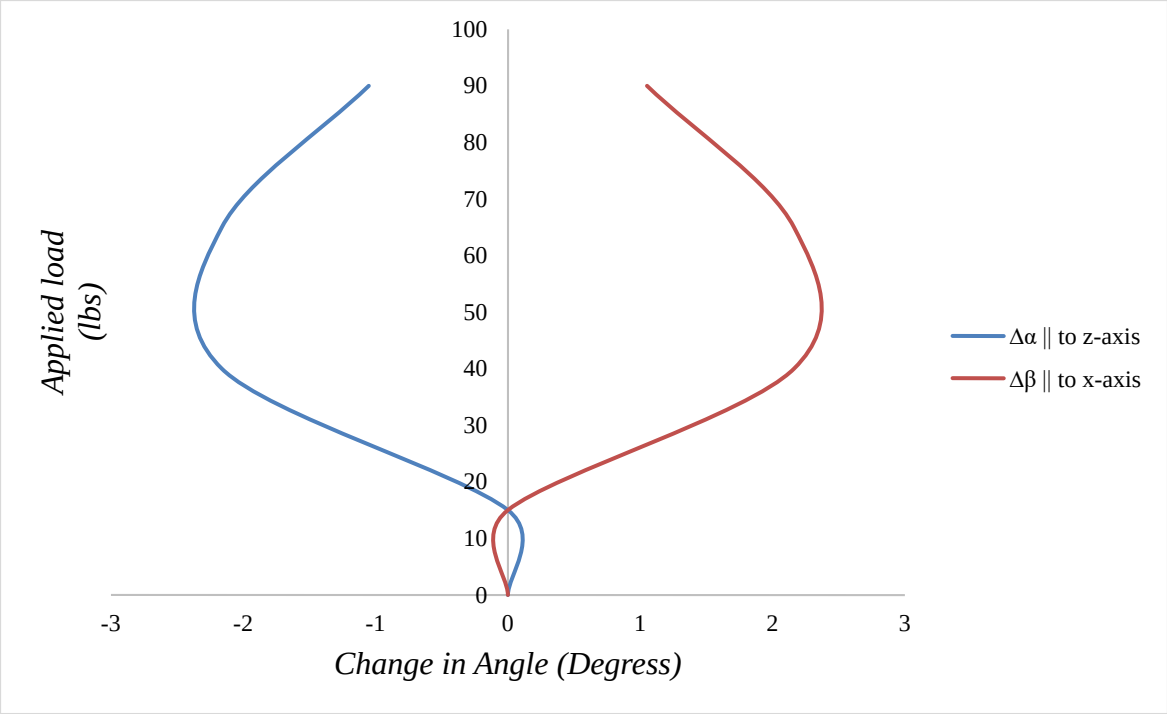

Figure (A.7): Records of Change in Angle in Rhombus 'R16' while Loading

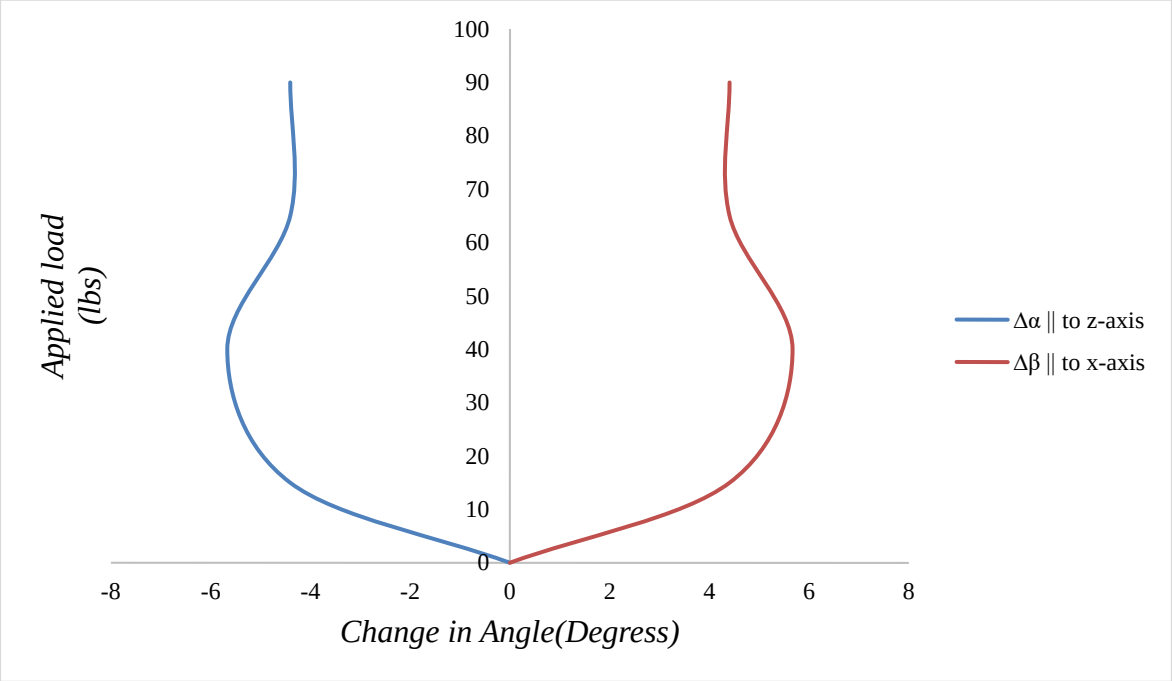

Figure (A.8): Records of Change in Angle in Rhombus 'R17' while Loading

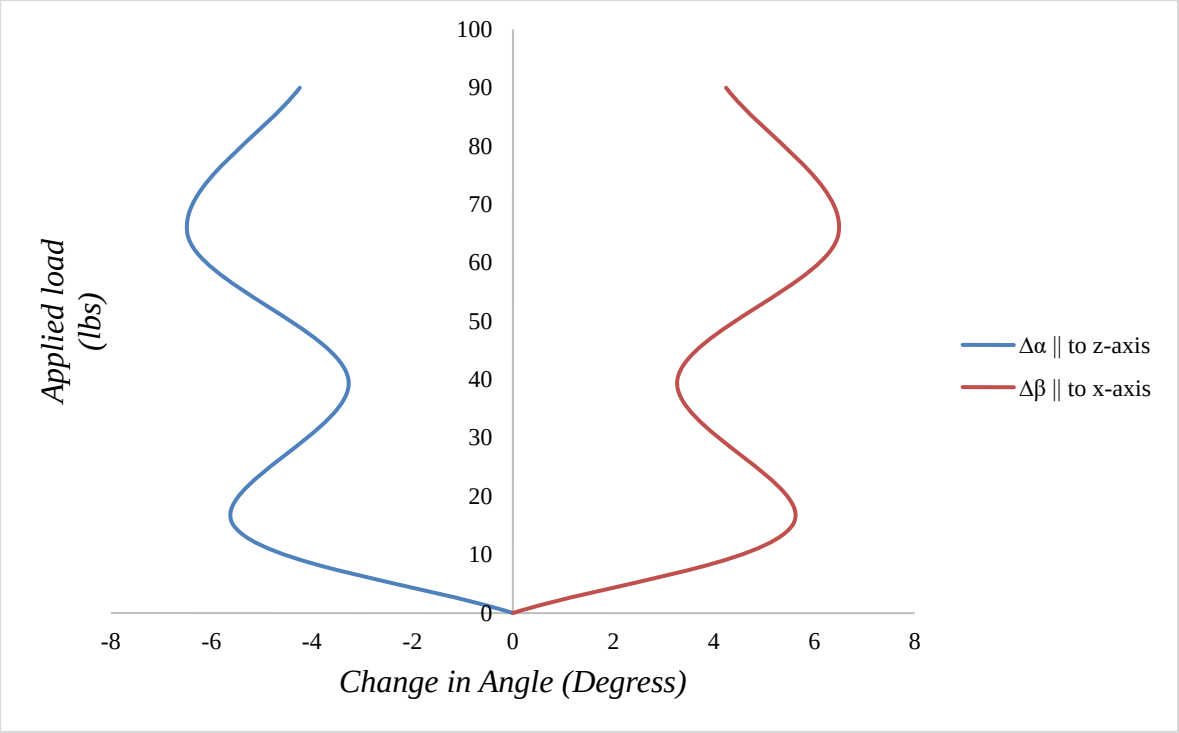

Figure (A.9): Records of Change in Angle in Rhombus 'R20' while Loading

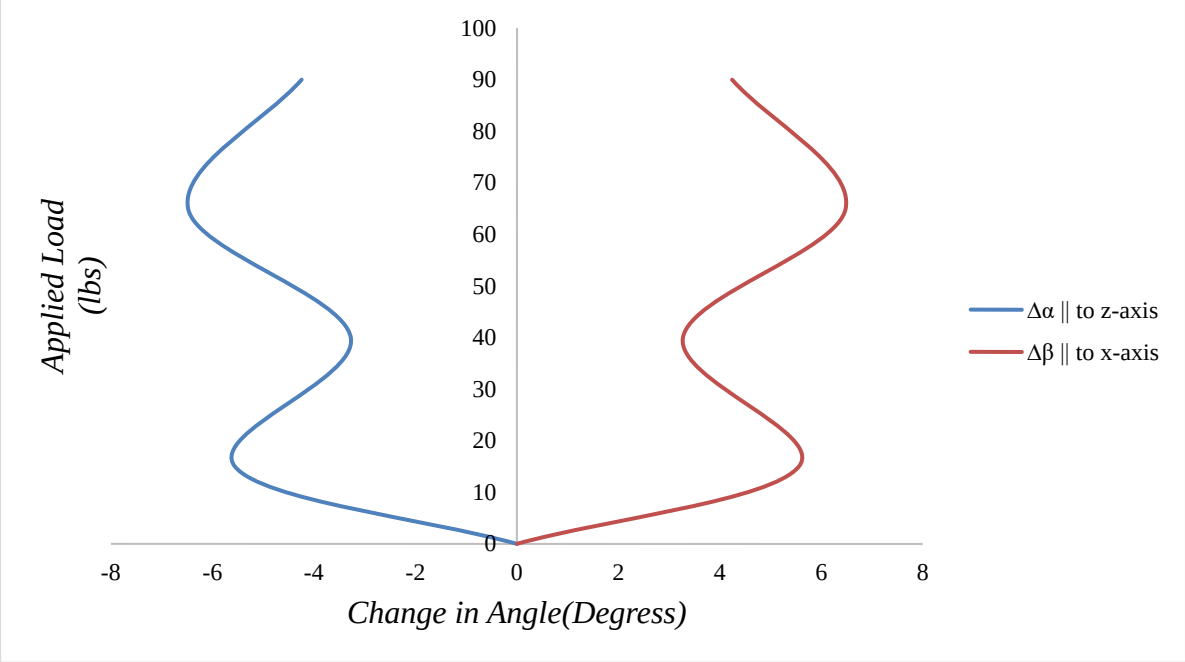

Figure (A.10): Records of Change in Angle in Rhombus 'R21' while Loading

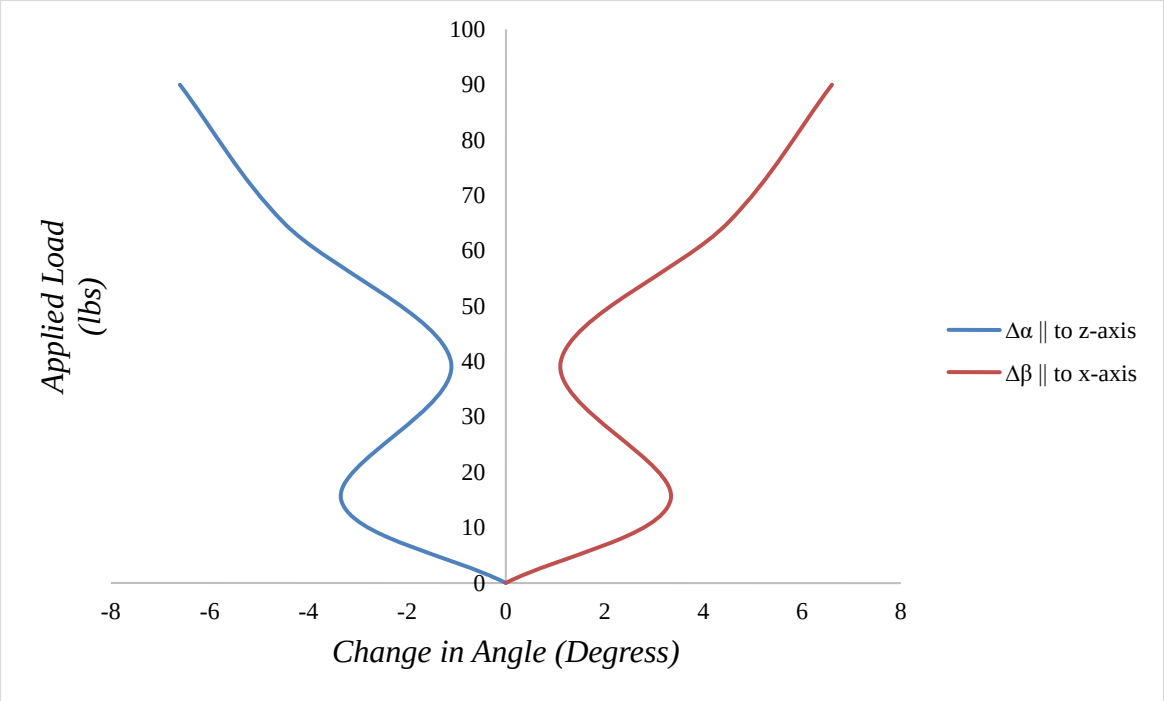

Figure (A.11): Records of Change in Angle in Rhombus 'R22' while Loading

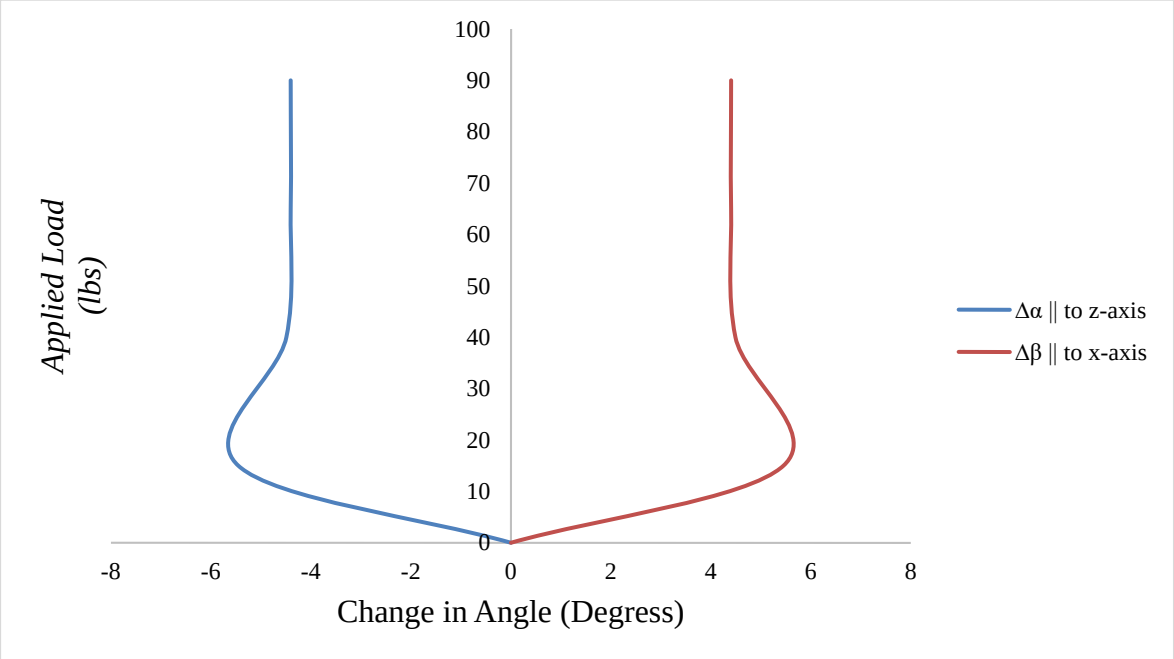

Figure (A.12): Records of Change in Angle in Rhombus 'R25' while Loading

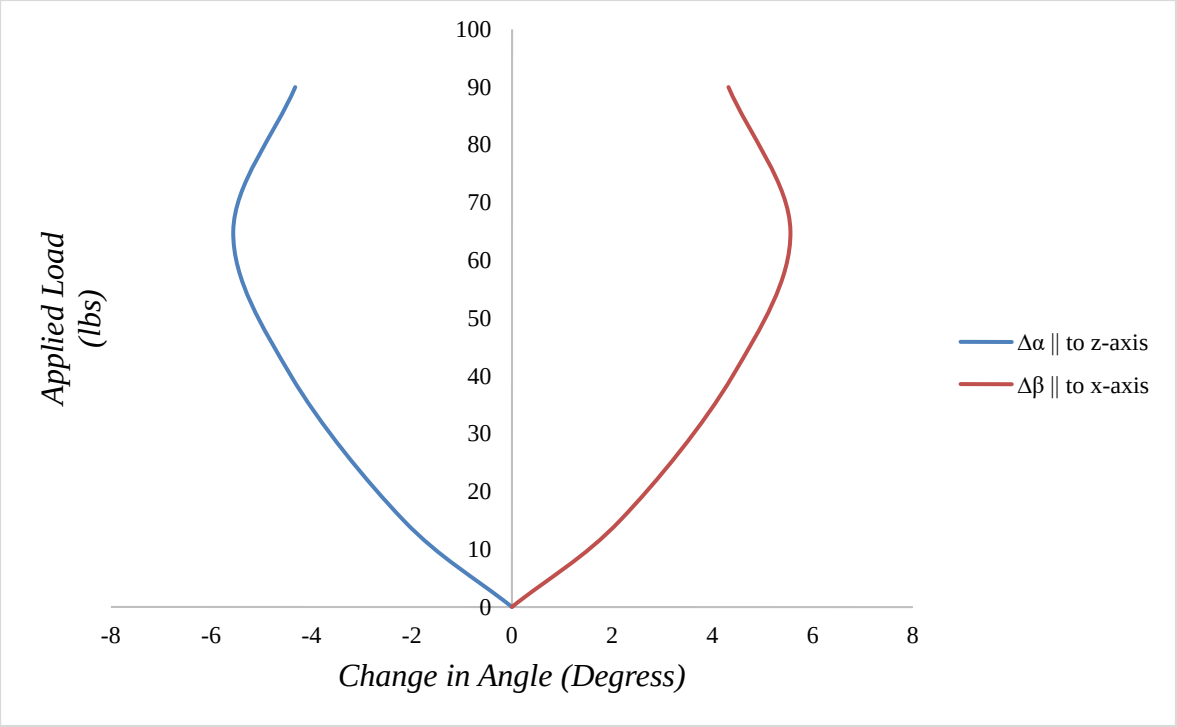

Figure (A.13): Records of Change in Angle in Rhombus 'R26' while Loading

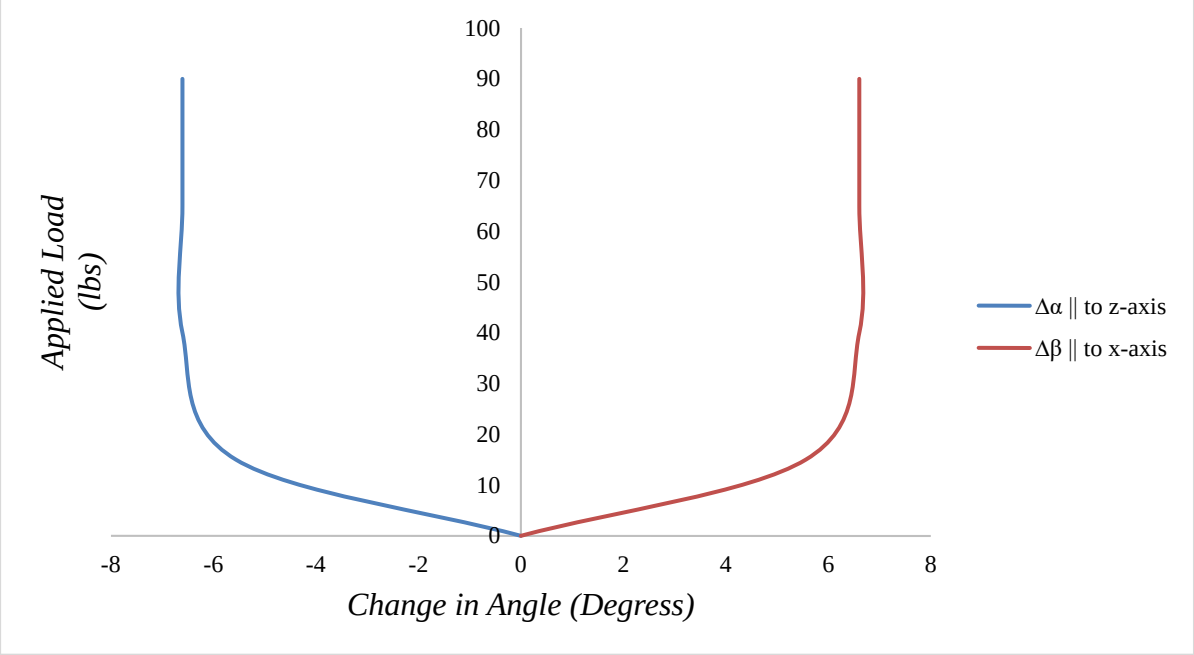

Figure (A.14): Records of Change in Angle in Rhombus 'R27' while Loading

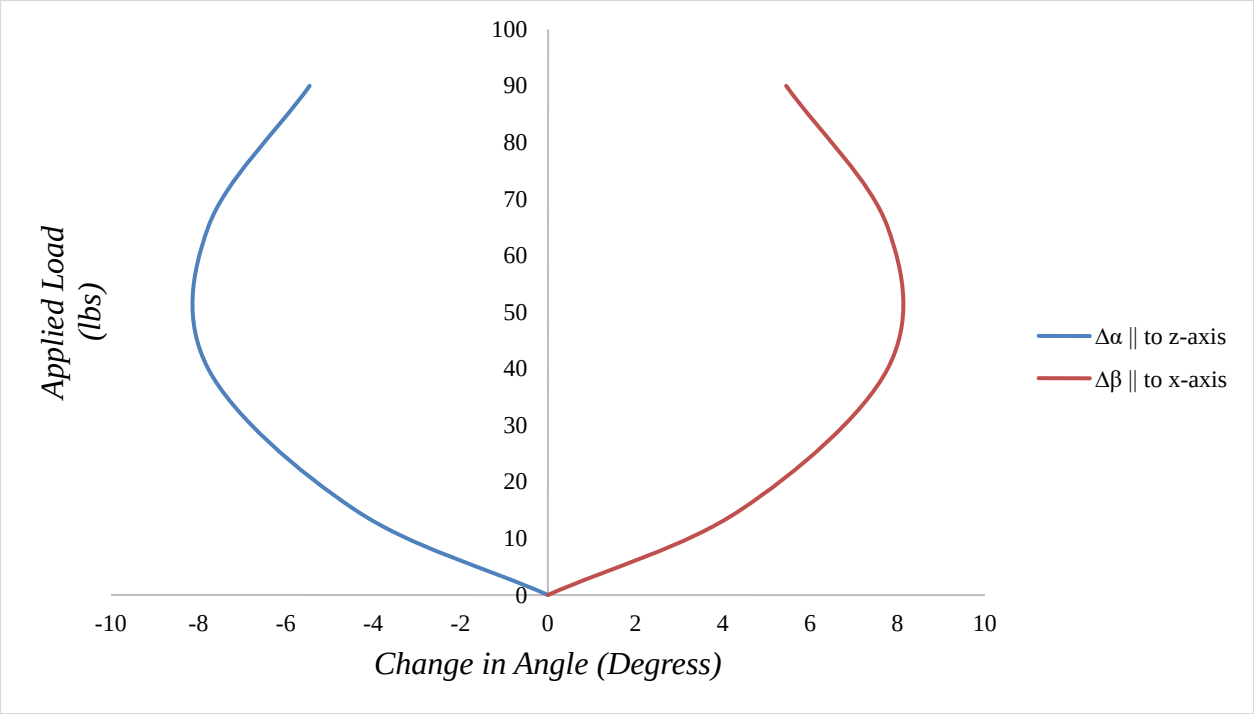

Figure (A.15): Records of Change in Angle in Rhombus 'R30' while Loading

APPENDIX (B)

RECORD OF TEST #1 UNDER UNLOADING

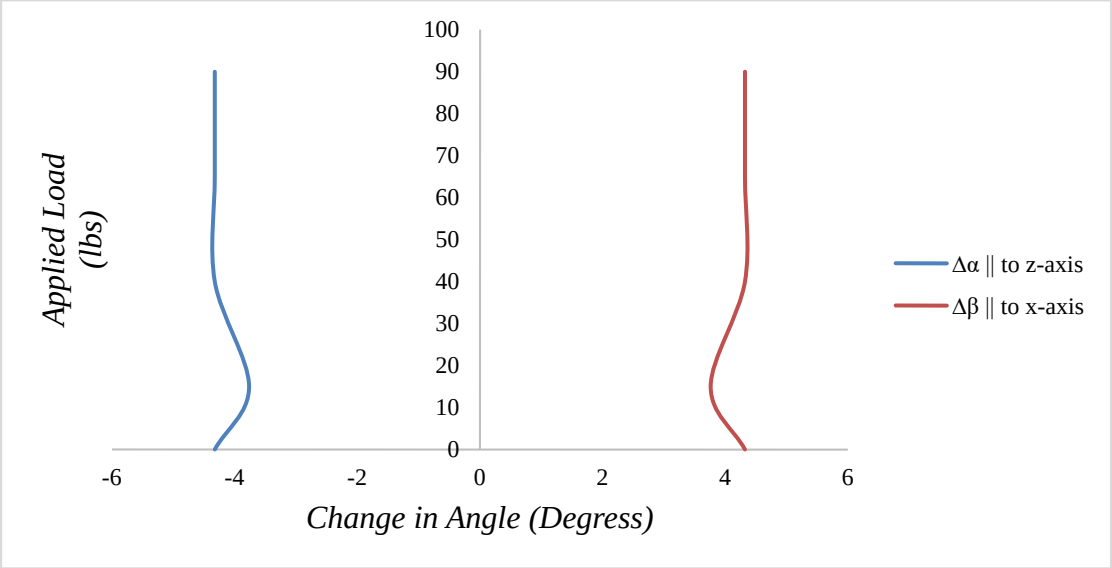

Figure (B.1): Records of Change in Angle in Rhombus 'R6' while Unloading

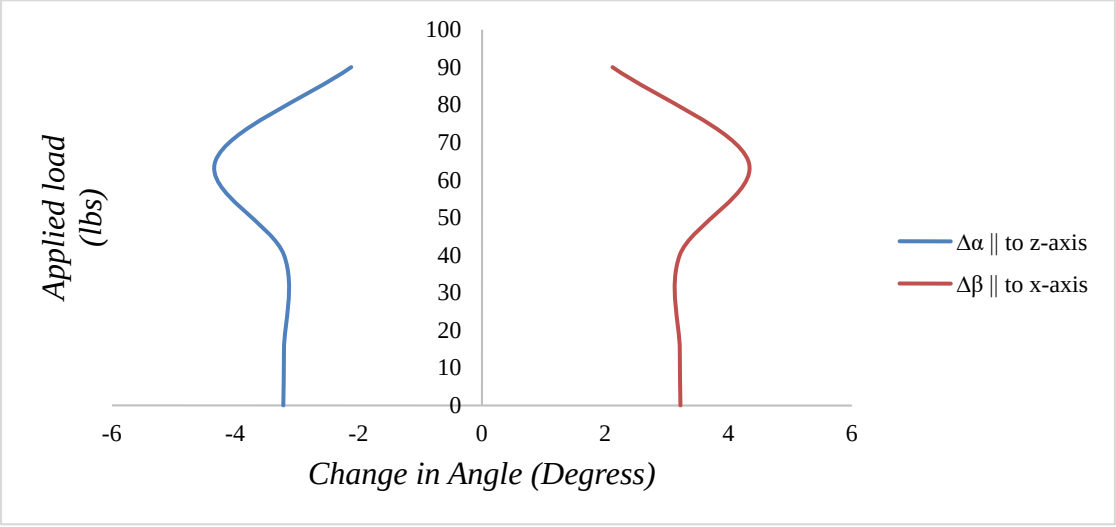

Figure (B.2): Records of Change in Angle in Rhombus 'R7' while Unloading

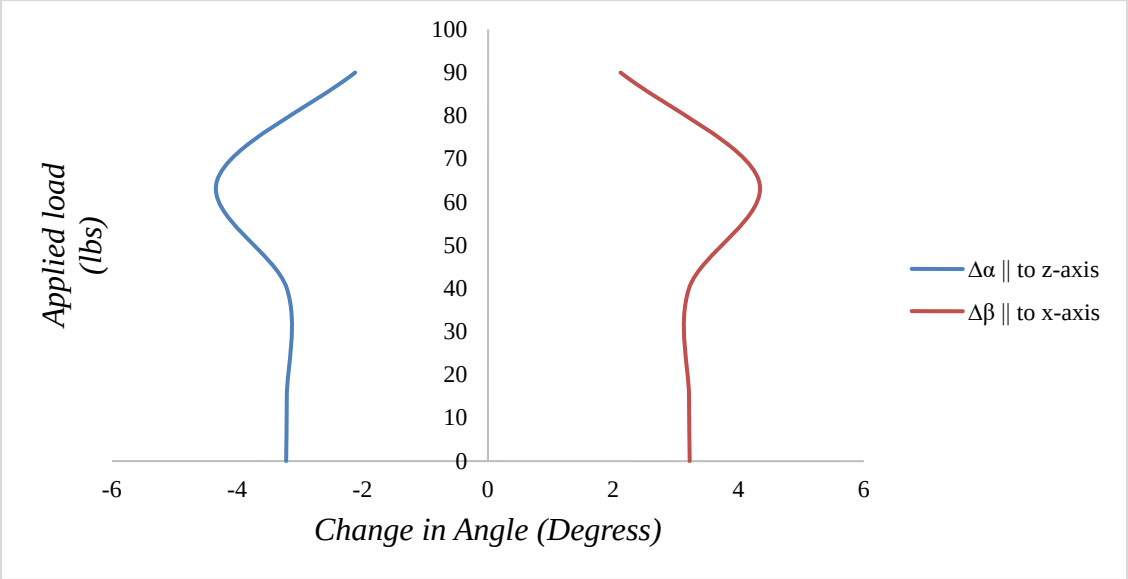

Figure (B.3): Records of Change in Angle in Rhombus 'R10' while Unloading

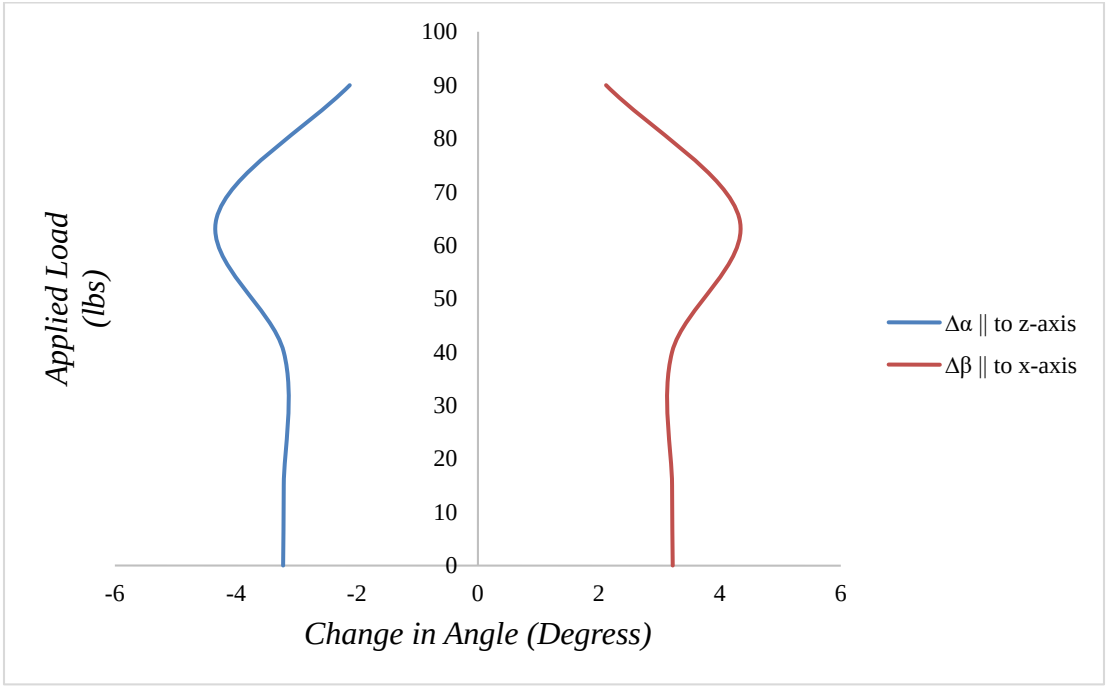

Figure (B.4): Records of Change in Angle in Rhombus 'R11' while Unloading

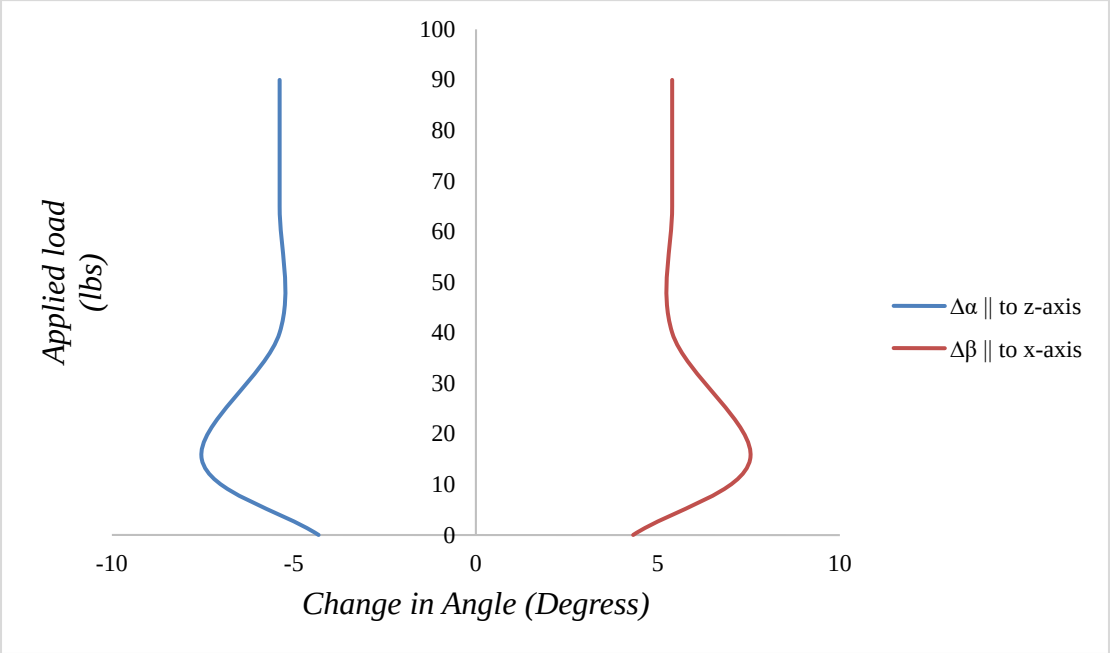

Figure (B.5): Records of Change in Angle in Rhombus 'R12' while Unloading

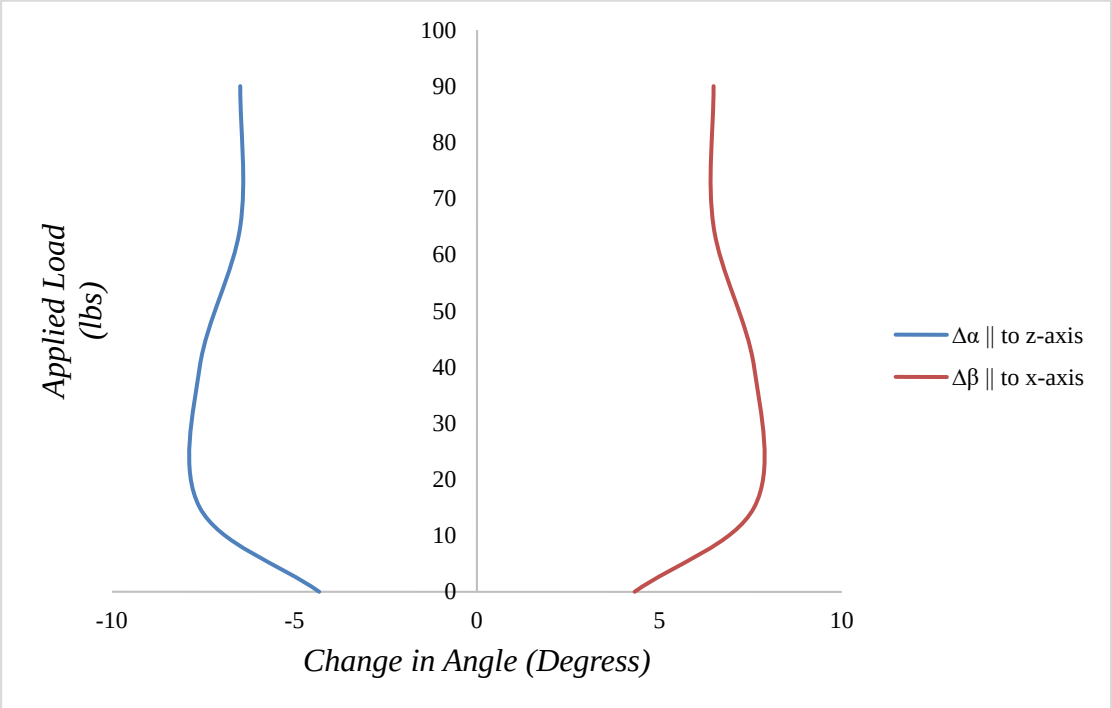

Figure (B.6): Records of Change in Angle in Rhombus 'R15' while Unloading

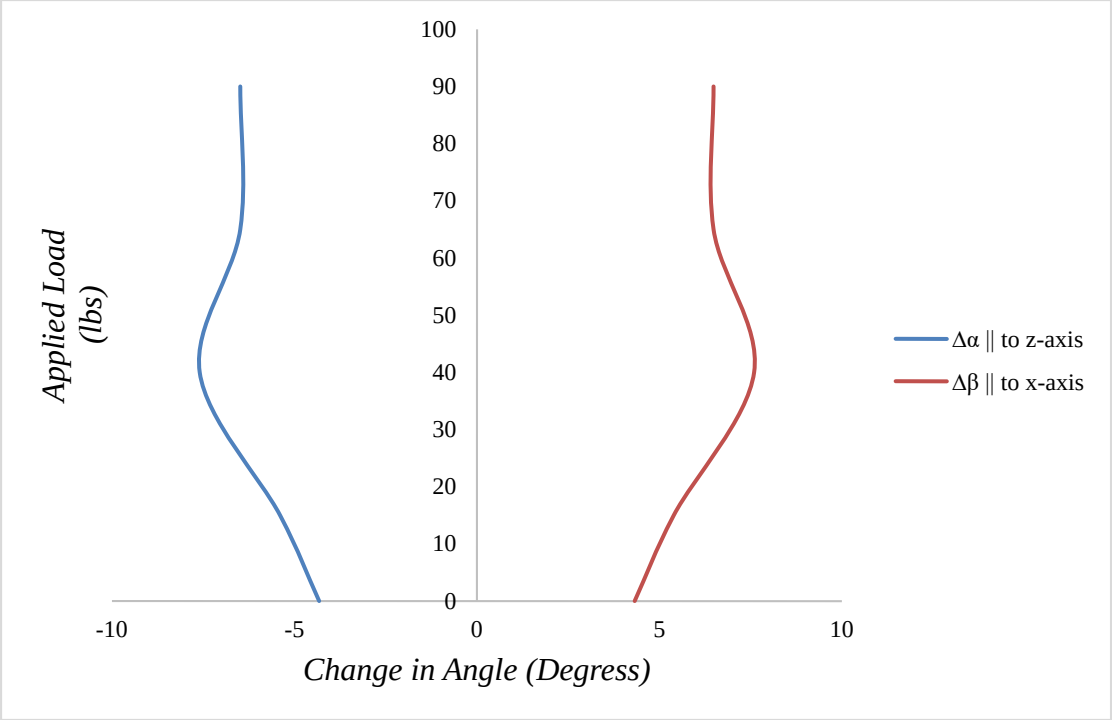

Figure (B.7): Records of Change in Angle in Rhombus 'R16' while Unloading

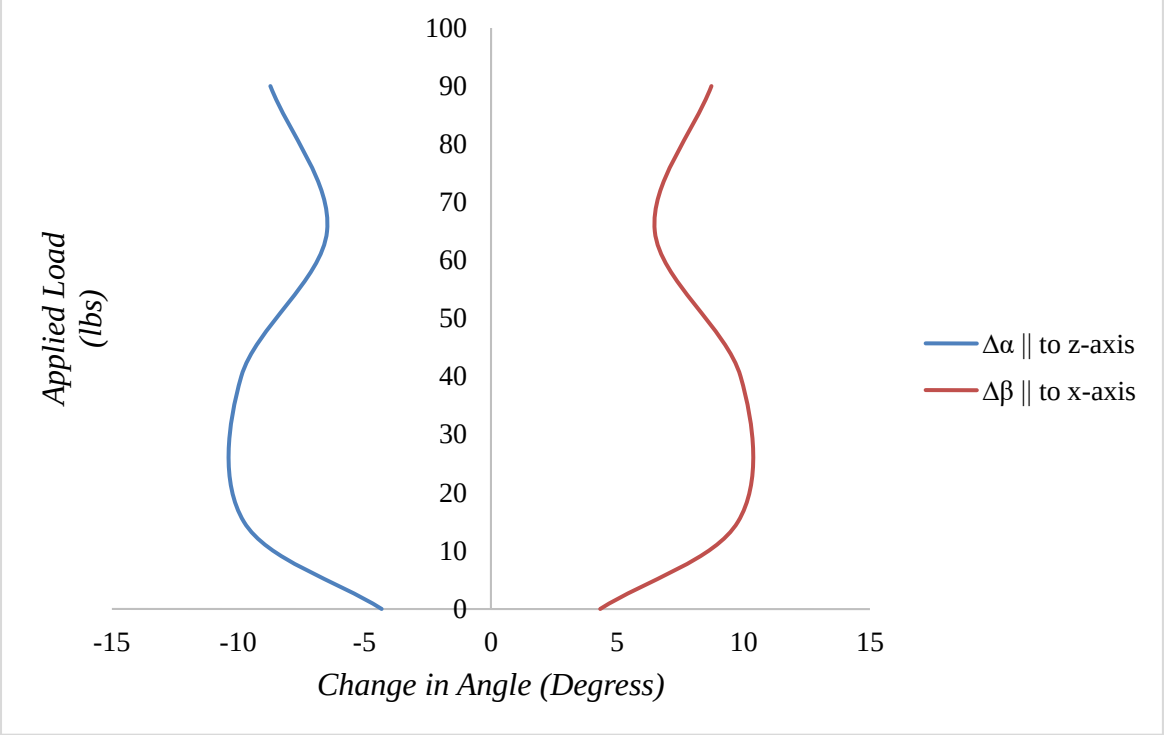

Figure (B.8): Records of Change in Angle in Rhombus 'R17' while Unloading

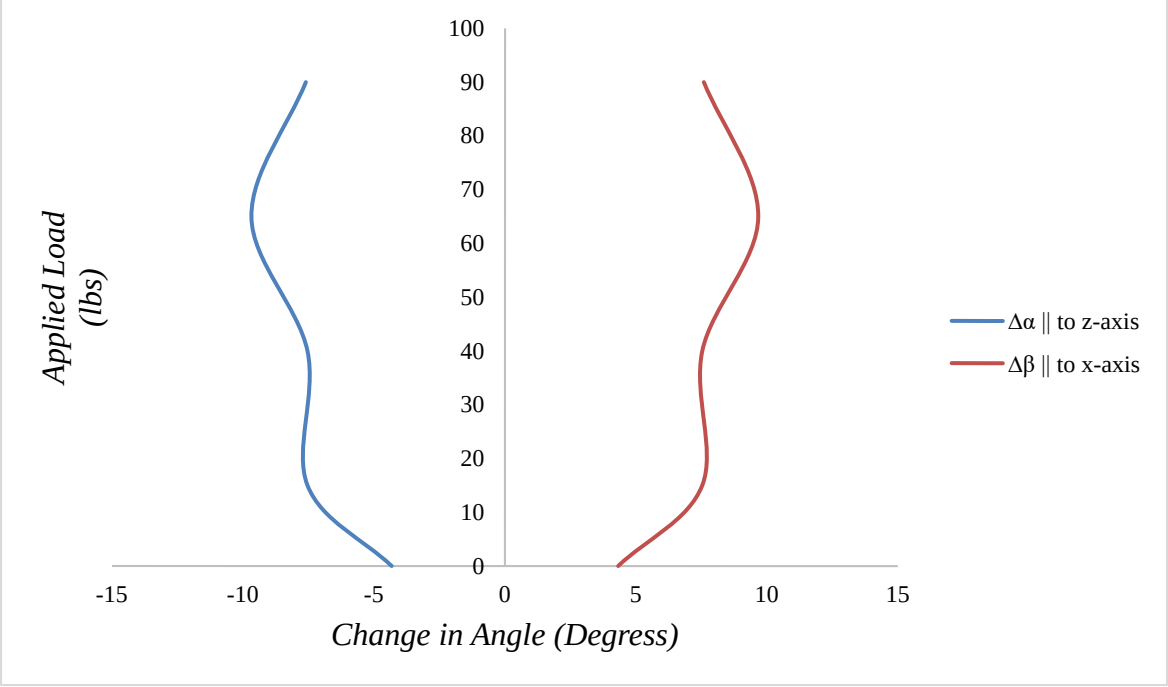

Figure (B.9): Records of Change in Angle in Rhombus 'R20' while Unloading

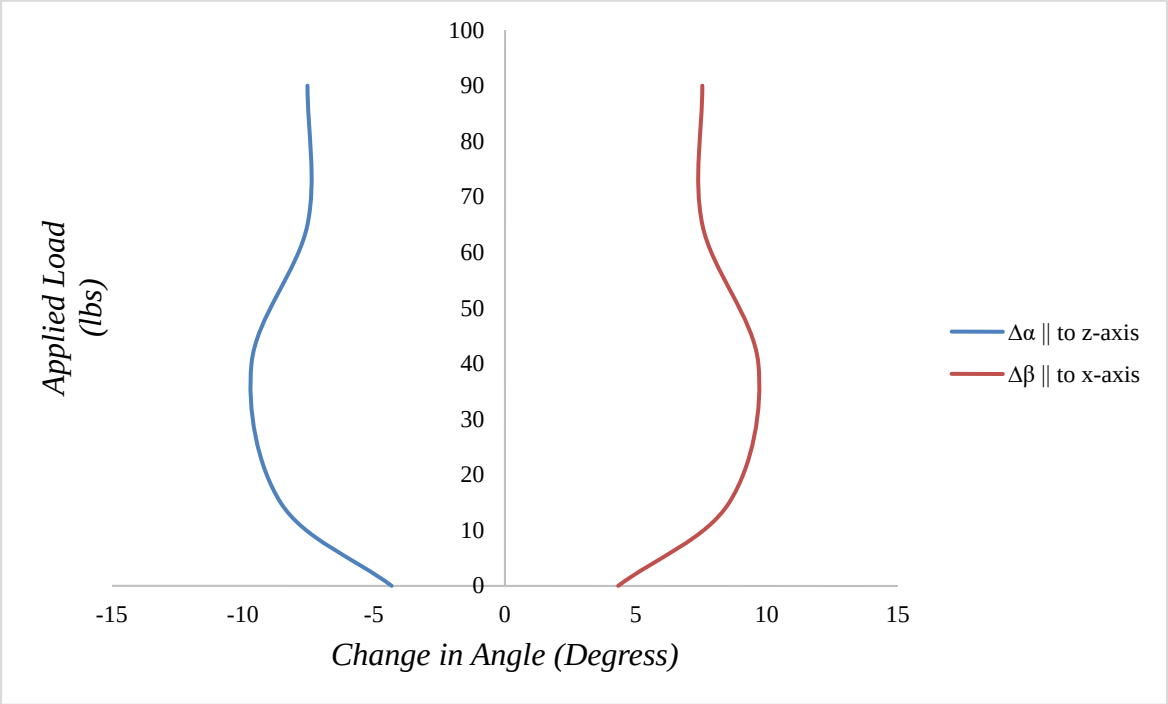

Figure (B.10): Records of Change in Angle in Rhombus 'R21' while unloading

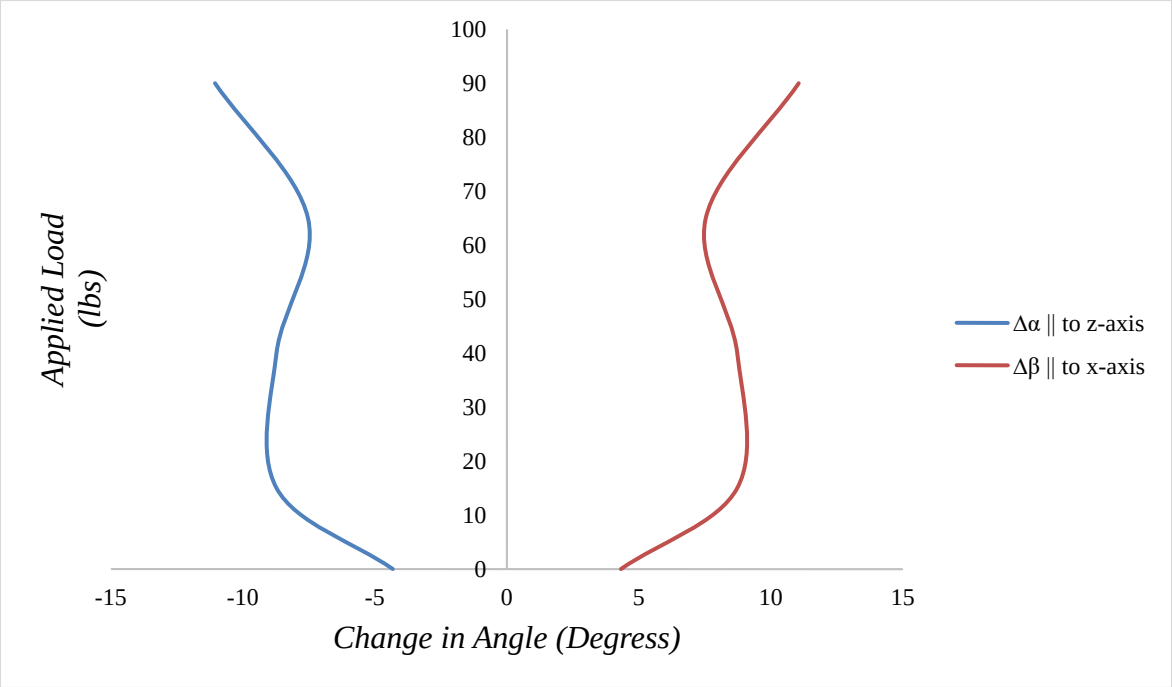

Figure (B.11): Records of Change in Angle in Rhombus 'R22' while Unloading

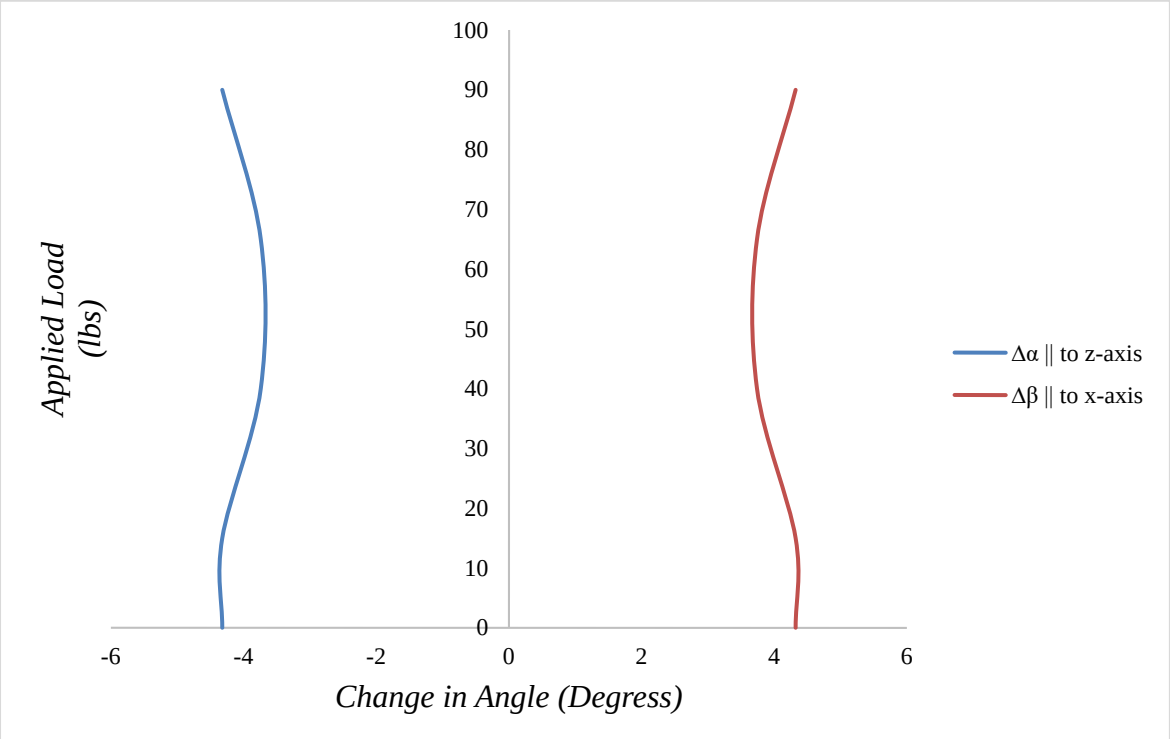

Figure (B.12): Records of Change in Angle in Rhombus 'R25' while Unloading

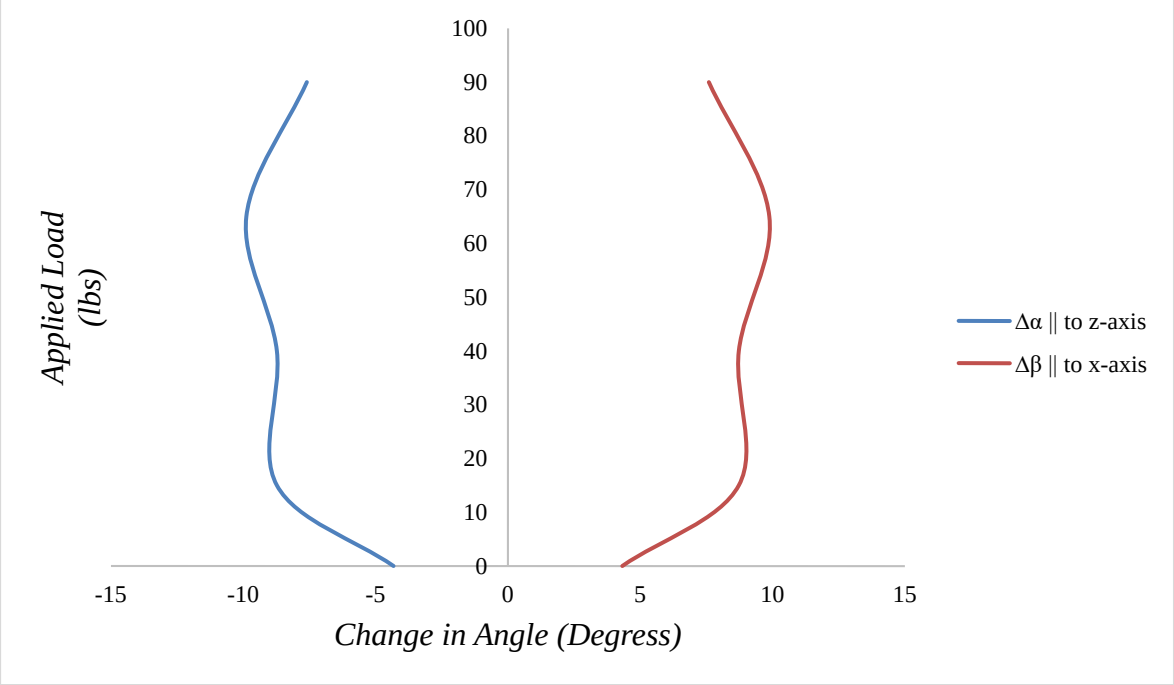

Figure (B.13): Records of Change in Angle in Rhombus 'R26' while Unloading

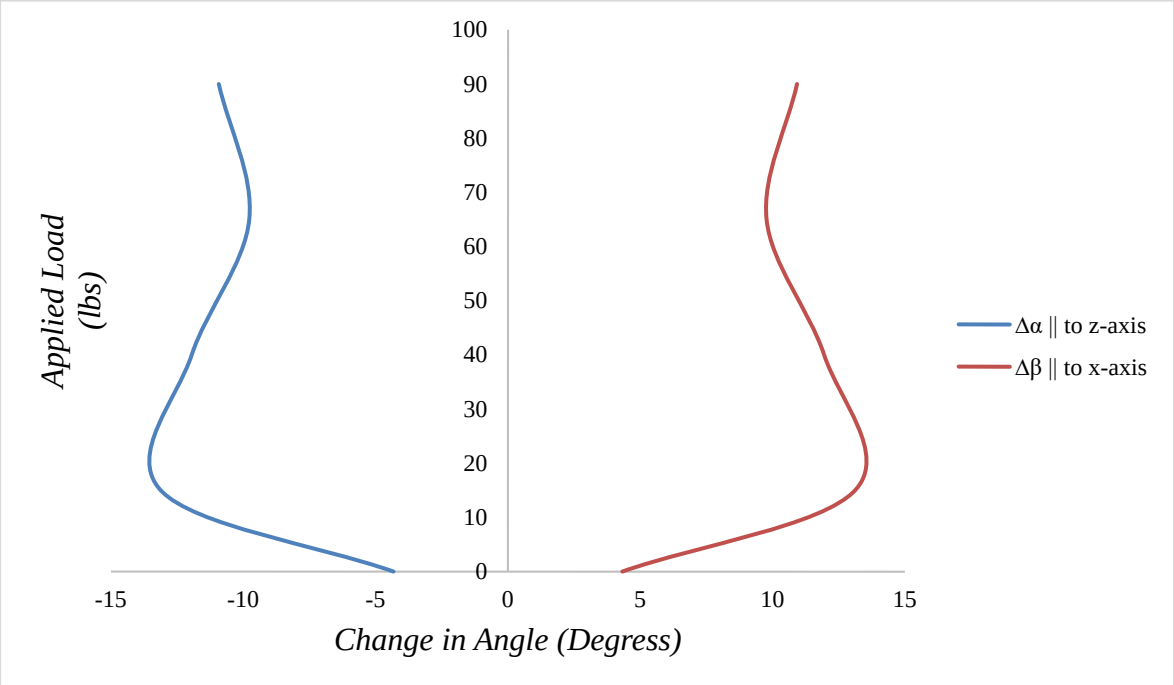

Figure (B.14): Records of Change in Angle in Rhombus 'R27' while unloading

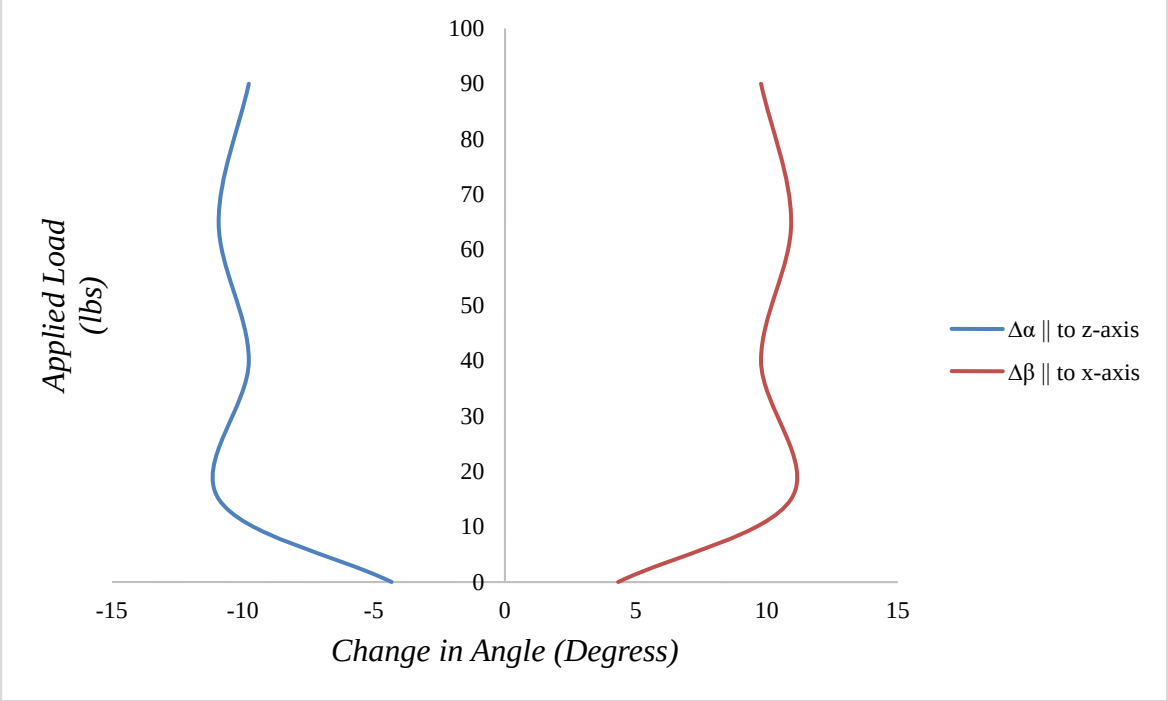

Figure (B.15): Records of Change in Angle in Rhombus 'R30' while Unloading

APPENDIX (C)

RECORD OF TEST #2 UNDER LOADING

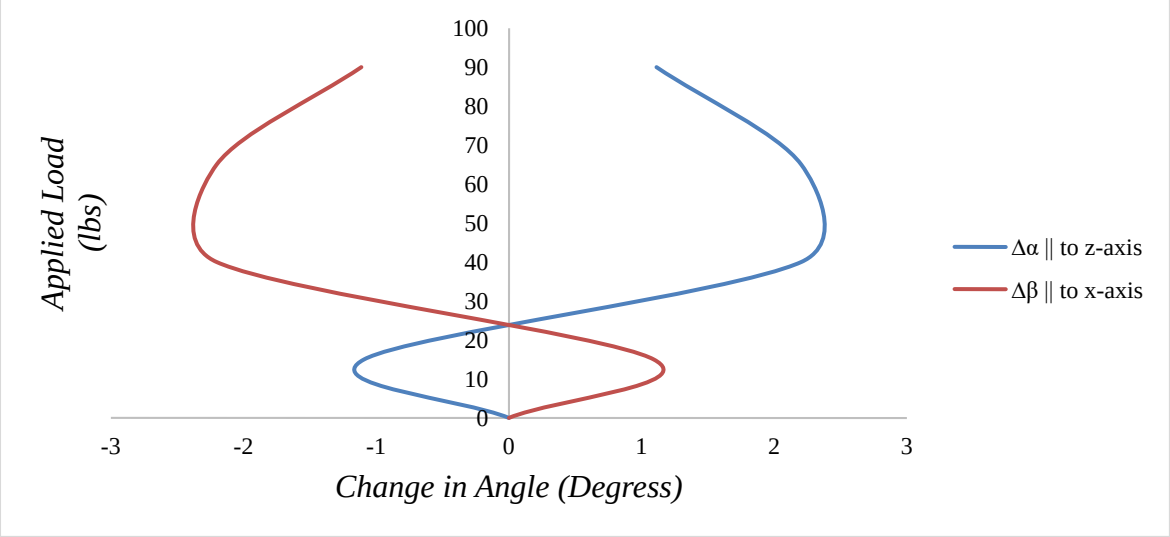

Figure (C.1): Records of Change in Angle in Rhombus 'R6' while Loading

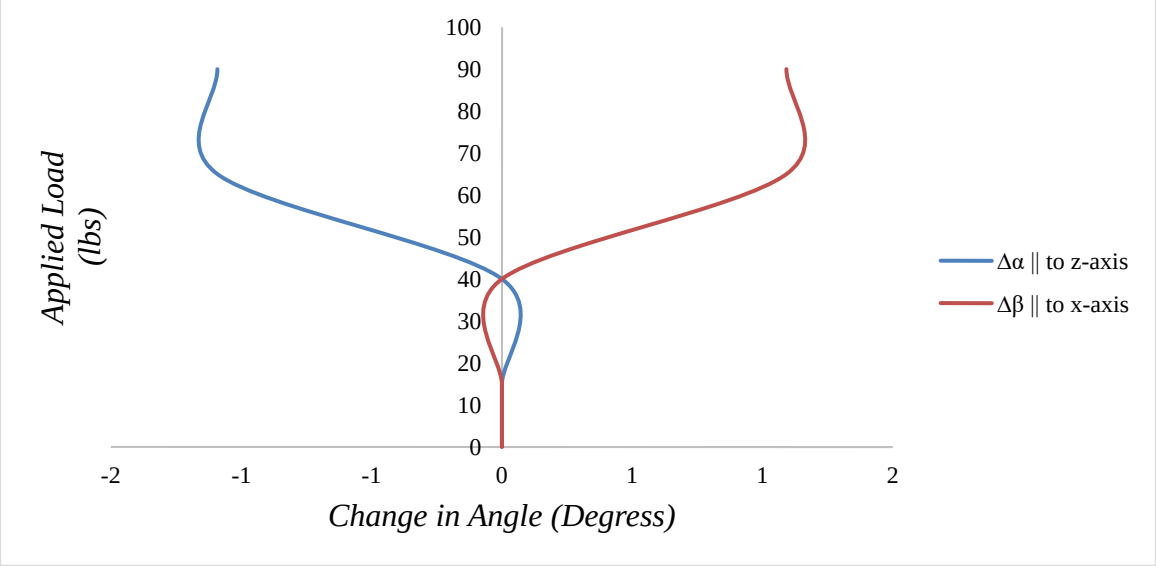

Figure (C.2): Records of Change in Angle in Rhombus 'R7' while Loading

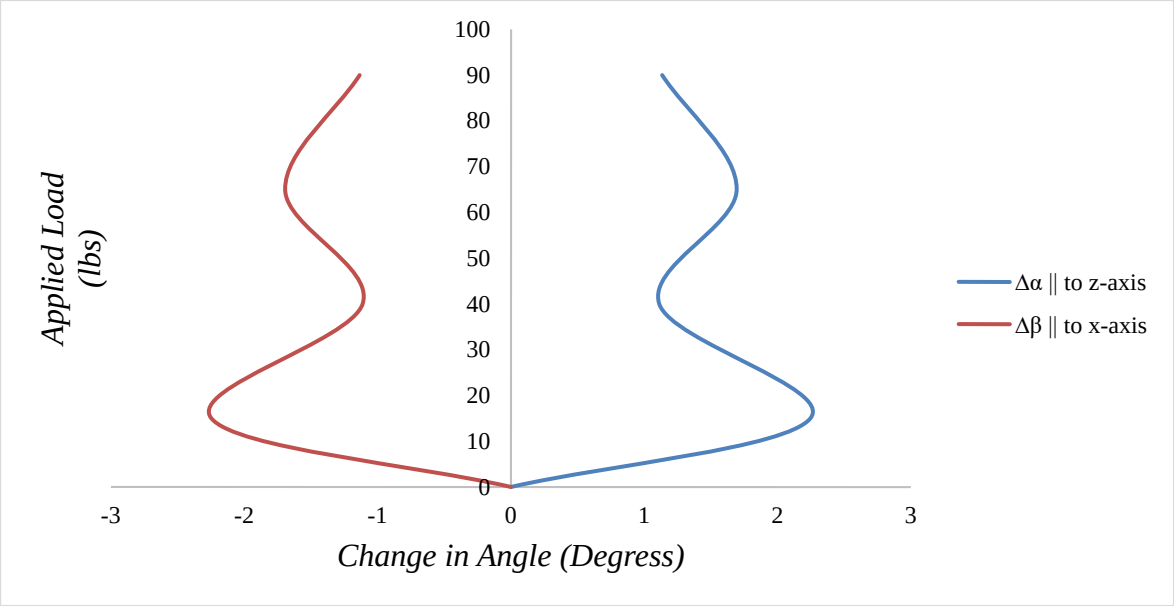

Figure (C.3): Records of Change in Angle in Rhombus 'R10' while Loading

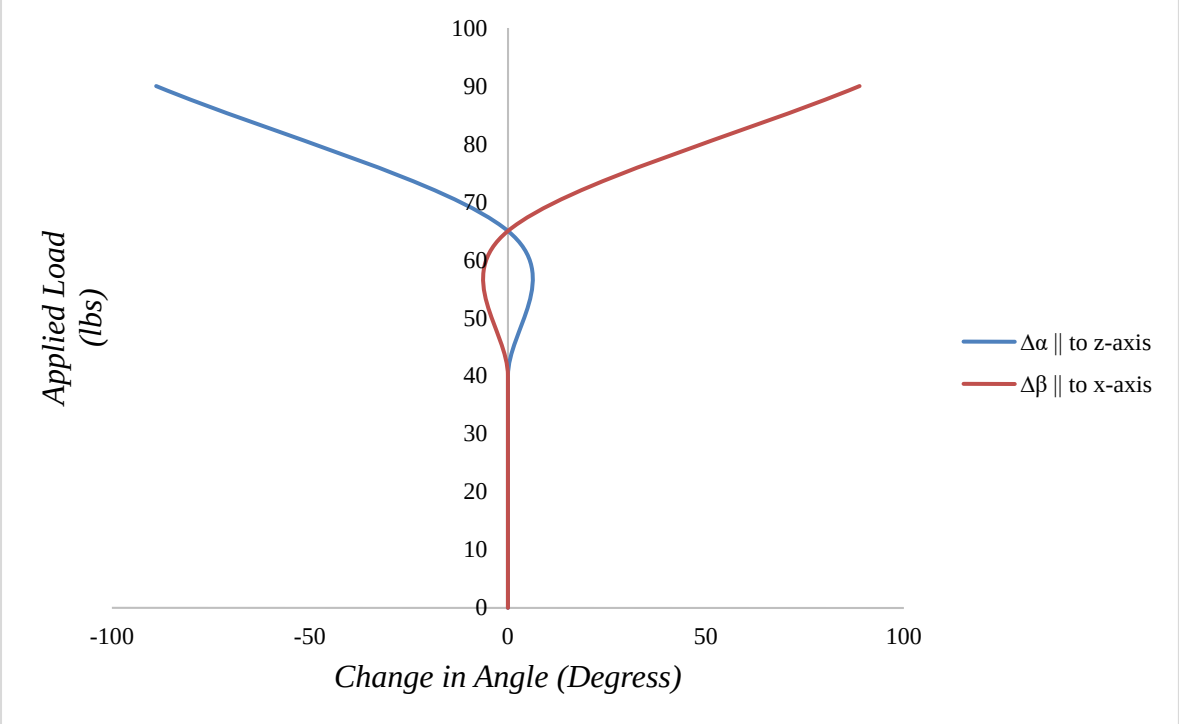

Figure (C.4): Records of Change in Angle in Rhombus 'R11' while Loading

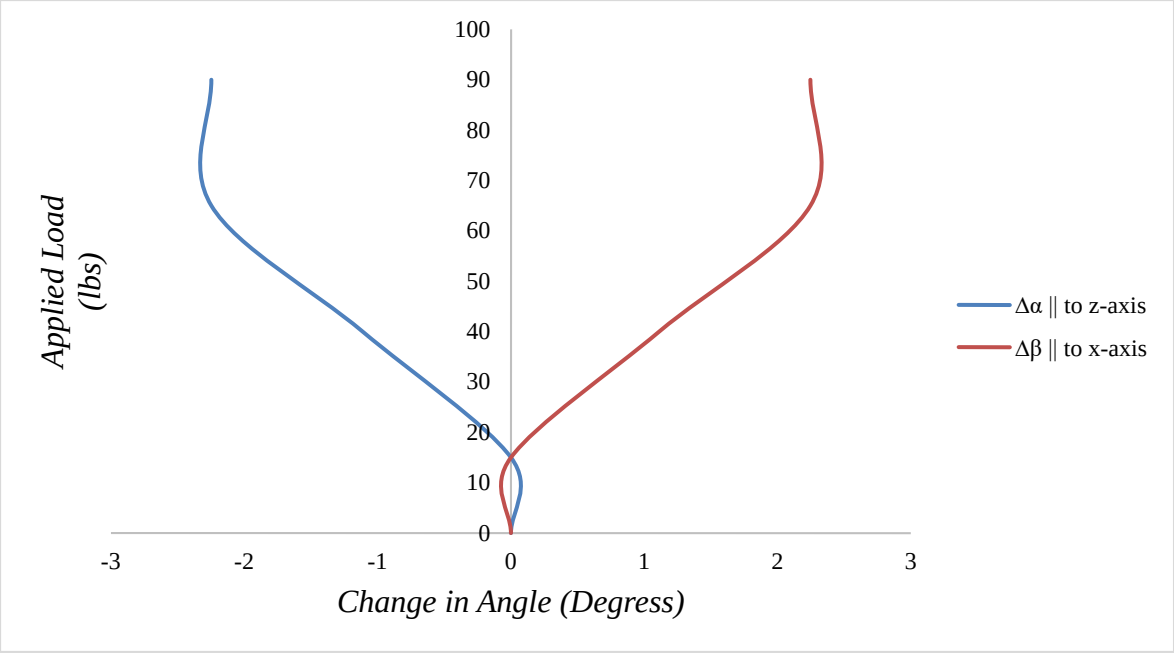

Figure (C.5): Records of Change in Angle in Rhombus 'R12' while Loading

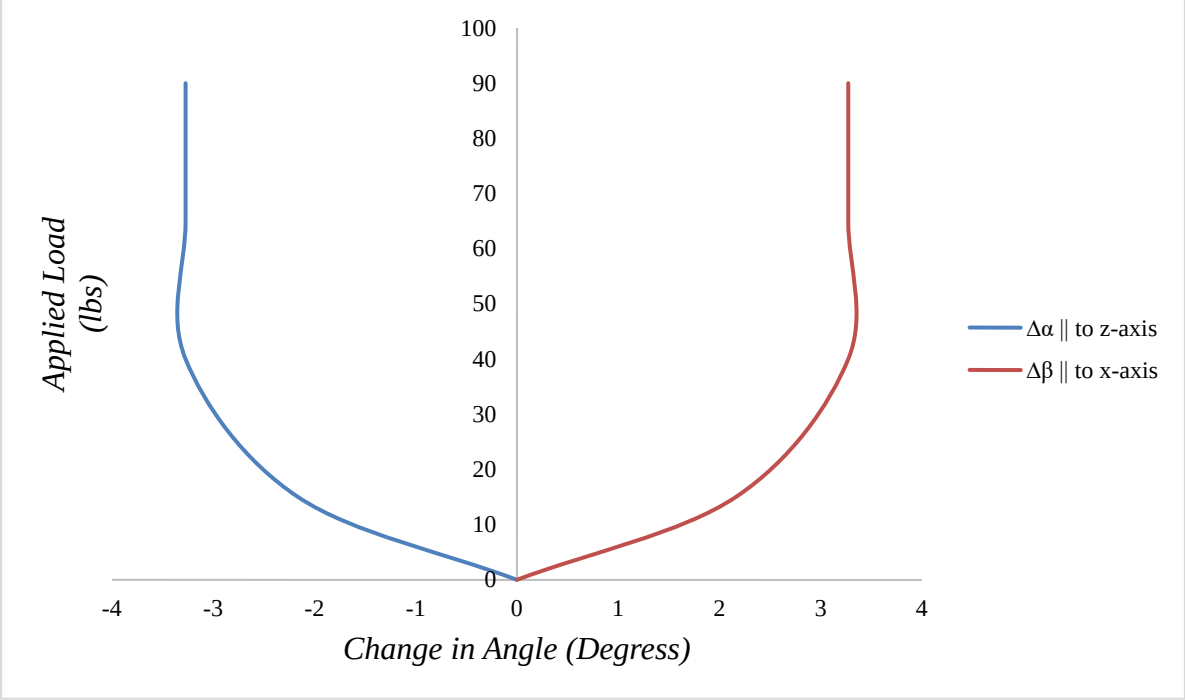

Figure (C.6): Records of Change in Angle in Rhombus 'R15' while Loading

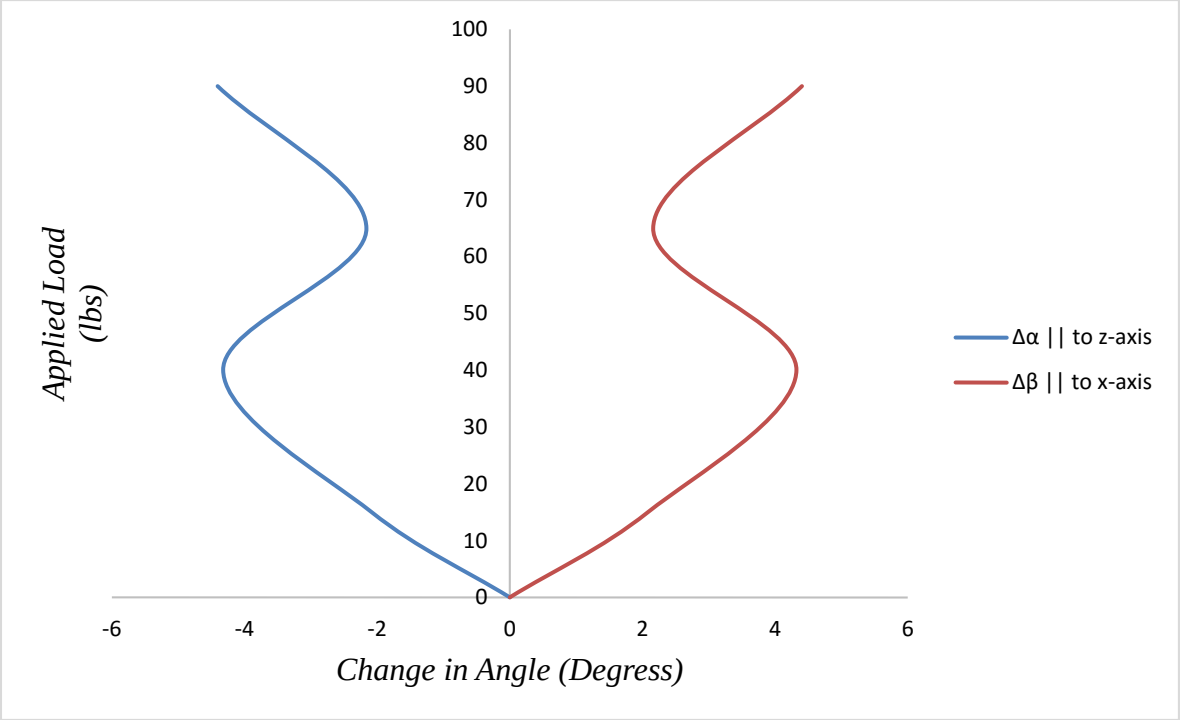

Figure (C.7): Records of Change in Angle in Rhombus 'R16' while Loading

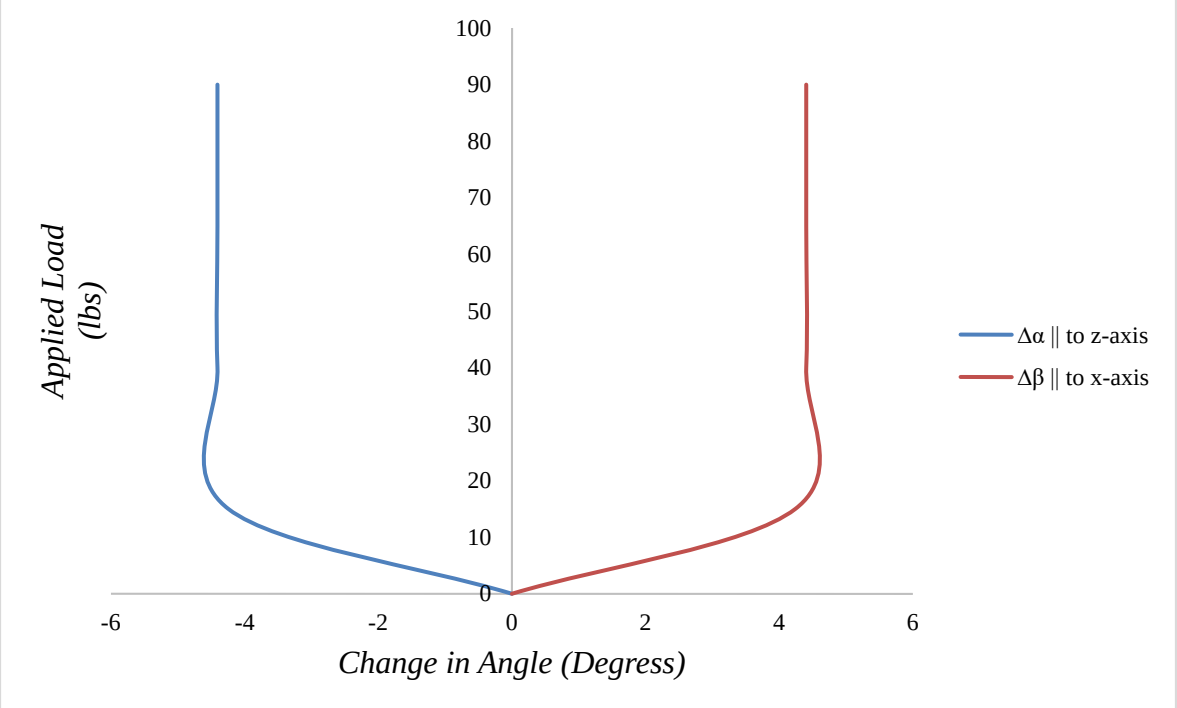

Figure (C.8): Records of Change in Angle in Rhombus 'R17' while Loading

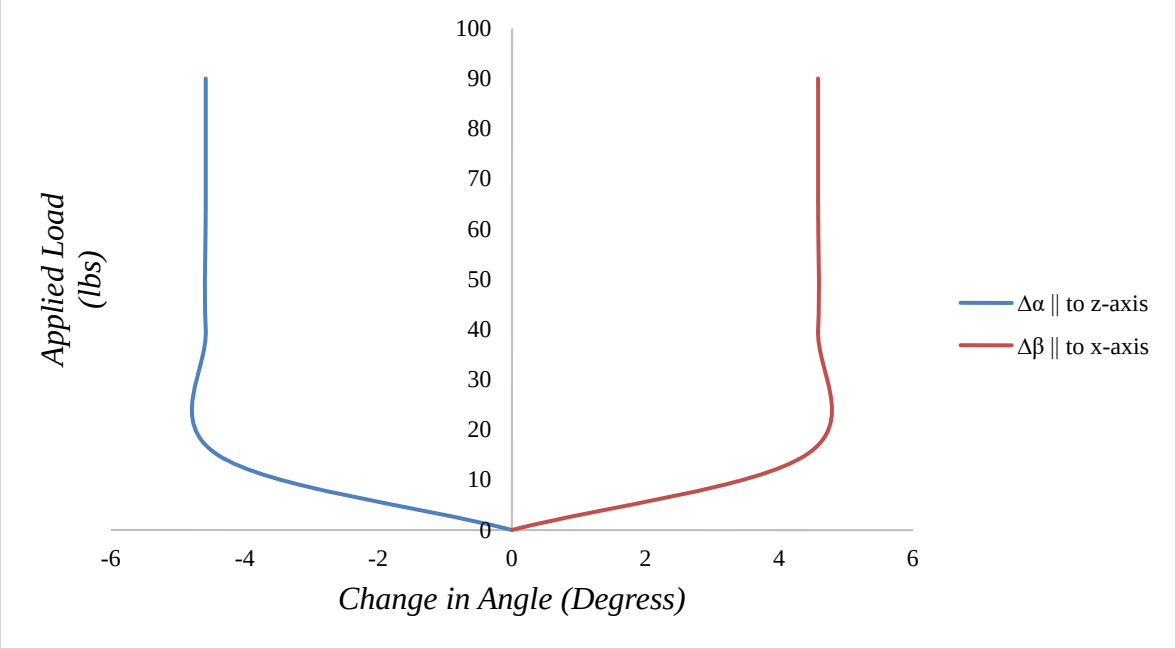

Figure (C.9): Records of Change in Angle in Rhombus 'R20' while Loading

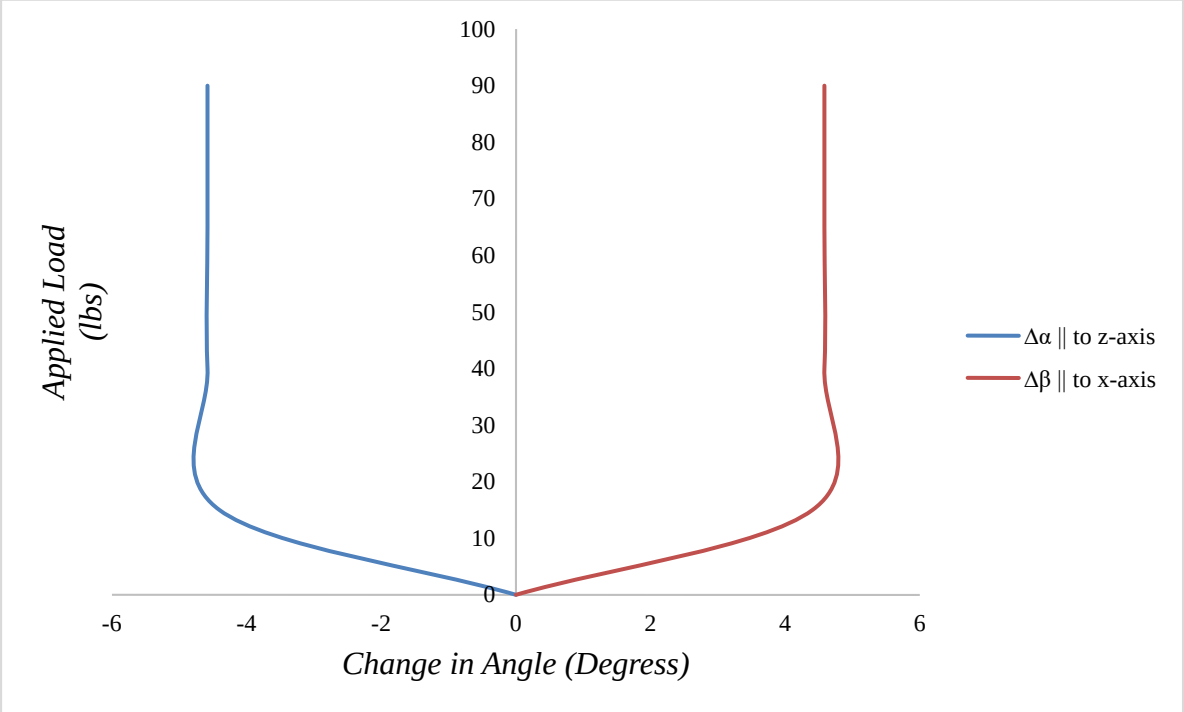

Figure (C.10): Records of Change in Angle in Rhombus 'R21' while Loading

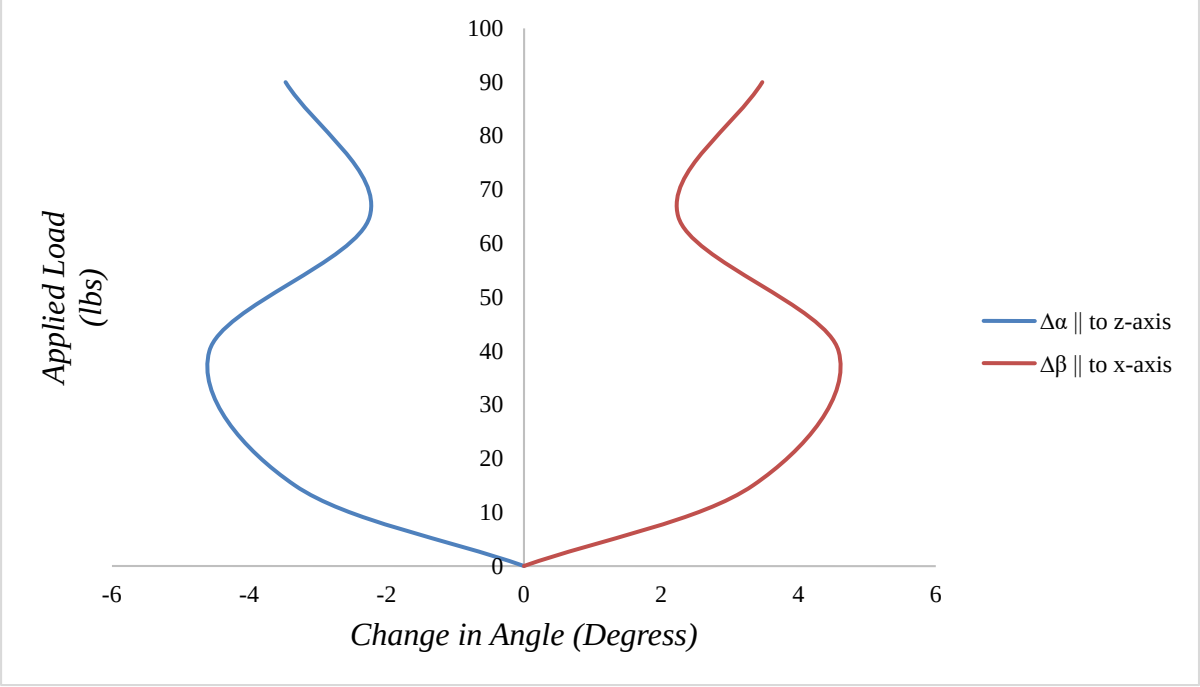

Figure (C.11): Records of Change in Angle in Rhombus 'R22' while Loading

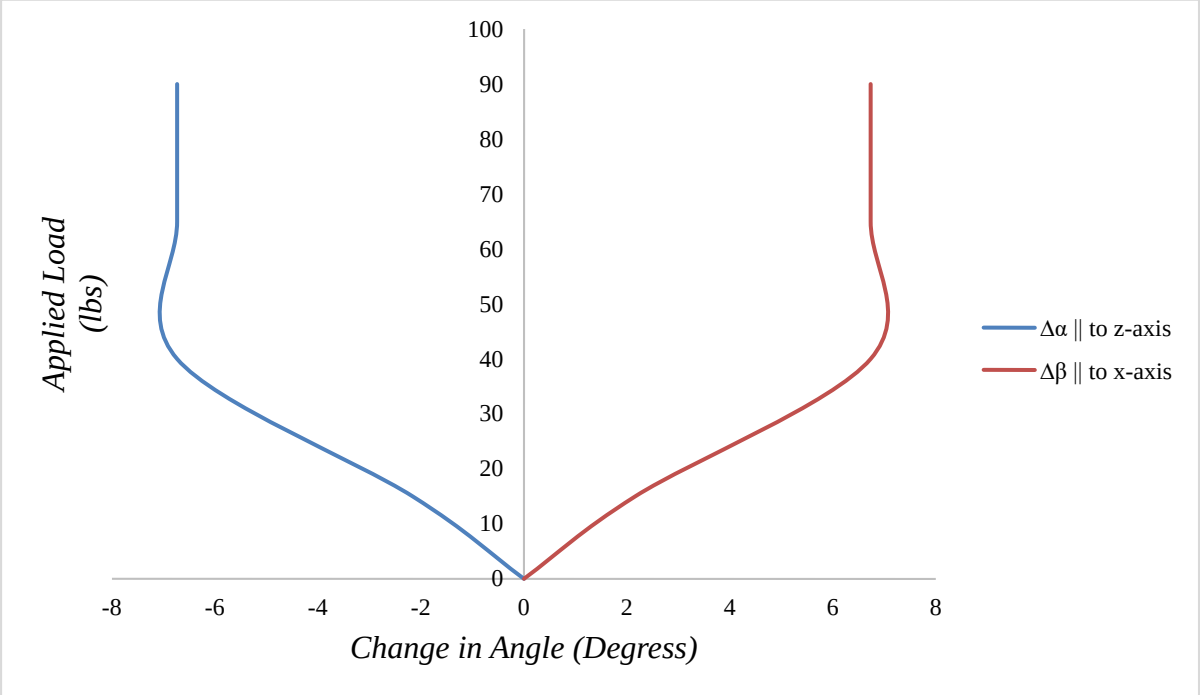

Figure (C.12): Records of Change in Angle in Rhombus 'R25' while Loading

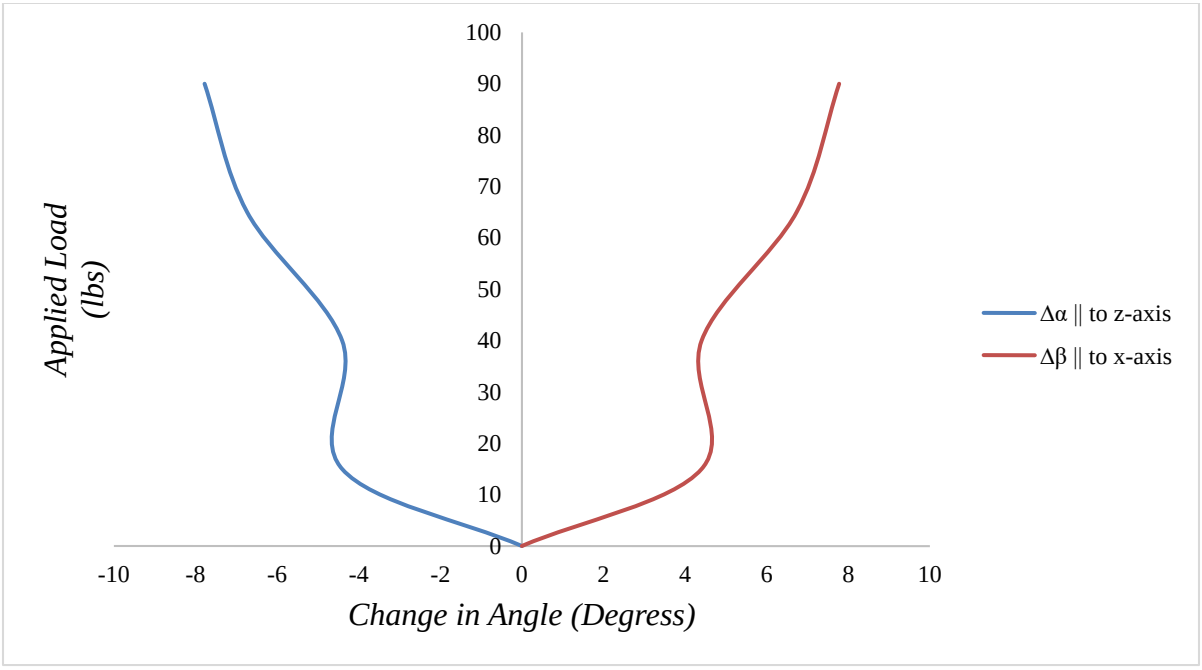

Figure (C.13): Records of Change in Angle in Rhombus 'R26' while Loading

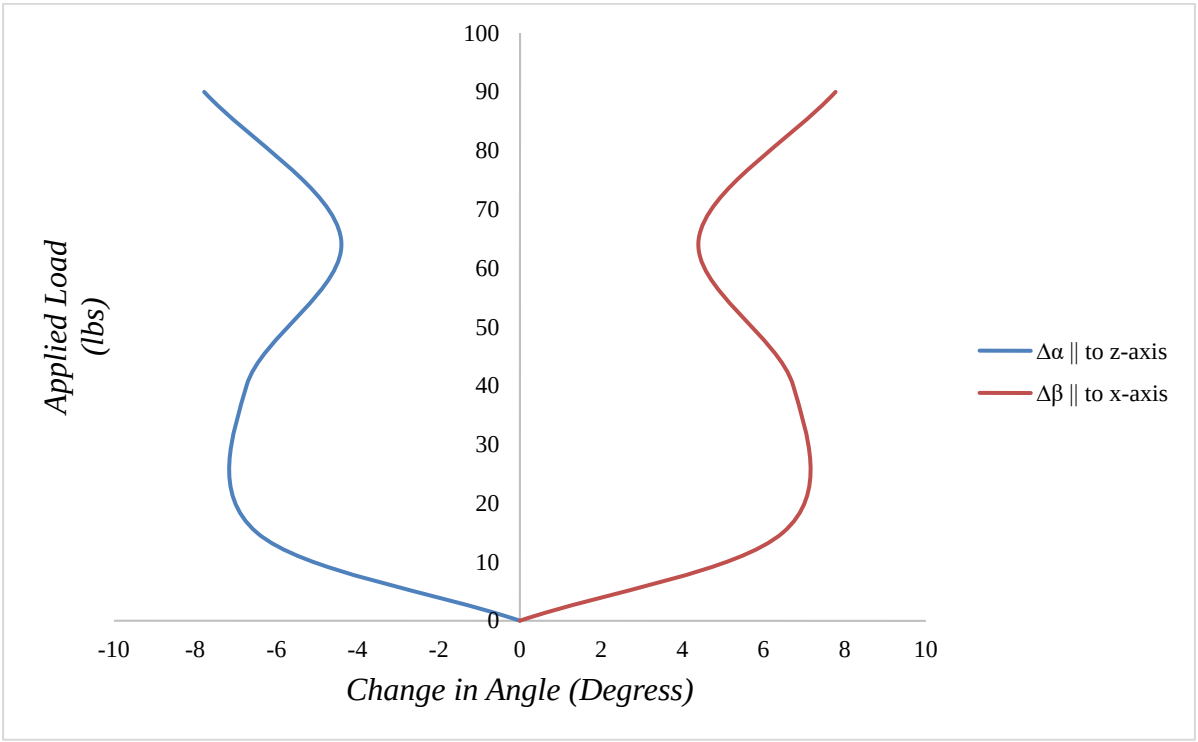

Figure (C.14): Records of Change in Angle in Rhombus 'R27' while Loading

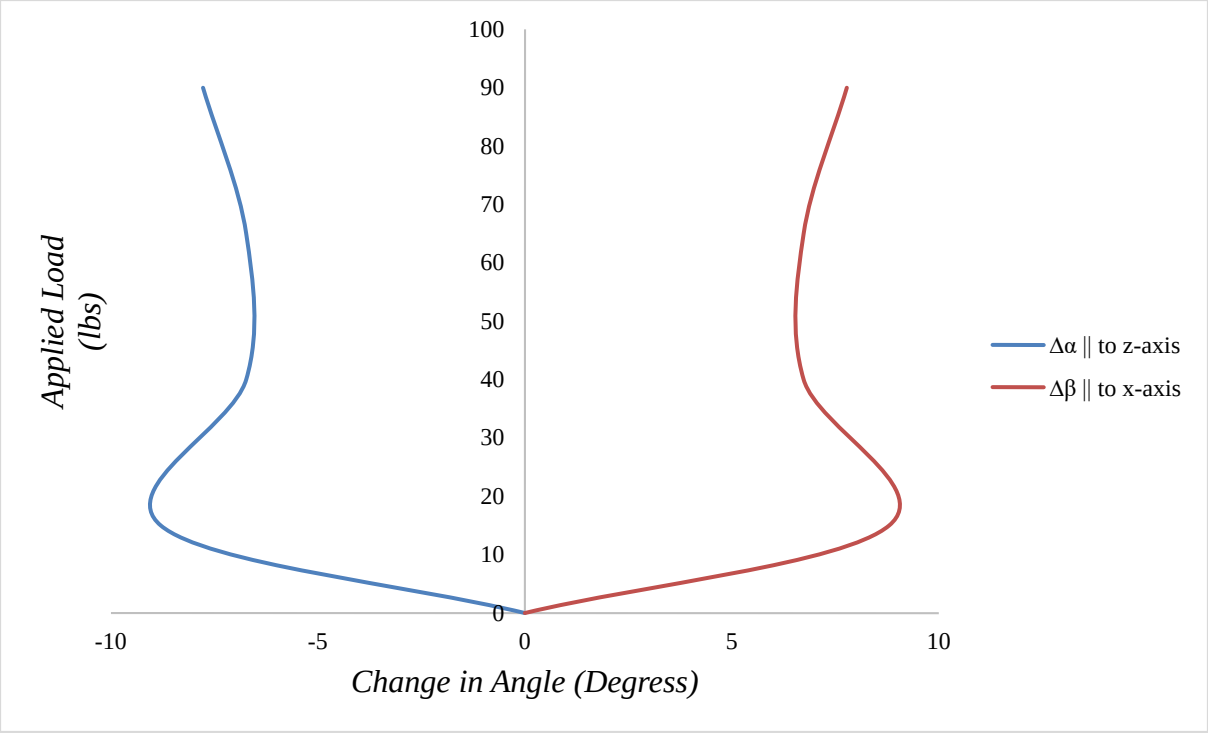

Figure (C.15): Records of Change in Angle in Rhombus 'R30' while Loading

APPENDIX (D)

RECORD OF TEST #2 UNDER UNLOADING

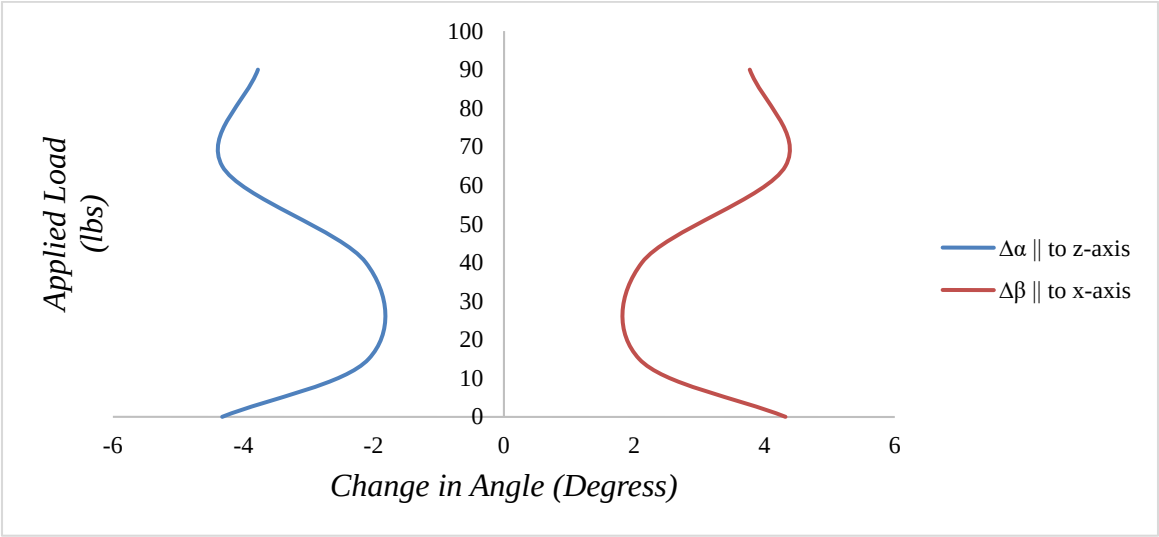

Figure (D.1): Records of Change in Angle in Rhombus 'R6' while Unloading

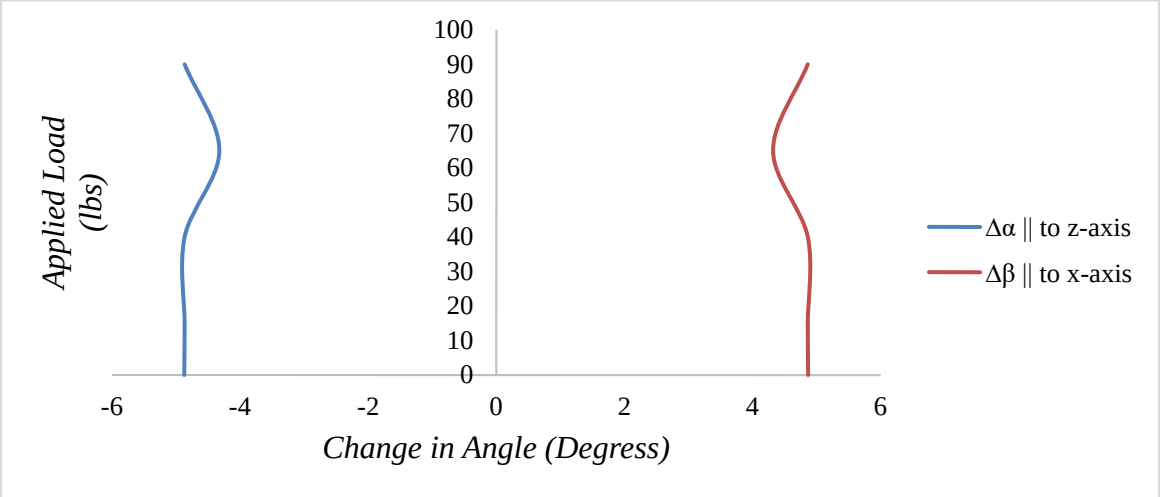

Figure (D.2): Records of Change in Angle in Rhombus 'R7' while Unloading

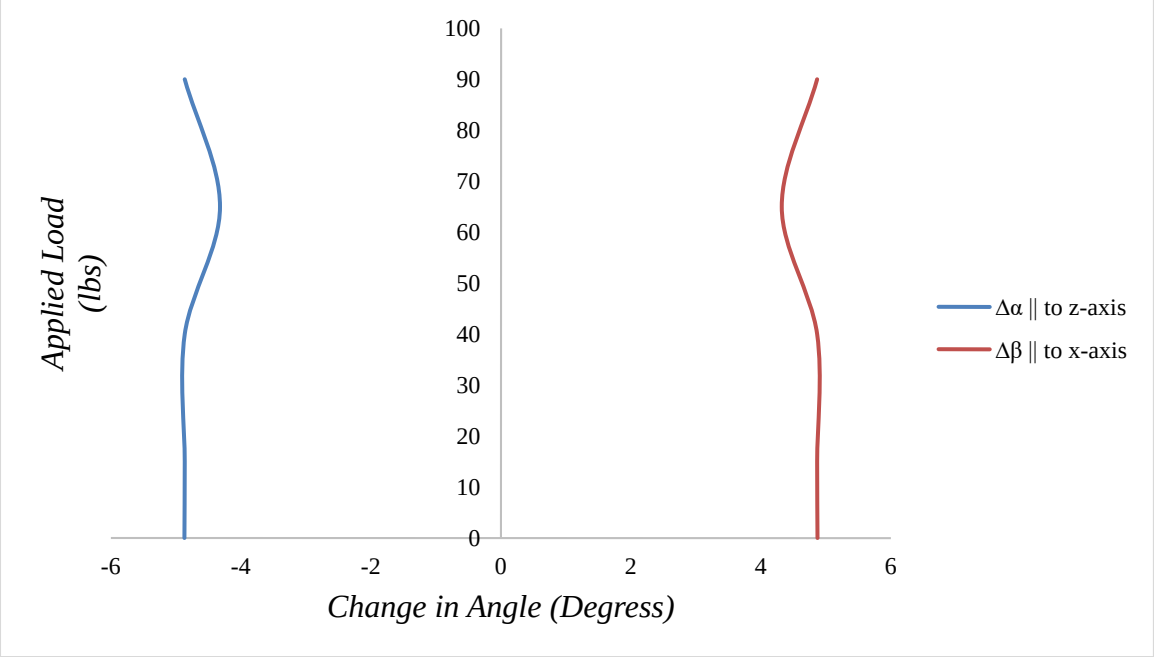

Figure (D.3): Records of Change in Angle in Rhombus 'R10' while Unloading

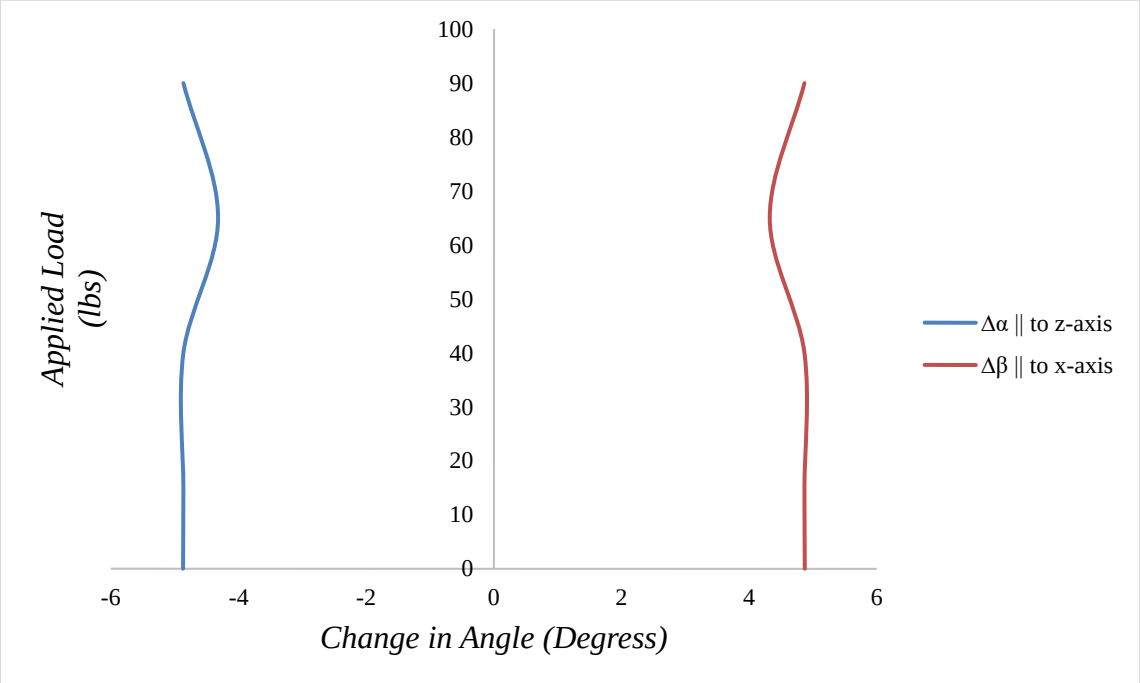

Figure (D.4): Records of Change in Angle in Rhombus 'R11' while Unloading

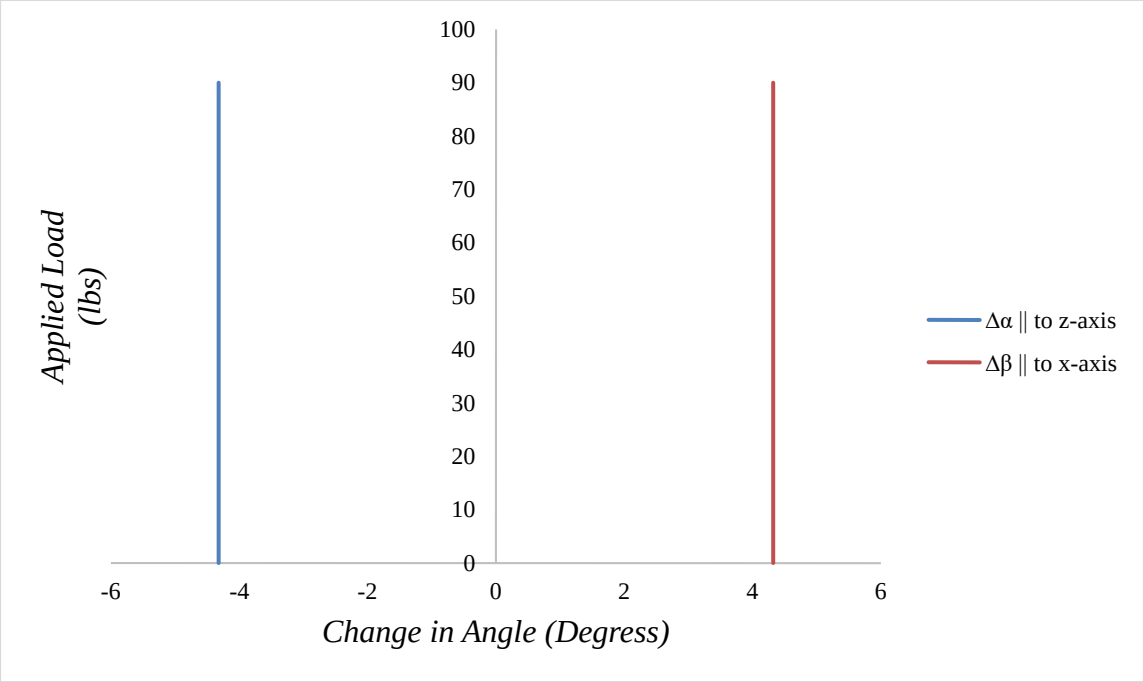

Figure (D.5): Records of Change in Angle in Rhombus 'R12' while Unloading

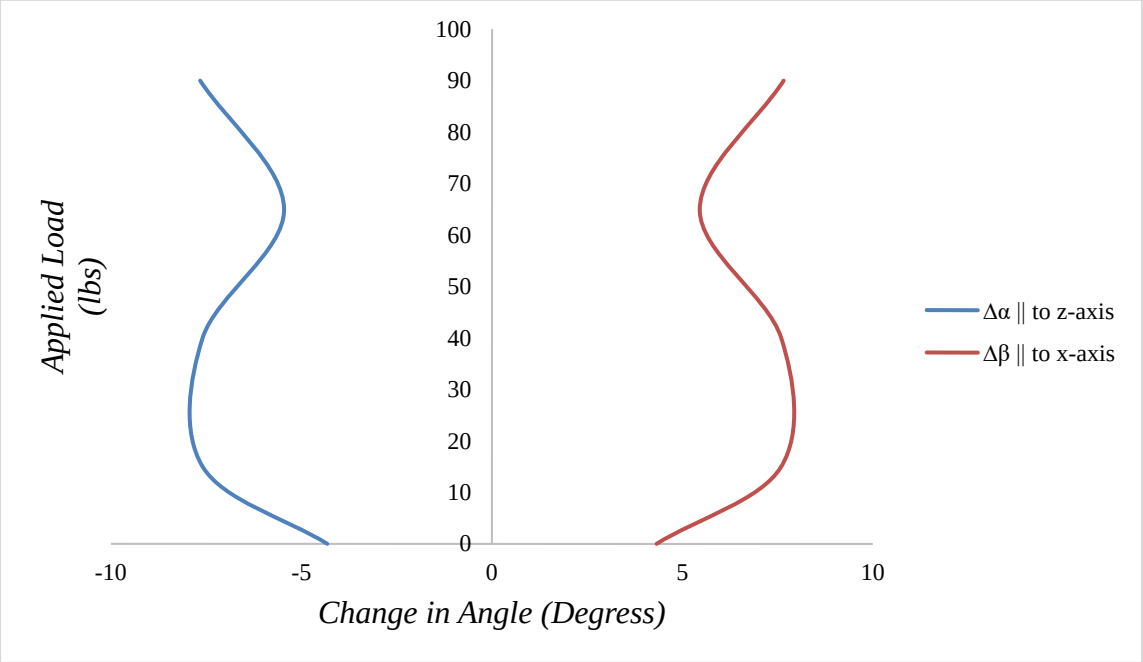

Figure (D.6): Records of Change in Angle in Rhombus 'R15' while Unloading

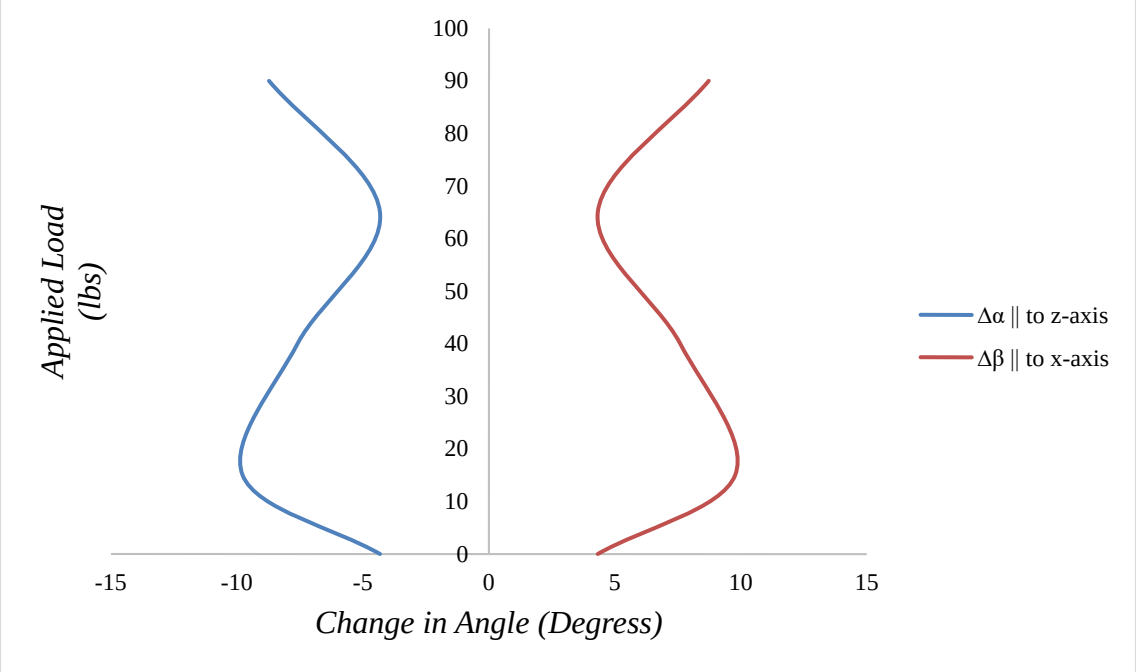

Figure (D.7): Records of Change in Angle in Rhombus 'R16' while Unloading

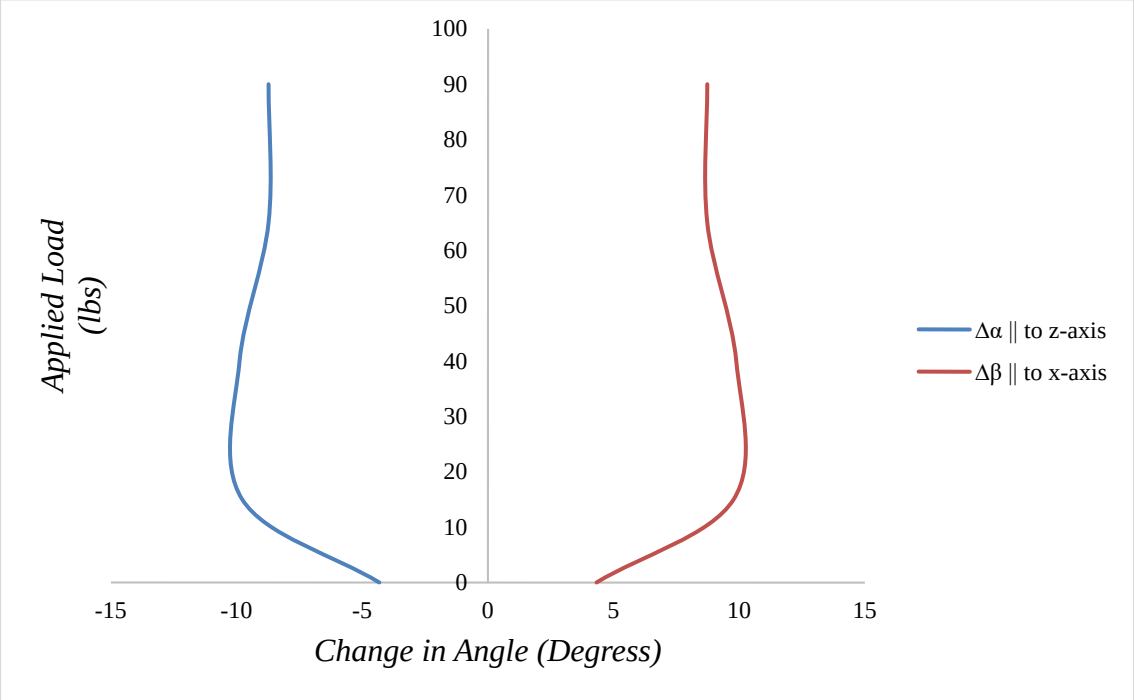

Figure (D.8): Records of Change in Angle in Rhombus 'R17' while Unloading

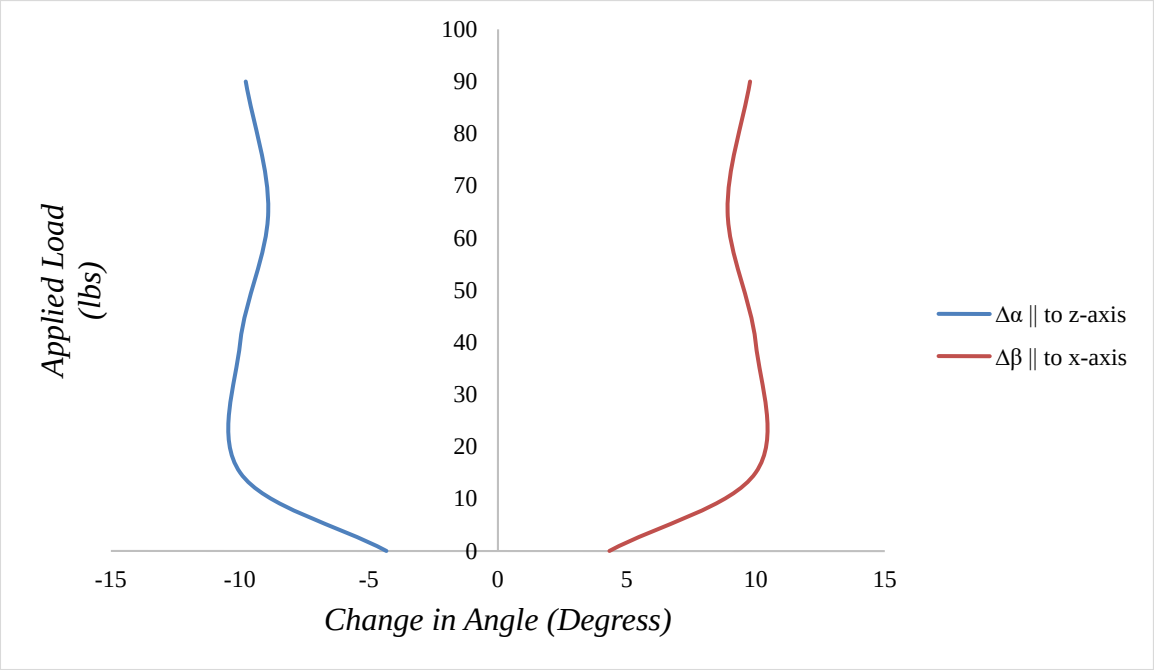

Figure (D.9): Records of Change in Angle in Rhombus 'R20' while Unloading

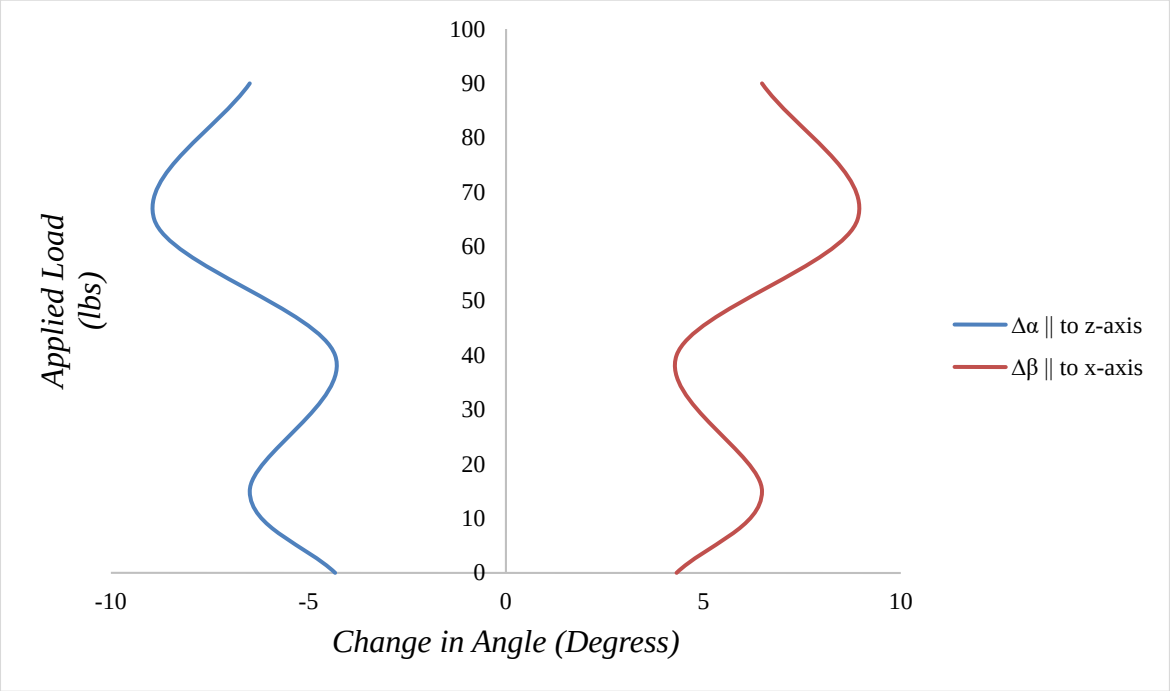

Figure (D.10): Records of Change in Angle in Rhombus 'R21' while Unloading

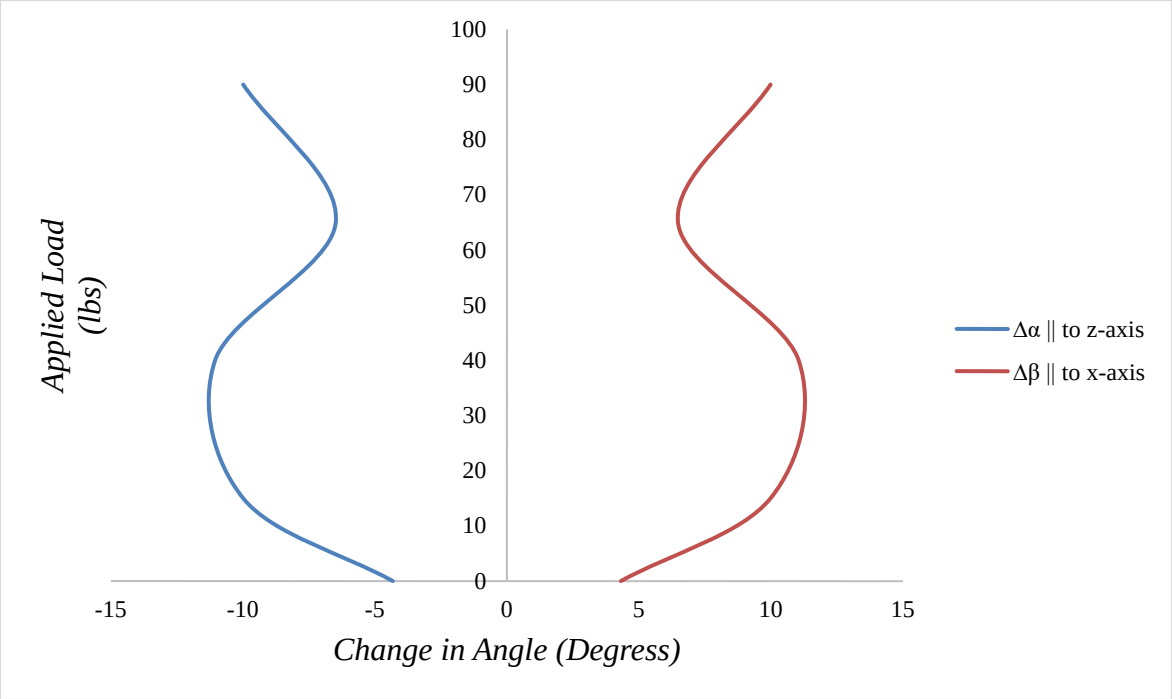

Figure (D.11): Records of Change in Angle in Rhombus 'R22' while Unloading

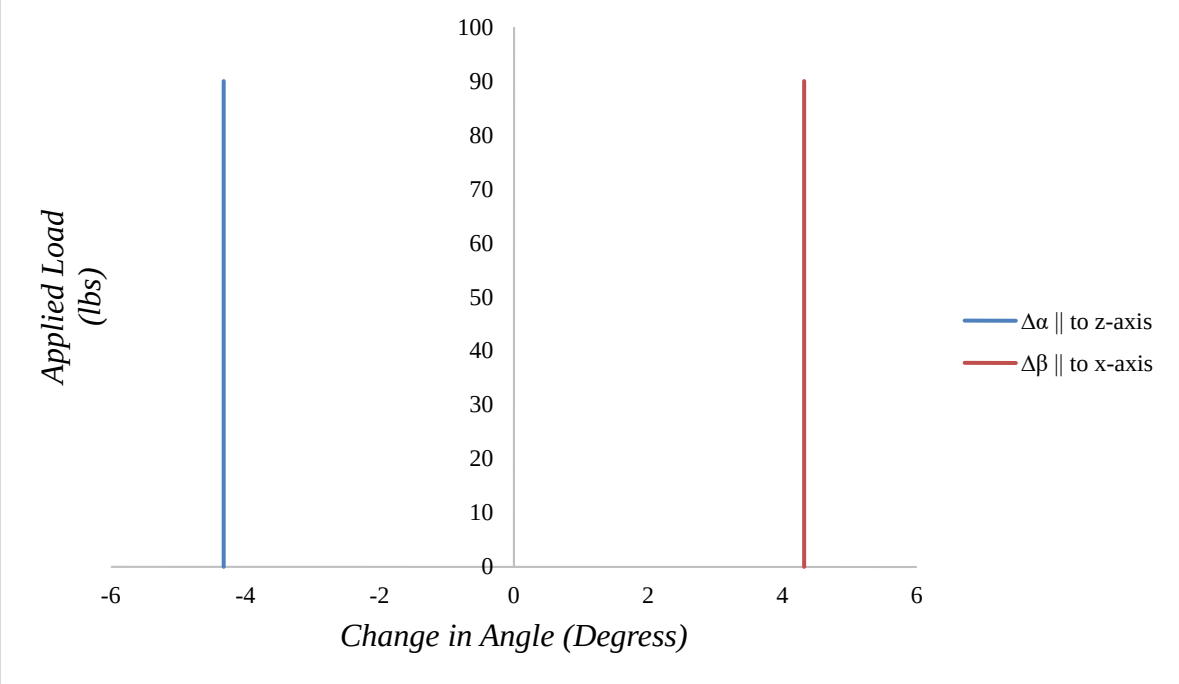

Figure (D.12): Records of Change in Angle in Rhombus 'R25' while unloading

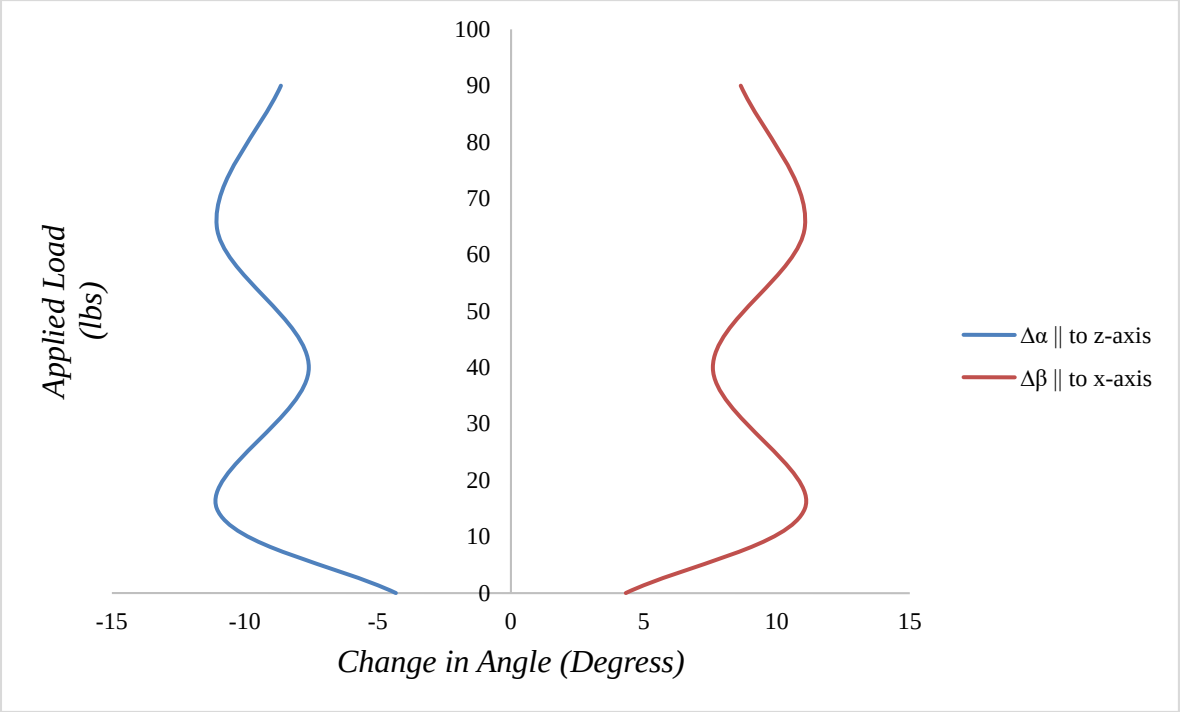

Figure (D.13): Records of Change in Angle in Rhombus 'R26' while Unloading

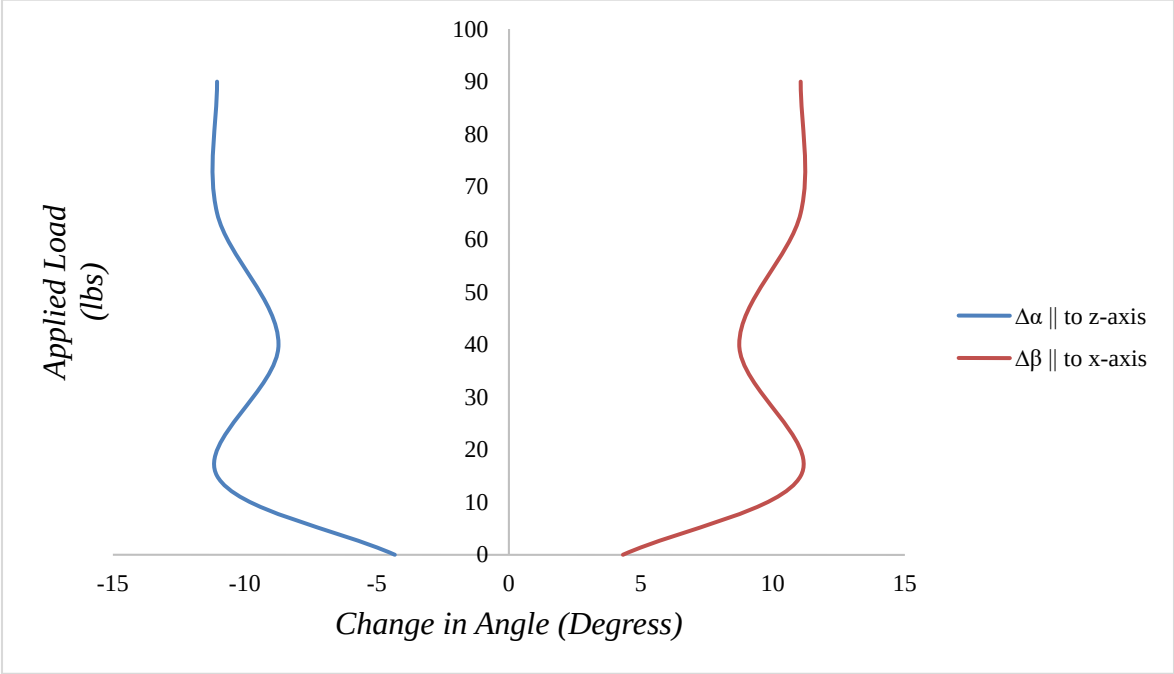

Figure (D.14): Records of Change in Angle in Rhombus 'R27' while Unloading

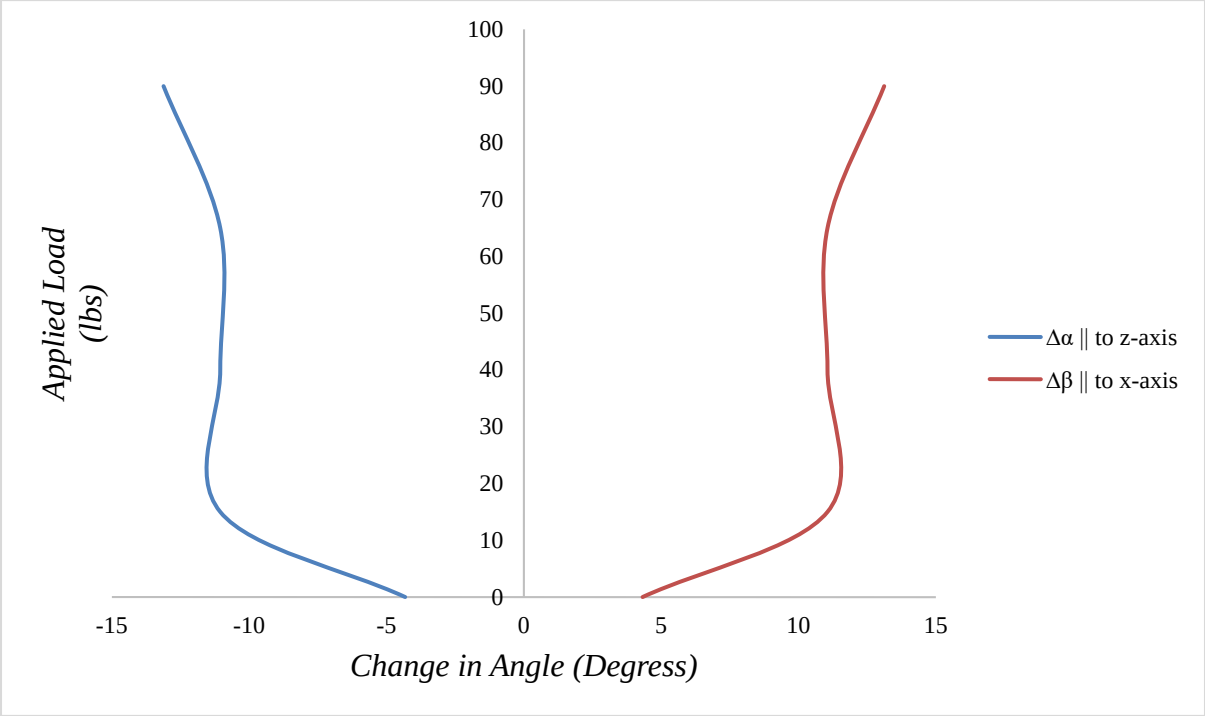

Figure (D.15): Records of Change in Angle in Rhombus 'R30' while Unloading

APPENDIX (E)

STRAIN GAUGES DETAIL

Kyowa Strain Gauge was used to record the strain in the sample. It has following properties:

1. Type: KFG-2N-120-C1-11L3M3R,

2. Gauge Factor (24˚C, 50% RH): 2.09 ± 1.0%,

3. Gauge Resistance (24˚C, 50% RH): 2 mm,

4. Adoptable Thermal Expansion: 11.7 PPM/˚C, and

5. Temperature Coefficient of gauge cement: CC-33A, EP-34B.

APPENDIX (F)

ANSYS FINITE ELEMENT CODE

ANSYS® (ANalysis SYStem) is multipurpose structural analysis finite element numerical software. This software has both linear and nonlinear capability for solving a wide scope of engineering problems including: stress, thermal, fluids, dynamics, vibrations, frequency analysis, acoustics, electromagnetism, optimization, etc.

To start ANSYS, double click on the ANSYS icon or *Start > Programs > ANSYS > ANSYS Product Launcher.* Then, enter the location for ANSYS file in the working directory and select run the MECHANICAL ADP 15.0 and the display window as shown in Figure (F.1).

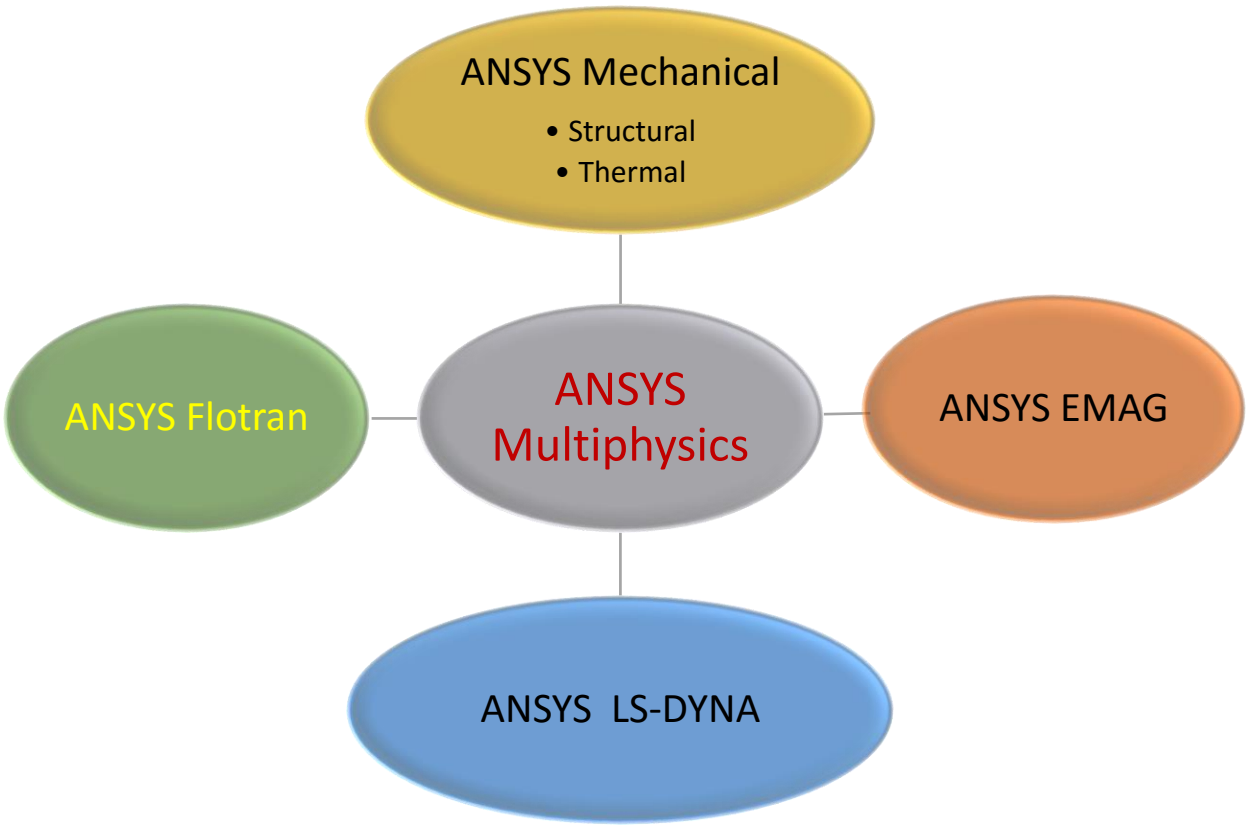

Figure (F.1): ANSYS Multiphysics

To model the numerical model following procedure was followed [3],

1. Main Menu/E-Preferences/E-Preferences for GUI Filtering,
2. Check Structural, accept default h-Method, and then press OK,
3. Main Menu/E-Preprocessor/E-Element Type/E-Add/Edit/Delete, (see Figure (F.2)),
4. In Element Types, pick Add/E-Library of element types, (see Figure (F.3)),
5. Select (Structural) Pipe and 3D Finite strain (in that, 2 node 288), and then press OK,

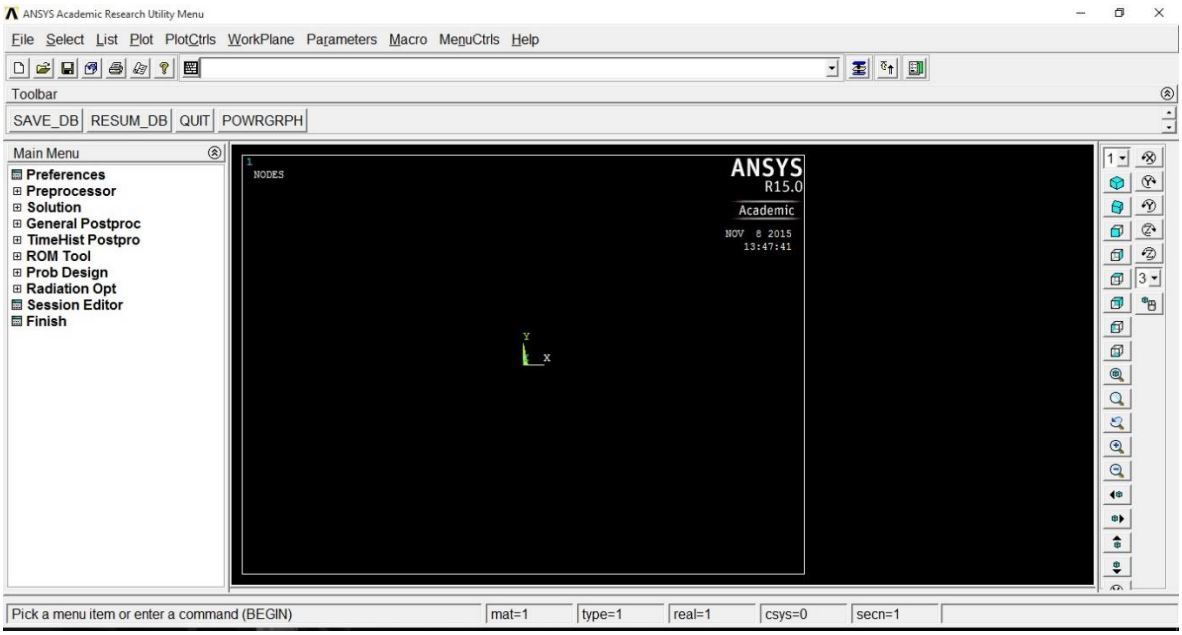

Figure (F.2): ANSYS MECHANICAL ADP 15.0 Display Screen

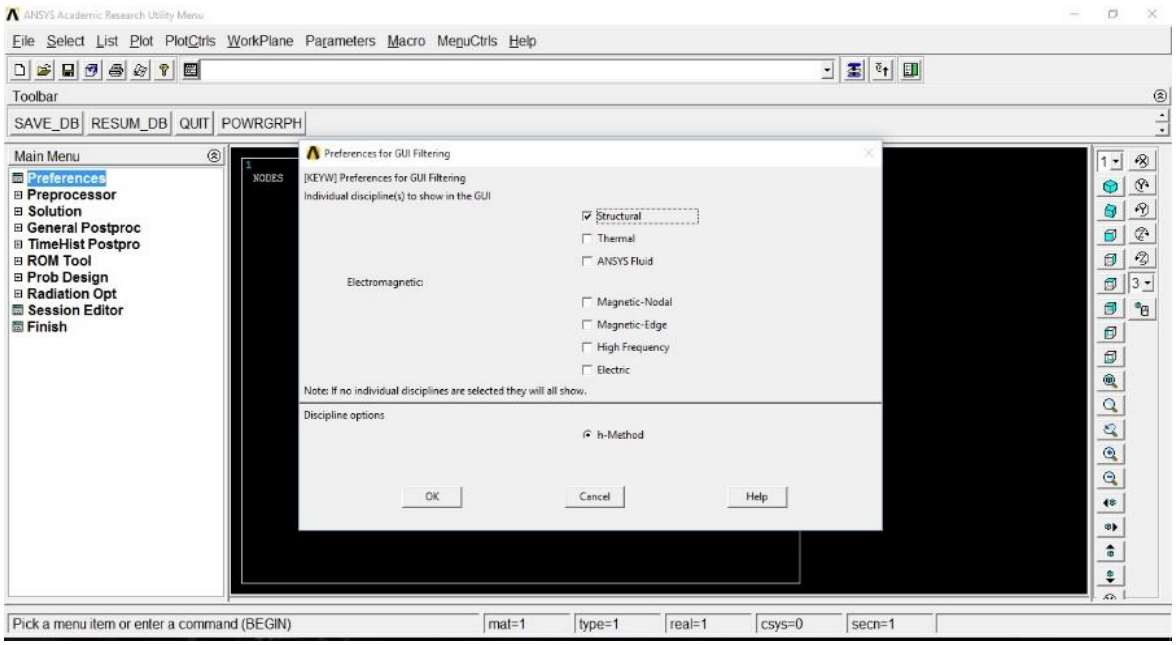

Figure (F.3): ANSYS MECHANICAL ADP 15.0 GUI Settings

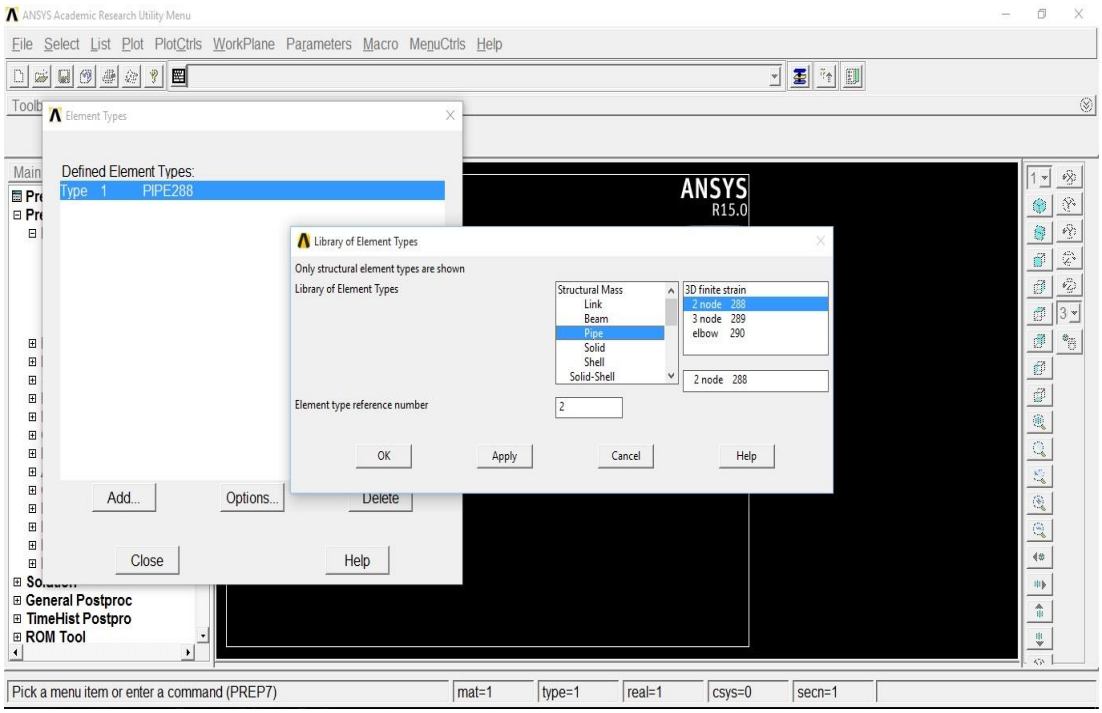

Figure (F.4): ANSYS MECHANICAL ADP 15.0 Element Addition

6. In Element Types and the click Close,

7. The element geometric properties data was provided to the element. The real conditions were replicated into the numerical model created in ANSYS software. Every element type requires one or more real constants, like area or moment of inertia, to describe it. Here, the geometric items for each type of pipe is area. Since the element type pipe 2 node 288 in order to supply real constant, the link was defined and properties were supplied as shown in Figure (F.4). To enter the various real constants to be referenced by the element types:

   i. Real Constants Type for real constants,

   ii. Select element type: Type 2 LINK 180, then press OK, (see Figure (F.5)),

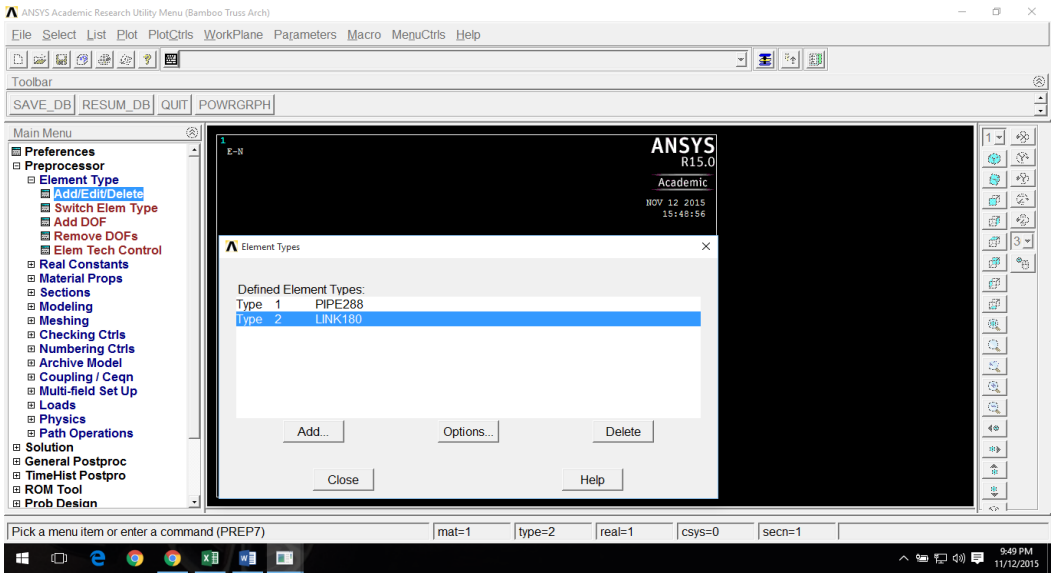

Figure (F.5): ANSYS MECHANICAL ADP 15.0 Link addition

   iii. In Real Constant Set Number 1, for LINK verify Set No. 1,

   iv. Enter 0.00174 m^2 (0.01875 ft^2) as cross-sectional area (AREA); (see Figure (F.6)), and then press OK, and

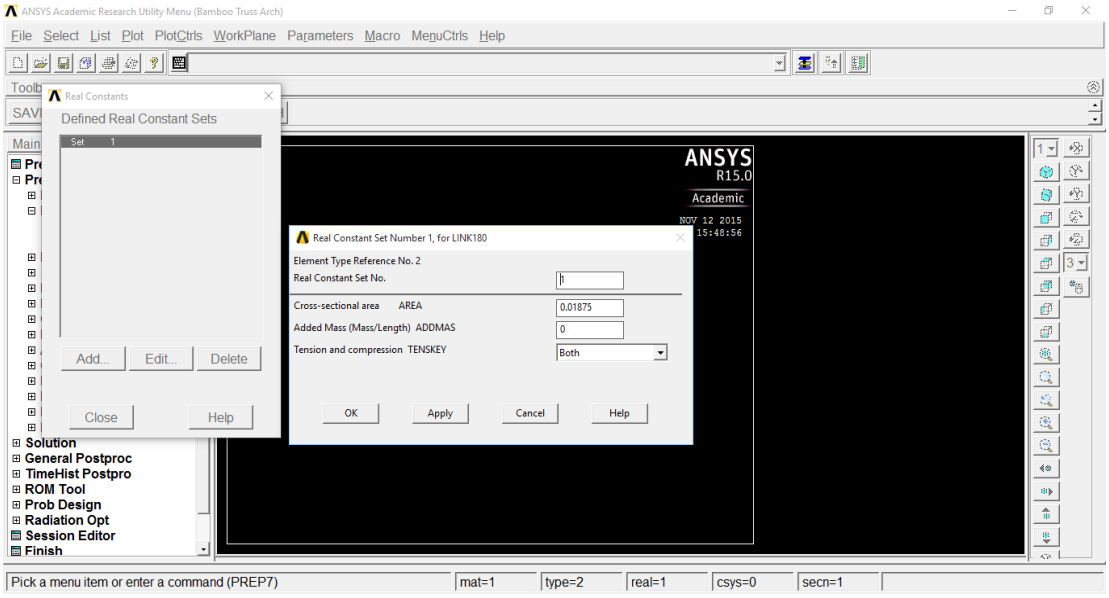

Figure (F.6): ANSYS Mechanical ADP 15.0 Defined Real Constant Sets

v. Set 1 appears in Real Constants. Select Close.

8. Now to declare material description. Activate the material properties with:

i. Main Menu/E-Preprocessor/E-Material Props/E-Material Models,

ii. Material Model Number 1 appears in define Material Model Behavior. Double click on Structural, then linear, elastic, orthotropic. In linear orthotropic properties for Material Number 1 enter for elastic modulus, Poisson's ratio and shear modulus as shown in Figure (F.7),

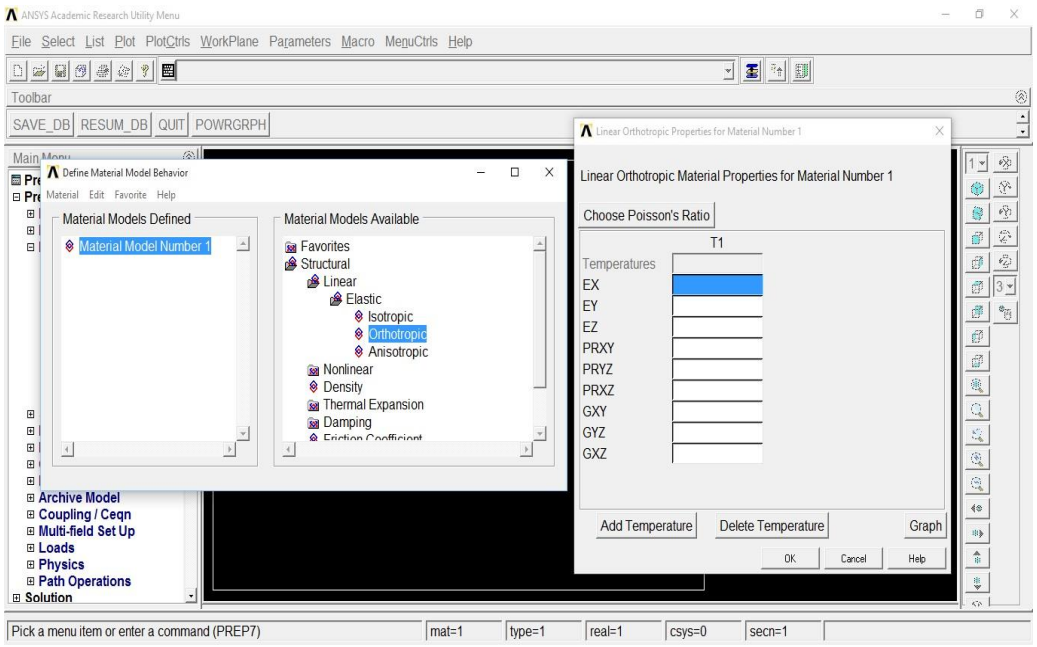

Figure (F.7): ANSYS MECHANICAL ADP 15.0 Material Properties

In linear isotropic properties for Material Number 2 enter for elastic modulus, Poisson's ratio as shown in Figure (F.8).

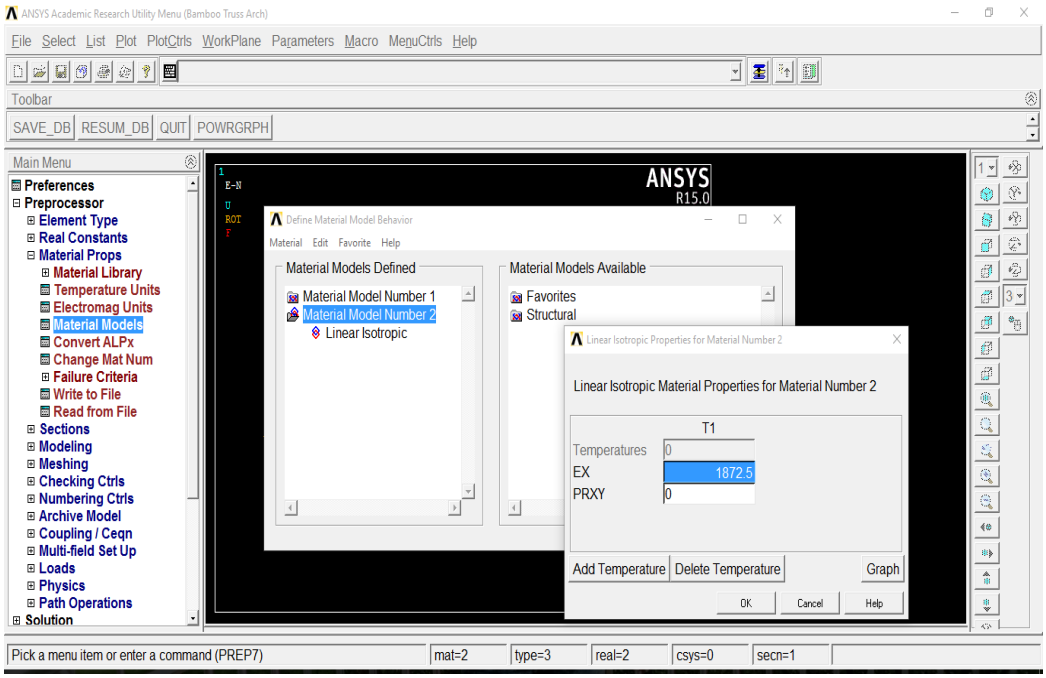

Figure (F.8): ANSYS MECHANICAL ADP 15.0 Material Properties

iii. The Table (F.1) shows the properties of Bamboo entered in ANSYS finite element software. In Figure (F.9) the properties direction was shown which was then used in table in terms of abbreviations,

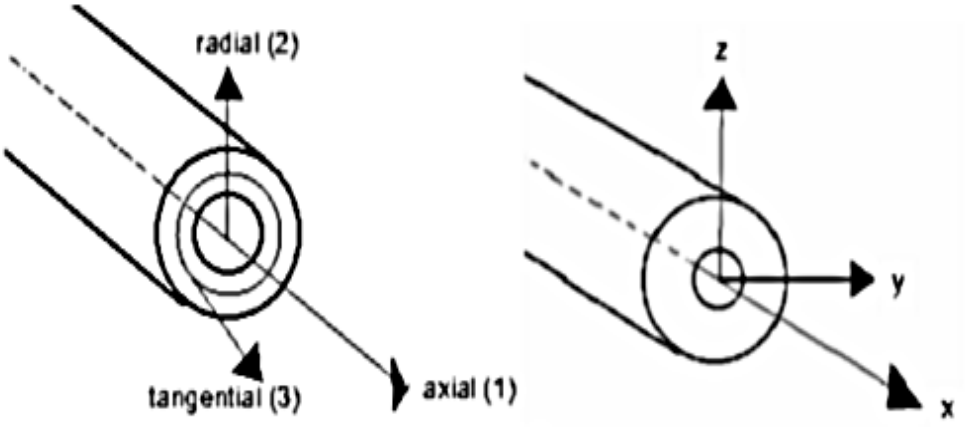

Figure (F.9): Bamboo Properties Directions [18]

Table (F.1): Physical and Mechanical Properties of Bamboo [18]

Properties	**Units**			
	SI		**US**	
Height of Culm	8.0 to 16.0	m	26.0 to 53.0	ft
Thickness	0.0075-0.015	m	0.025-0.05	ft
Cross-section diameter	0.025-0.08	m	0.08-0.26	ft
Distance between nodes	0.20-0.45	m	0.7-1.5	ft
Density	500.0-800.0	kg/m^3	31.0-50.0	lb/ft^3
Moisture Content	9 to 10			%
Young's Modulus, E1	$15{,}000 \times 10^6$	N/m^2	313.3×10^6	psf
Young's Modulus, E2	$6{,}200 \times 10^6$	N/m^2	130.0×10^6	psf
Young's Modulus, E3	$6{,}200 \times 10^6$	N/m^2	130.0×10^6	psf
Shear Modulus, G12	132.0×10^6	N/m^2	2.8×10^6	psf
Shear Modulus, G23	$1{,}650 \times 10^6$	N/m^2	34.5×10^6	psf

Shear Modulus, G31	93.50 x 10^6	N/m^2	2.0 x 10^6	psf
Poisson's Ratio μ_{12}	0.39 (inner)-0.58 (outer)		0.485 (avg)	
Poisson's Ratio μ_{13}	0.39 (inner)-0.58 (outer)		0.485 (avg)	
Poisson's Ratio μ_{21}	0.0177			
Poisson's Ratio μ_{31}	0.0177			
Poisson's Ratio μ_{32}	0.30			
Poisson's Ratio μ_{23}	0.30			
Ultimate Tensile Strength	160.0 x 10^6	N/m^2	3.40 x 10^6	psf

In this table, the properties were taken from past research performed on common bamboo species used in structural applications. These values were taken into account in developing the numerical model developed in this study. The generalized value of material properties was used because the design of structure is applicable to almost all types of bamboo and do not create any material constraints in the capacity of structure.

9. In next step to create the geometry the nodes were created and followed by elements. The x, y, z-coordinates of each node were identified for the ANSYS with its number.

Main Menu > Preprocessor > Modeling > Create > Nodes > In Active CS

(see Figure (F.10))

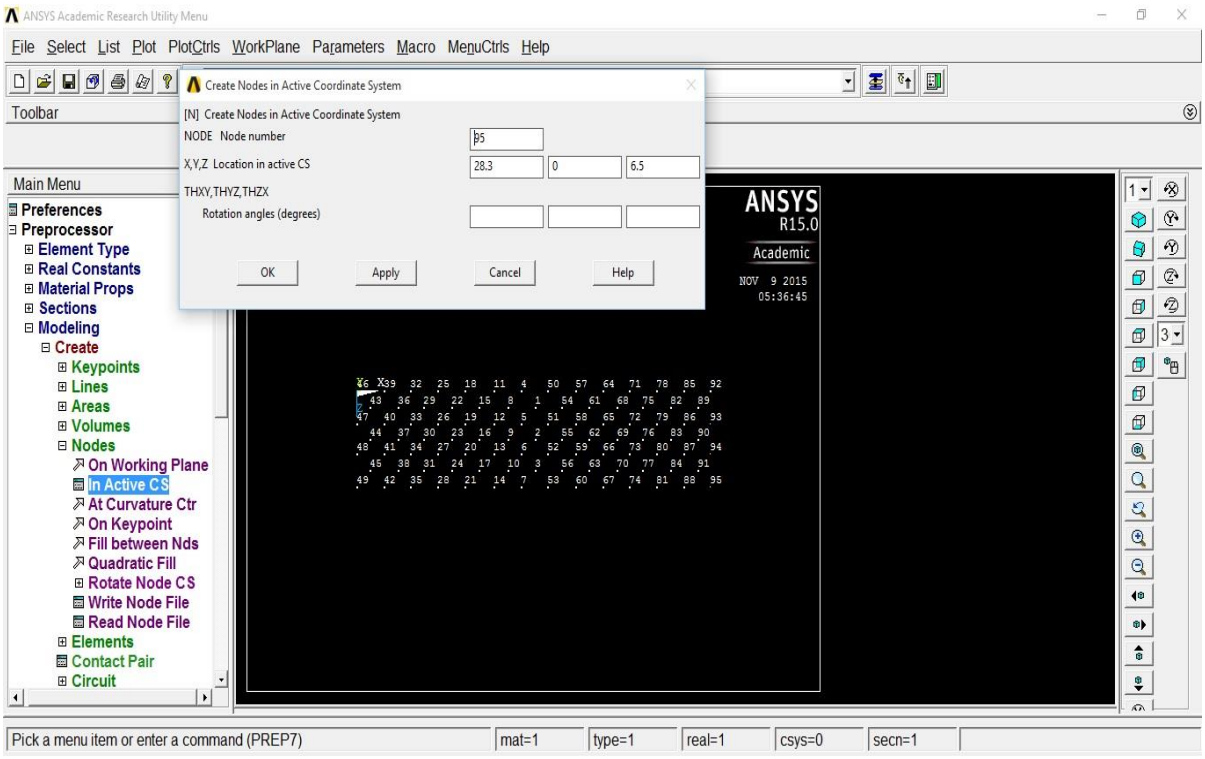

Figure (F.10): ANSYS Figures Shows the Created Nodes

Creating the element is done using the mouse only. Two nodes were connected to join elements as shown in Figure (F.11).

Main Menu > Modeling > Create > Elements > Auto Numbered > Thru Nodes

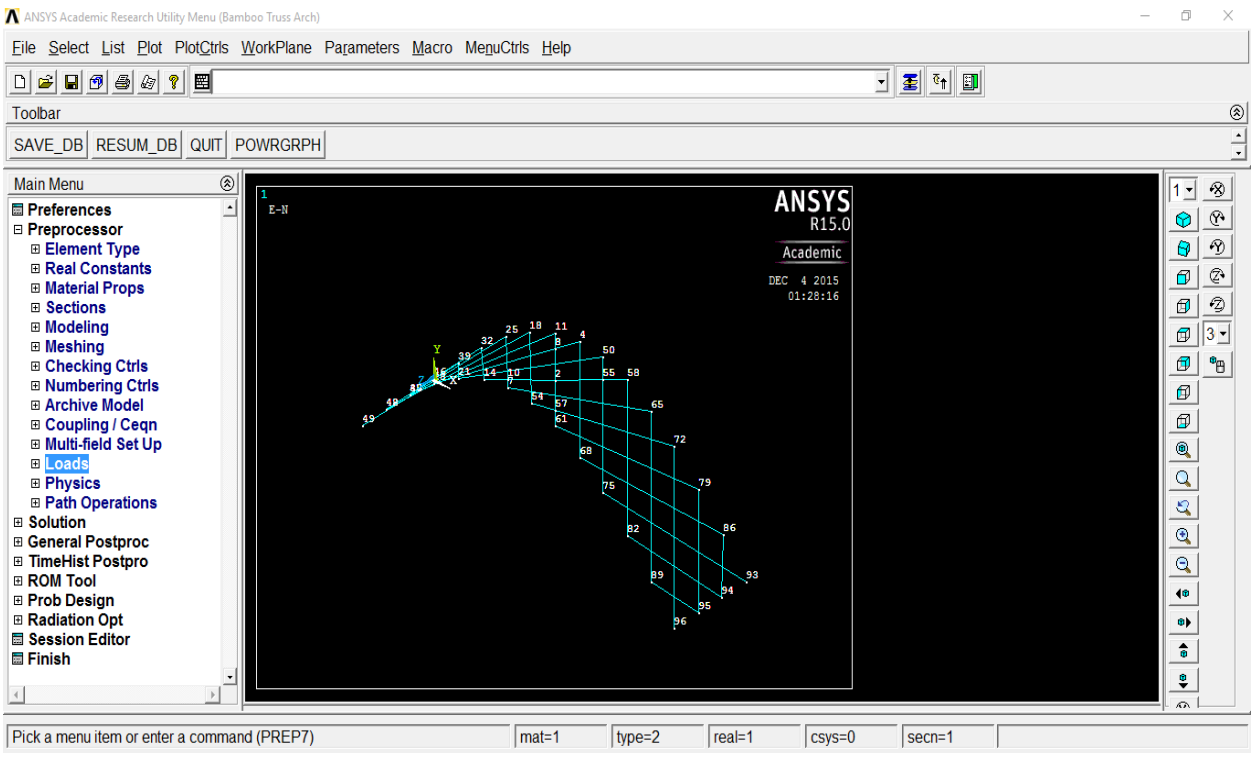

Figure (F.11): ANSYS Figures Shows the Elements

These steps summaries the finite element modeling in ANSYS of the structure with material properties and appropriate assumption. In Table (F.2), the node numbers and their respective observational node numbers were enlisted. In Figure (F.12), the element with their numbers and connection is shown.

10. The solution task starts here. Nodal forces and displacement were applied (see Figures 4.17 and 4.18]. Starting with force or displacements will not affect the solution. A zero displacement to the Z-direction for each was assigned and it means that node is fixed.

Main Menu > Solution > Define Load > Apply > Structural > Displacement > On Nodes

Table (F.2): ANSYS Model Node Numbers and Coordinates

ANSYS Model Node Numbers	Nodes	X	Y	Z
		(foot)	(foot)	(foot)
1	X1	14.3	9.0	1.1
2	X2	14.3	8.7	3.3
3	X3	14.3	9.0	5.4
4	1	13.2	9.2	0
5	2	13.2	8.7	2.2
6	3	13.2	8.7	4.3
7	4	13.2	9.2	6.5
8	5	12.1	8.7	1.1
9	6	12.1	8.4	3.3
10	7	12.1	8.7	5.4
11	8	11	8.7	0
12	9	11	8.1	2.2
13	10	11	8.1	4.3
14	11	11	8.7	6.5
15	12	9.8	7.8	1.1
16	13	9.8	7.5	3.3
17	14	9.8	7.8	5.4
18	15	8.7	7.6	0
19	16	8.7	7.1	2.2
20	17	8.7	7.1	4.3
21	18	8.7	7.6	6.5
22	19	7.6	6.7	1.1
23	20	7.6	6.3	3.3
24	21	7.6	6.7	5.4
25	22	6.5	6.2	0
26	23	6.5	5.7	2.2
27	24	6.5	5.7	4.3
28	25	6.5	6.2	6.5
29	26	5.4	5.0	1.1
30	27	5.4	4.8	3.3
31	28	5.4	5.0	5.4
32	29	4.3	4.3	0
33	30	4.3	3.9	2.2
34	31	4.3	3.9	4.3
35	32	4.3	4.3	6.5
36	33	3.3	3.0	1.1
37	34	3.3	2.9	3.3
38	35	3.3	3.0	5.4
39	36	2.2	2.2	0

40	37	2.2	1.9	2.2
41	38	2.2	1.9	4.3
42	39	2.2	2.2	6.5
43	40	1.1	1.9	1.1
44	41	1.1	1.9	3.3
45	42	1.1	1.9	5.4
46	43	0	0.0	0
47	44	2.2	0.0	2.2
48	45	4.3	0.0	4.3
49	46	6.5	0.0	6.5
50	1	15.3	9.2	0
51	2	15.3	8.7	2.2
52	3	15.3	8.7	4.3
53	4	15.3	9.2	6.5
54	5	16.4	8.7	1.1
55	6	16.4	8.4	3.3
56	7	16.4	8.7	5.4
57	8	17.5	8.7	0
58	9	17.5	8.1	2.2
59	10	17.5	8.1	4.3
60	11	17.5	8.7	6.5
61	12	18.6	7.8	1.1
62	13	18.6	7.5	3.3
63	14	18.6	7.8	5.4
64	15	19.7	7.6	0
65	16	19.7	7.1	2.2
66	17	19.7	7.1	4.3
67	18	19.7	7.6	6.5
68	19	20.8	6.7	1.1
69	20	20.8	6.3	3.3
70	21	20.8	6.7	5.4
71	22	21.8	6.2	0
72	23	21.8	5.7	2.2
73	24	21.8	5.7	4.3
74	25	21.8	6.2	6.5
75	26	22.9	5.0	1.1
76	27	22.9	4.8	3.3
77	28	22.9	5.0	5.4
78	29	24	4.3	0
79	30	24	3.9	2.2
80	31	24	3.9	4.3
81	32	24	4.3	6.5
82	33	25.1	3.0	1.1
83	34	25.1	2.9	3.3

84	35	25.1	3.0	5.4
85	36	26.2	2.2	0
86	37	26.2	1.9	2.2
87	38	26.2	1.9	4.3
88	39	26.2	2.2	6.5
89	40	27.3	1.9	1.1
90	41	27.3	1.9	3.3
91	42	27.3	1.9	5.4
92	43	28.3	0.0	0
93	44	28.3	0.0	2.2
94	45	28.3	0.0	4.3
95	46	28.3	0.0	6.5

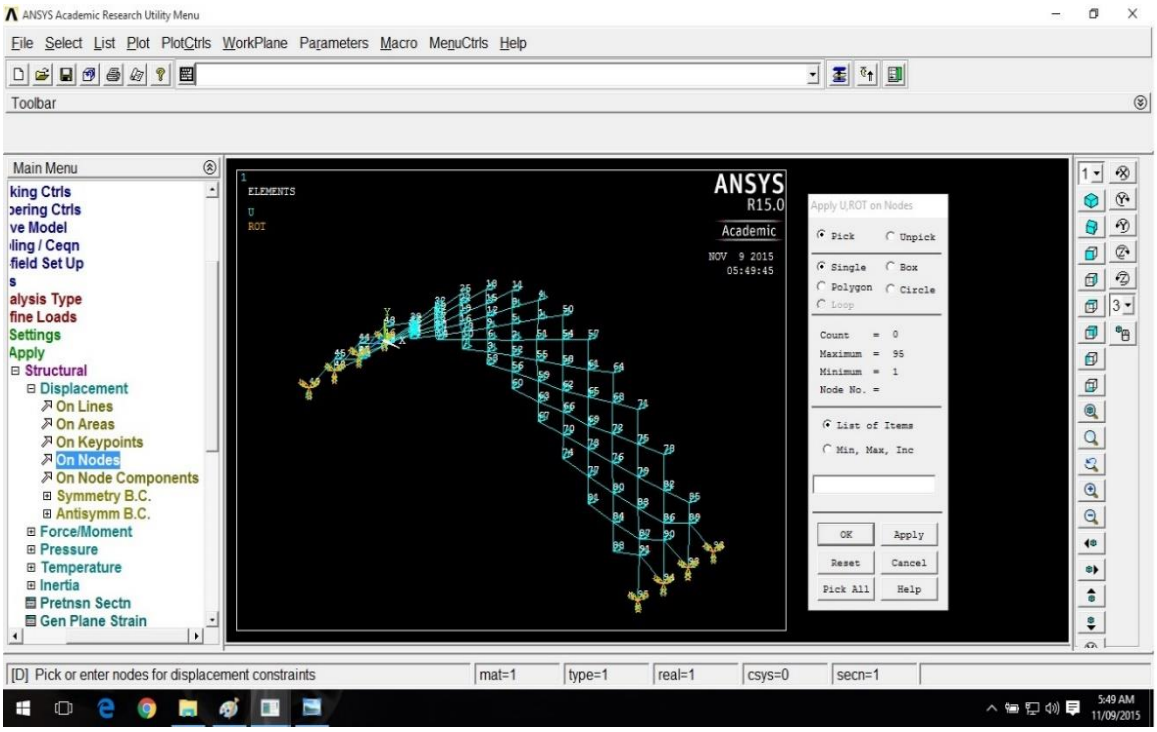

Figure (F.12): ANSYS Pictorial Show of the Displacement Boundary Condition

Main Menu > Solution > Define Load > Apply > Structural > Force/Moment > On Nodes

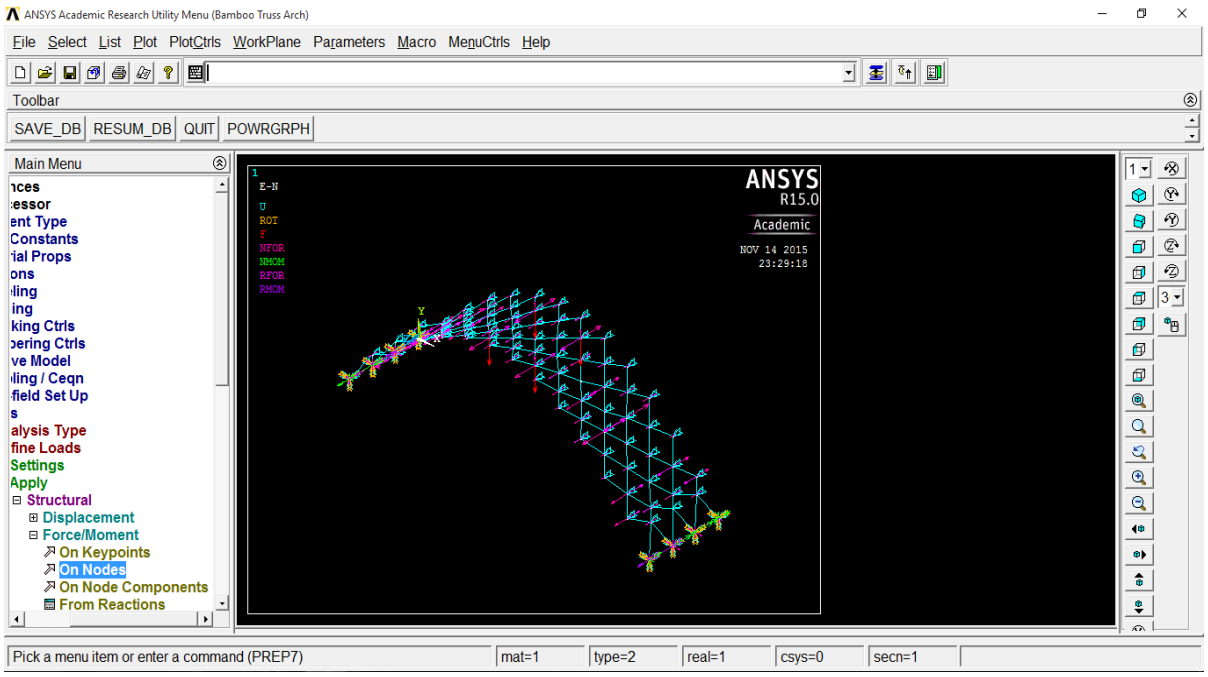

Figure (F.13): ANSYS Pictorial Show of the Force Boundary Condition

Main Menu > Solution > Define Load > Apply > Function > Define/Edit

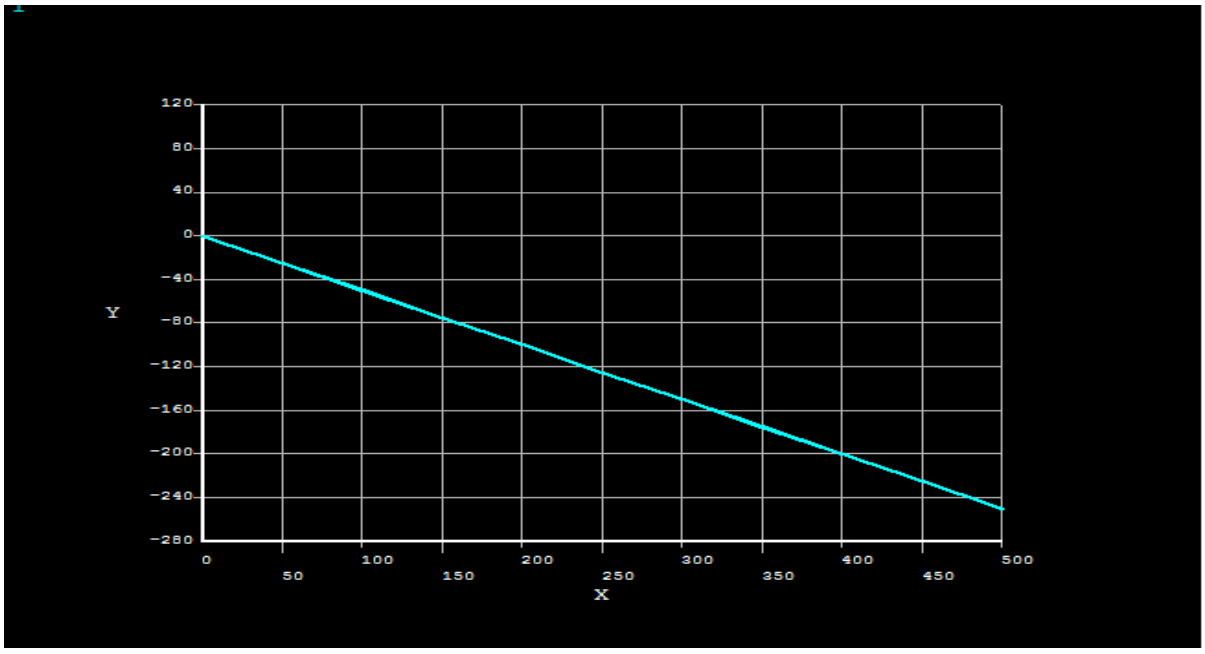

Figure (F.14): ANSYS Figure shows a Function of Force

(Y- Force Function, X – Time)

The negative FY function was applied at each node such to replicate the experimental loading for comparison purpose and negative direction represents the downward direction of the force applied (see Figure (F.14)).

11. The final step is to initiate the solution. ANSYS software will assemble the stiffness matrix, apply the boundary conditions and solve the stiffness matrix.

Main Menu > Solution > Solve > Current LS

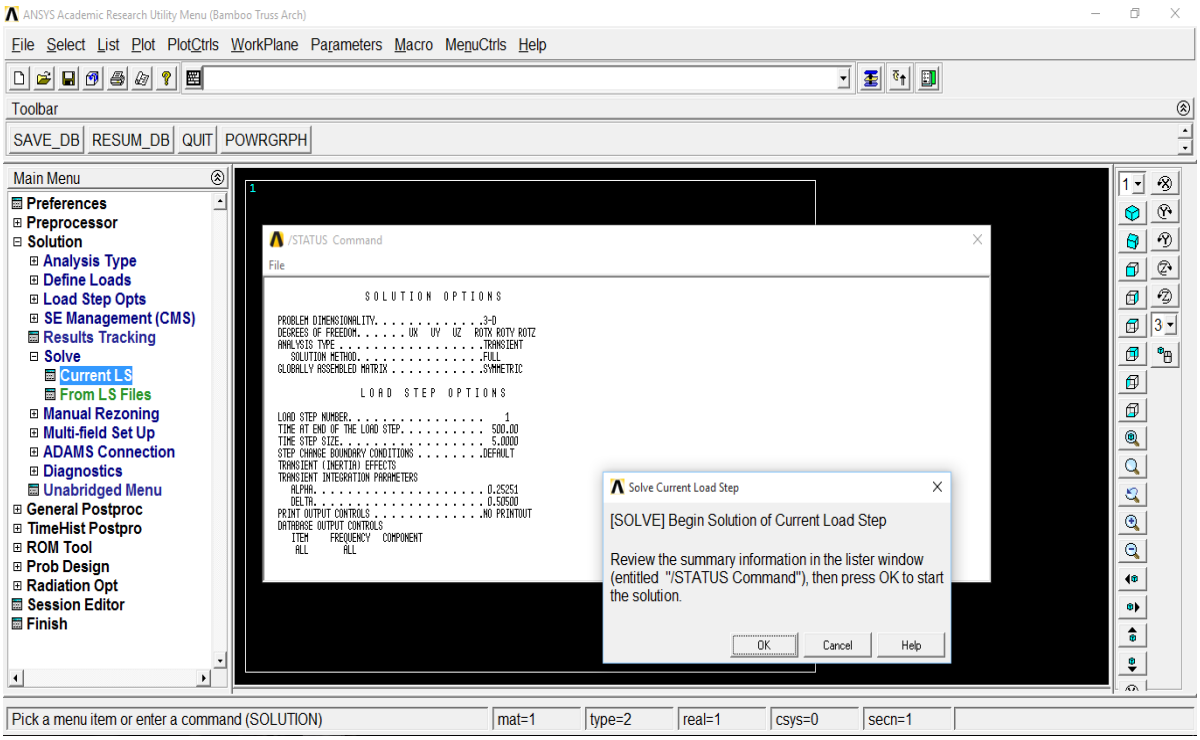

Figure (F.15): ANSYS Force Function per Time

After following all the process, the numerical model was ready to get the results for comparison with experimental model.